8-6-2007

KIR Channels in CO2 Central Chemoreception: Analysis with a Functional Genomics Approach

Asheebo Rojas

KIR CHANNELS IN CO_2 CENTRAL CHEMORECEPTION: ANALYSIS WITH A FUNCTIONAL GENOMICS APPROACH

by

ASHEEBO ROJAS

Under the Direction of Chun Jiang

ABSTRACT

The process of respiration is a pattern of spontaneity and automatic motor control that originate in the brainstem. The mechanism by which the brainstem detects CO_2 is termed central CO_2 chemoreception (CCR). Since the early 1960's there have been tremendous efforts placed on identification of central CO_2 chemoreceptors (molecules that detect CO_2). Even with these efforts, what a central CO_2 chemoreceptor looks like remain unknown. To test the hypothesis that inward rectifier K^+ (Kir) channels are CO_2 sensing molecules in CCR, a series of experiments were carried out. **1)** The first question asked was whether the Kir4.1-Kir5.1 channel is expressed in brainstem chemosensitive nuclei. Immunocytochemistry was performed on transverse medullary and pontine sections using antibodies raised against Kir4.1 and Kir5.1. Positive immunoassays for both Kir4.1 and Kir5.1 subunits were found in CO_2 chemosensitive neurons. In the LC the Kir4.1 and Kir5.1 were co-expressed with the neurokinin-1 receptor that is the natural receptor for substance P. **2)** The second question asked was whether the Kir4.1-Kir5.1 channel is subject to modulation by neurotransmitters critical for respiratory control. My studies demonstrated that indeed the Kir4.1-Kir5.1 channel is

subject to modulation by substance P, serotonin and thyrotropin releasing hormone. **3)** I performed studies to demonstrate the intracellular signaling system underlying the Kir4.1-Kir5.1 channel modulation by these neurotransmitters. The modulation by all three neurotransmitters was dependent upon the activation of protein kinase C (PKC). The Kir4.1-Kir5.1 but not the Kir4.1 channel was modulated by PKC. Both the Kir4.1 and Kir5.1 subunits can be phosphorylated by PKC in vitro. However, systematic mutational analysis failed to reveal the phosphorylation site. **4)** The fourth question asked was whether Kir channels share a common pH gating mechanism that can be identified. Experiments were performed to understand the gating of the Kir6.2+SUR1 channel as specific sites for ligand binding and gating have been demonstrated. I identified a functional gate that was shared by multiple ligands that is Phe168 in the Kir6.2. Other Kir channels appear to share a similar gating mechanism. Taken together, these studies demonstrate the modulation of Kir channels in central CO_2 chemoreception.

INDEX WORDS: Kir4.1-Kir5.1, Kir6.2+SUR1, Central CO_2 Chemoreception, Neuromodulation, Phosphorylation, Channel Gating, Ligand Modulation, CO_2/pH sensing

KIR CHANNELS IN CO_2 CENTRAL CHEMORECEPTION: ANALYSIS WITH A FUNCTIONAL GENOMICS APPROACH

by

ASHEEBO ROJAS

A Dissertation Submitted in Partial Fullfillment of the Requirements for the Degree of

Doctor of Philosophy

In the College of Arts and Sciences

Georgia State University

2007

KIR CHANNELS IN CO_2 CENTRAL CHEMORECEPTION: ANALYSIS WITH A FUNCTIONAL GENOMICS APPROACH

by

ASHEEBO ROJAS

Major Professor: Chun Jiang
Committee: Delon Barfuss
Deborah Baro
Teryl Frey

Electronic Version Approved:

Office of Graduate Studies
College of Arts and Sciences
Georgia State University
August 2007

A. ACKNOWLEDGEMENTS

Pursuing a doctoral degree is one of the most challenging and important events in my life which requires not only my personal efforts but also support from my surroundings. My sincere appreciation is extended to all who have provided assistance, advice and encouragement to me during my Ph.D. study.

First of all, I would like to thank my advisor, Dr. Chun Jiang, for all his instruction, encouragement and help in brining this dissertation into reality and completion. He has a tremendous influence not only to my career, but also to my personality. I am also indebted to the faculty and staff of the Department of Biology at Georgia State University for their advice and generous assistance during my Ph.D. program. I am particularly grateful to Drs. Delon Barfuss, Deborah Baro, and Teryl Frey for serving on my dissertation committee and their invaluable advisements in my thesis design and accomplishment.

I would like to express my appreciation to the members in Dr. Jiang's lab for their involvement in the discussions of my research projects and numerous technical assistances. Special thanks to Dr. Junda Su and Dr. Ningren Cui for their help in the whole cell recordings, Dr. Jianping Wu and Dr. Ningren Cui for their help with patch clamp, Drs. Haoxing Xu, Hailan Piao, Li Li, and Runping Wang for their assistance in DNA reconstruction, purification and molecular biology, Dr. Liang Yang, Dr. Junda Su, Ms. Xiaoli Zhang, and Mr. Ming Lee for their help with immunocytochemistry, Ms. Vivian Onyebuchi, Ms. Carmen Adams, Ms. Ying Wang, Ms Dyanna Fountain, and Mr. Jean-Pierre Muhumuza for their technical assistance.

I also give special thanks to Ms. Ping Liang-Jiang for her help with the DNA sequencing and making primers. My appreciation is also extended to the many members of the Department of Biology that I shared this experience with for their advice and assistance during my Ph. D. program.

Finally, my most heartfelt thanks goes to my family, my beautiful wife Tychay Rojas and my lovely Kids, Asheebo Rojas jr. and Kaitlyn Ashlee Rojas for their love, encouragement and support. I thank my parents and siblings for giving me my early scientific education and encouraging me to pursue this Ph.D. degree. I am extremely grateful to my mother and all of my extended family for all of their support.

B. TABLE OF CONTENTS

C. LIST OF TABLES

D. LIST OF FIGURES

E. ABBREVIATIONS

5-HT	5-hydroxytryptamine (serotonin)
5-HT2A	serotonin receptor 2A
ADP	adenosine diphosphate
ADS	antibody dilution solution
ATP	adenosine triphosphate
BSA	bovine serum albumin
C	closed state
CCHS	congenital central hypoventilation syndrome
CCR	central chemoreceptor
CNG	cyclic nucleotide-gated
CO_2	carbon dioxide
DAB	diaminobenzidine
DAG	diacylglycerol
DOI	25-dimethoxy-4-iodophenyl-2-aminopropane
EGTA	ethylene glycol-bis-β-aminoethylether-N,N,N',N'-tetraacetic acid
FVPP	fluoride, vanadate, and pyrophosphate
GFP	green fluorescent protein
GIRK	G protein-coupled inward rectifier K^+ channels
GPCR	G protein coupled receptors
h	hill coefficient
HEK	human embryonic kidney cells
HEPES	4-(2-hydroxyethyl)-1-piperazineethanesulfonic acid
IC_{50}	concentration for 50% inhibition
IP_3	inositol 1 4 5-triphosphate receptor
K^+	potassium ion
K_{ATP}	ATP-sensitive K^+ channel
KcsA	K^+ channel protein from bacterium Streptomyces lividans
Kir	inward rectifiier K^+ channel

Kir6.2ΔC36	inward rectifiier K^+ channel 6.2 with 36 amino acids truncated
LC	locus coeruleus
MAP2	microtubule associated protein 2
MOR	mu-opioid receptor
Ni-DAB	nickel enhanced diaminobenzidine
NK1R	neurokinin-1 receptor
O	open state
P	pore-forming loop
PBS	phosphate buffered saline
P_{CO2}	partial pressure of CO_2
PCR	polymerase chain reaction
PDD	phorbol 12,13-didecanoate
pH	potential of hydrogen
pH_i	intracellular pH
PI3K	phosphoinositide-3 kinase
PIP_2	phosphatidylinositol bisphosphate
PIPES	piperazine-N,N'-bis-2-2ethanesulfonic acid
pKa	pH value at 50% effect
PKA	protein kinase A
PKC	protein kinase C
PMA	phorbol 12-myristate 13-acetate
P_o	open-state probability
P_{open}	open-state probability
S.E.	standard error
SP	substance-P
SUR	sulphonyl urea receptor
TASK	twik-related acid-sensitive K^+ channel
TBS	tris buffered saline
TEVC	two-electrode voltage clamp

TH	tyrosine hydroxylase
TM1	first membrane-spanning helix
TM2	second membrane-spanning helix
TRH	thyrotropin releasing hormone
TRH-R1	thyrotropin releasing hormone receptor 1
TRH-R2	thyrotropin releasing hormone receptor 2
VLM	ventallateral medulla
VRG	ventral respiratory group
WT	wild-type

F. SPECIFIC AIMS AND HYPOTHESES

Central chemoreception, defined as the physiological response of the central nervous system to chemical stimuli (CO_2 and H^+) has been a puzzling area of medical science for the past 40-50 years. Although new information is constantly being produced in the literature about this topic, what a central chemoreceptor looks like remains elusive. Recent studies indicate that there are specific neurons in the brainstem that are CO_2 chemosensitive (Ballantyne & Scheid, 2001; Feldman et al., 2003; Nattie & Li, 2002; Paterson et al., 2006; Richerson et al., 2001). However, because of the diversity of cell types in the brainstem, the difficulty for finding the central chemoreceptor molecule has proven to be rather difficult. One approach to overcome this difficulty is to find molecules instead of cells, which are responsible for CO_2 sensing, as proposed in our laboratory. Based on the criteria established recently by Jiang et al., 2001, a number of ion channels qualify as potential CO_2/pH sensing candidates, i.e., various inward rectifier K^+ channels (KIR), twik-related acid-sensitive K^+ channels (TASK), and non selective cation channels such as transient receptor potential channels (TRP) and cyclic nucleotide gated channels (CNG). Immunocytochemistry and in situ hybridization studies have proposed the existence of members of these channel families in brainstem neurons. The brainstem neuronal expression of these channels may implicate an involvement in central CO_2 chemoreception. In addition to brainstem expression these potential candidates satisfy other properties that are required of central CO_2 chemoreceptors such as a high sensitivity to CO_2/pH and an ability to detect both alkaline and acidic pH levels. Although many of these channels meet the criteria, the inward rectifier K^+ (Kir) channels

are leading candidates because there is evidence showing that certain intrinsic Kir channel properties are detected in known chemosensitive neurons during changes in CO_2 (Kawai et al., 2006; Pineda & Aghajanian, 1997; Schultz et al., 2003). One major finding from studies involving these Kir channels is that they have the ability to change cellular excitability (Cui et al., 2001; Isomoto et al., 1997; Nichols & Lopatin, 1997). This is important because central CO_2 chemoreception involves a change in neuronal excitability, such as a depolarization of brainstem chemosensitive neurons resulting in an increase in the firing rate of these neurons when challenged with acidosis. Over the past decade a number of Kir channels suggested to play a role in central CO_2 chemoreception have declined because they fail to satisfy most or all of the requirements of a central CO_2 chemoreceptor. The heteromeric Kir4.1-Kir5.1 channel and the K_{ATP} channel (composed of Kir6.2/SUR1) remain strong candidates for a major involvement in central CO_2 chemoreception. However, even with extensive *in vitro* electrophysiological and protein modification studies carried out on these channels their neuronal specific function has not been elucidated. Therefore, a neuron-specific functional genomics approach is important because this may eventually lead to an identification of the long-searched central CO_2 chemoreceptors. However, it is not clear whether the Kir4.1-Kir5.1 protein is expressed in chemosensitive brainstem nuclei; whether the Kir4.1-Kir5.1 channel is modulated by neurotransmitters critical for respiratory control; what intracellular signaling mechanisms account for the modulation; and whether Kir6.2 modulation by ATP is important for central chemoreception. To address the issue of the Kir4.1-Kir5.1 and Kir6.2 channels

being central CO_2 chemoreceptors, I have designed experiments to target four specific aims:

A. **To demonstrate the expression of the heteromeric Kir4.1-Kir5.1 channel protein in chemosensitive brainstem nuclei.**

B. **To show the modulation of the Kir4.1-Kir5.1 channel by neurotransmitters critical for respiratory control.**

C. **To elucidate the molecular basis for the modulation of the Kir4.1-Kir5.1 channel by neurotransmitters.**

D. **To understand a general gating mechanism shared by the Kir channels and its effect on CO_2 central chemoreception.**

The following hypotheses will be tested:

1. **The Kir4.1-Kir5.1 channel protein is expressed in the plasma membrane of chemosensitive neurons in the brainstem where it is co-localized with the natural receptor for the neurotransmitter Substance-P (NK1R).**

2. **The Kir4.1-Kir5.1 channel is modulated by the neurotransmitters substance-P, serotonin, and thyrotropin releasing hormone, where channel activity is reduced by receptor activation via a protein kinase C-dependent mechanism.**

3. **Kir4.1-Kir5.1 channel activity is reduced by PKC activation and channel phosphorylation and such a regulation requires the presence of the Kir5.1 subunit.**

4. **Kir6.2+SUR1 channel gating involves a bulky phenylalanine residue located at the narrowest sector of the ion conductive pore where it allows the channel to affect cellular excitability.**

G. BACKGROUND

The ability to respire (breathe) is a basic fundamental function for human survival. Respiration can simply be defined as the process of gas exchange within the body. The final goal of respiration is to maintain adequate concentrations of O_2, CO_2, and hydrogen ions in the body. It is fortunate therefore, that changes in the levels of these three molecules or any of the three results in increase respiratory activity to regulate the changes. When we breathe, we consume O_2 during inhalation and liberate CO_2 during exhalation. This exchange of gases is the respiratory system's means of getting O_2 to the blood where it is then delivered to all regions of the body by red blood cells. Unlike O_2, during metabolic processes CO_2 is produced by the tissues of the body. It enters the vascular system where it is transported to the lungs so it can be expired. For this gas exchange process to be effective and efficient there has to be mechanisms in the body for the constant detection of the levels of O_2 and CO_2 that are present. O_2 sensing and detection is carried out mainly by peripheral chemoreceptors, whereas CO_2 sensing is mainly carried out by central CO_2 chemoreceptors located within the brainstem (Donnelly & Carroll, 2005; Lahiri & Forster, 2003; Lahiri et al., 2006; Nattie, 1999; O'Regan & Majcherczyk, 1982). O_2 does not have a significant direct effect on the respiratory center of the brain. Instead O_2 acts on the peripheral chemoreceptors which were found to be located in the carotid and aortic bodies in the base of the neck (Lahiri et al., 2006). The effect of O_2 on the carotid and aortic bodies is transmitted to the respiratory center in the brainstem via nerves. The information then travels from the respiratory center to the respiratory muscles. Changes in CO_2 stimulate the respiratory center in the brain directly

resulting in increases in both inspiratory and expiratory drive that are transmitted to the respiratory muscles, thus affecting ventilation. Indirectly, changes in CO_2 are also detected by peripheral chemoreceptors via a change in arterial pH similar to O_2 sensing

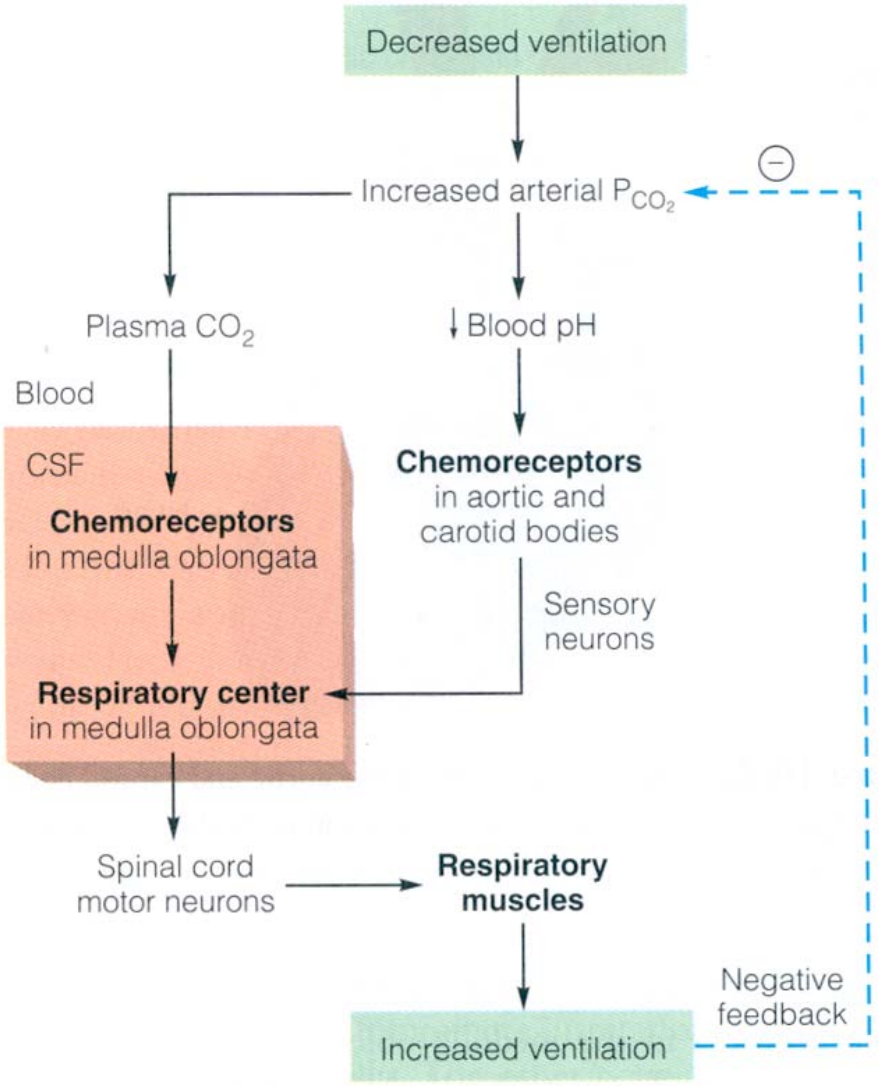

Fig. G-1. A schematic demonstrating the flow of information in the respiratory system when ventilation is reduced and CO_2 is increased.

(Fig. 1).

Although the brainstem contains the respiratory center that is responsible for generating the involuntary respiratory rhythm, our conscious though processes also affect respiration. Higher brain centers such as the cerebrum and hypothalamus may send signals to the respiratory center and alter the activity of the central pattern generator leading to a change in ventilation. These higher brain centers, although can affect and modulate respiratory drive are not necessary for respiration as experiments in animals with severe damage to higher brain areas demonstrate normal breathing. It is also known that respiration is affected by emotional processes such as fear and excitement. Under these conditions the neural pathway may bypass the central pattern generator in the brainstem and go directly to the somatic motor neurons that innervate respiratory muscles. No matter what information is sent to the respiratory center the chemoreceptor reflex is still dominant. We cannot override the chemoreceptor reflex although consciously we can alter our respiratory output. No matter how long we hold our breath voluntarily the increased P_{CO2} in our system will activate the chemoreceptor reflex and we will be forced to breath. Therefore, the strong CO_2 stimulus cannot be ignored.

G-1. Central CO_2 chemoreception

The process by which the respiratory center in the brainstem detects CO_2 is termed central CO_2 chemoreception (CCR). Central CO_2 chemoreception is an important process in the maintenance of brain function. The brain tightly monitors changes in pH in both acidic and alkaline directions. The presence of the blood-brain barrier does not allow

H^+ to get from the periphery of the body into the brain. However, CO_2 can cross the blood-brain barrier. Gaseous CO_2 is recognized as the molecule that diffuses across the blood-brain barrier, but pH is the actual stimulus that elicits a response by chemosensing neurons leading to a change ventilation (Erlichman & leiter, 1997; Feldman et al., 2003; Jiang et al., 2001; Kawai et al., 2006; Lahiri & Forster, 2003; Lahiri et al., 2006; Lamanna, 2003; Nattie et al., 2002; Sugama et al., 1997). This leads to the question: What is the relationship between CO_2 and H^+? Gaseous CO_2 in the presence of the enzyme carbonic anhydrase is rapidly hydrated by water to form carbonic acid. Carbonic acid dissociates into a proton and bicarbonate ion. The rate limiting factor in this reaction is the enzyme carbonic anhydrase. This enzyme allows for the extremely rapid conversion of gaseous CO_2 to carbonic acid.

$$CO_2\,(g) + H_2O \overset{CA}{\rightleftarrows} H_2CO_3$$

$$H_2CO_3 \rightleftarrows HCO_3^- + H^+$$

Fig. G-2. Diagram showing the relationship between CO_2 and H^+.

Therefore, increases in CO_2 (hypercapnia) physiologically result in very rapid increases in hydrogen ions. The increase in hydrogen ions results in a decrease in pH (acidosis). Although pH is the accepted stimulus that elicits a ventilatory response, it is still possible that some central chemoreceptors can detect CO_2 directly. This possibility cannot be completely excluded although there is no evidence supporting this idea.

G-2. Inability to identify the central CO_2 chemoreceptor

Unfamiliarity with the research conducted in the field of central CO_2 chemoreception may lead someone to the conclusion that the field is long on problems and short on solutions. Although this conclusion would be false, it is justified due to the inability of many researchers over a long period of time to detect and characterize the central chemoreceptor which is the molecule responsible for detecting changes in CO_2 within the brainstem. Although researchers have been unable to find the long searched for chemoreceptor molecule, many breakthroughs and accomplishments have occurred over the last 50-60 years within this field. For example, one important finding involving central chemoreception over the past decade has been the role of the brainstem in CO_2 chemoreception (Coates et al., 1993; Feldman et al., 2003; Lamanna et al., 2003; Nattie, 2000;). The discovery that the brainstem is the area of the brain responsible for pH chemosensitivity is no longer controversial. However, although the location of the modulation of breathing in the brain is known (respiratory center in the brainstem), exactly how CO_2 and pH can be detected by this area to generate a pattern of breathing remains elusive and is an area of interest. With the knowledge of the brainstem's role in chemoreception researchers tried to detect specific cells in this region of the brain that are potential candidates for sensing changes in CO_2 and pH and coupling this sensing to a ventilatory response.

G-3. Various CO_2 chemosensitive nuclei within the brainstem

The search for chemosensitive neurons within the brainstem has led to the identification of many CO_2 chemosensitive nuclei within the brainstem. These

chemosensitive nuclei share several common features. For example, the level of C-fos (the gene that encodes the nuclear protein FOS) increases in these areas when challenged with CO_2 (Anton et al., 1991; Haxhiu et al., 1996; Ribas-Salgueiro et al., 2006; Sato et al., 1992). Also, individual neurons in these nuclei exhibit CO_2 chemosensitivity in vitro as measured by their firing activity (Dean et al., 1989; Dean et al., 1990; Guyenet et al., 2005a; Guyenet et al., 2005b; Li & Nattie, 2006; Richerson et al., 2005; Severson et al., 2003; Sugama et al., 1997). And, focal acidification of these chemosensitive nuclei stimulates breathing in vivo (Budzinska et al., 1985; Hodges et al., 2004a; Hodges et al., 2004b; Li & Nattie, 1997; Li et al, 2006; Nattie et al., 1991; Nattie & Li, 1994; Nattie & Li, 2002a; Nattie & Li, 2002b; Taylor et al., 2005; Wenninger et al., 2004). In addition to this, neurons in some chemosensitive nuclei have been shown to detect changes in intracellular CO_2 and pH resulting in changes in membrane excitability (Kawai et al., 2006; Lahiri & Forster, 2003; Nattie, et al., 2002; Sugama et al., 1997).

For much of the history of CCR it was believed that the central chemoreceptors were located on the ventral surface of the medulla in an area known as the ventral lateral medulla (VLM). The VLM is now believed to be the area where the central pattern generators for respiration are located (Solomon, 2003a; Solomon, 2003b; Wu et al, 2005; Guyenet et al., 2005). In addition to the VLM we now know that there are chemosensitive sites located throughout the brainstem. Such nuclei as the nucleus tractus solatarius (NTS), the retrotrapezoid nucleus (RTN), nucleus paragigantocellularis, midline raphé nuclei in the medulla and midbrain, ventral respiratory column, area postrema, nucleus ambiguous, etc, have all been demonstrated to be CO_2 chemosensitive nuclei (Dean et al.,

1989; Dean et al., 1990; Guyenet et al., 2005a, Guyenet et al., 2005b; Hodges et al., 2004a; Hodges et al., 2004b; Li & Nattie, 1997; Li et al., 2006; Miura et al., 1998; Nattie et al., 1991; Nattie et al., 1994; Nattie & Li, 2002). There are even CO_2 chemosensitive nuclei within the dorsal pons such as the locus coeruleus (LC) nucleus and the Kolliker Fuse nucleus (Li & Nattie, 2006; Mizusawa et al., 1995; Pineda & Aghajanian, 1997). All of these chemosensitive nuclei have been classified into three groups that are the ventral respiratory group (VRG), the dorsal respiratory group (DRG), and the pontine respiratory group (PRG) (Fig. 3). The identification of these multiple chemosensitive nuclei located throughout the brainstem has raised the question; why are there so many CO_2 chemosensitive sites within the brainstem? One potential explanation is perhaps these chemosensitive sites are communicating with each other allowing for fine tuning of the respiratory system. Or, maybe these various sites allow for integration between the respiratory system and other neuronal systems. These multiple CO_2 chemosensitive sites may be involved in the control of breathing, cardiovascular regulation, and other sympathetic functions such as hypercapnia-induced arousal, anxiety and aggression. The exact reason there are so many chemosensitive sites within the brainstem is not known. However, all of these CO_2 chemosensitive nuclei appear to be important for the whole body response to changes in CO_2 as ablation of these sites individually results in impaired respiration in animals.

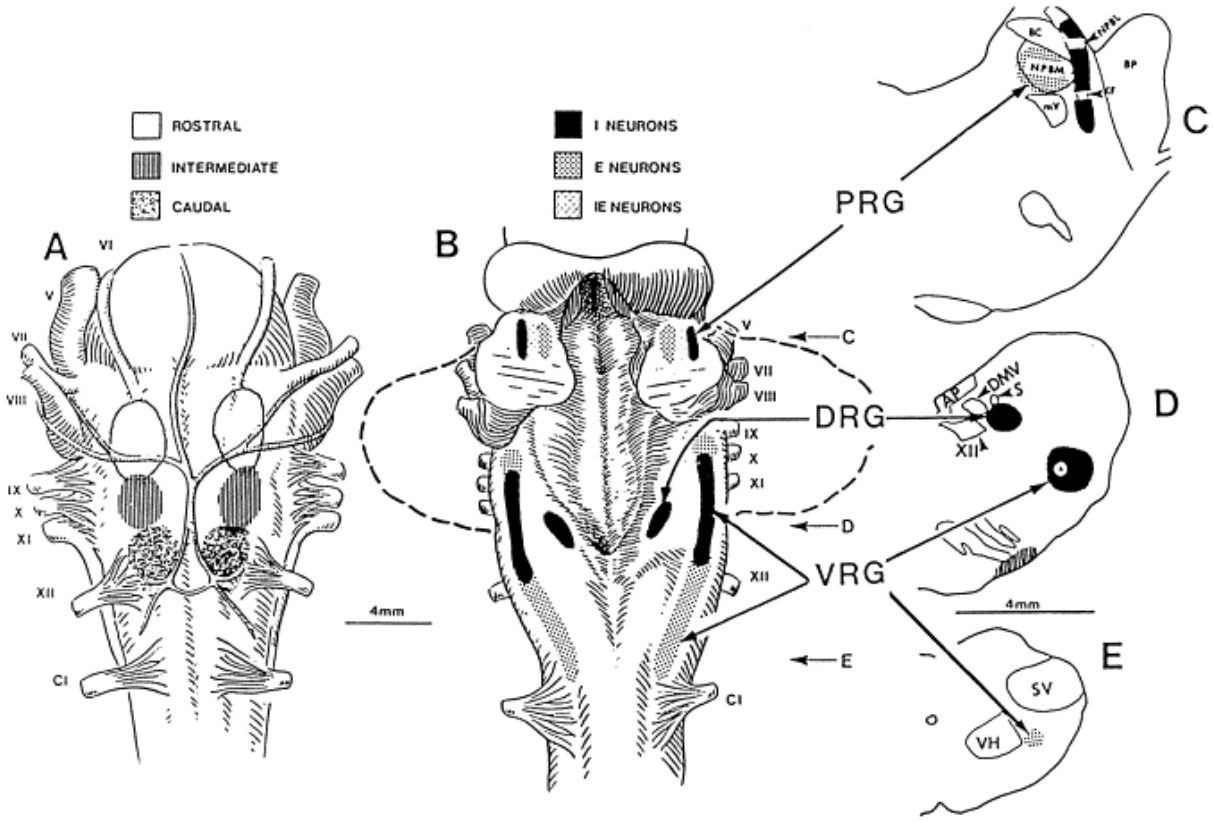

Fig. G-3. Brainstem anatomy demonstrating the location of the various respiratory groups. *A*. Ventral view of the brainstem. *B*. Dorsal view of the brainstem. *C*, *D*, *E*. Representative transverse sections taken at different locations of the respiratory groups. PRG=pontine respiratory group, DRG=dorsal respiratory group (medulla), VRG=ventral respiratory group (medulla). (Nattie, 1999)

G-4. The involvement of neurotransmitter systems in central CO_2 chemoreception

Recently, the importance of neurotransmitter systems in central CO_2 chemoreception has been under intense investigation. One reason for this is that there must be amplification of the stimulus during central CO_2 chemoreception. There is a

significant discrepancy in central CO_2 chemoreception. This discrepancy stems from results obtained from experiments conducted in vitro versus those that were conducted in vivo. Based on the results from in vivo experiments none of the potential chemoreceptor candidates studied thus far demonstrates a CO_2/pH sensitivity that is required of a central CO_2 chemoreceptor molecule in vivo. The central CO_2 chemoreceptor molecule should possess the capability to detect very minute changes in CO_2. A change in pCO_2 as low 1mm Hg is sufficient enough to produce a 20-30% change in ventilation (Nattie, 1999; Putnam et al., 2004). No molecule identified to date demonstrates such sensitivity to CO_2/pH. Therefore, perhaps there is amplification of the signal in central CO_2 chemoreception. The involvement of neurotransmitter systems in this process may allow for amplification of the signal. Indeed, several neurotransmitters have been shown to be important for respiratory control. Different approaches have been used to demonstrate the importance of neurotransmitters in the control of respiration. The neurotransmitters substance P (SP), serotonin (5-HT), thyrotropin releasing hormone (TRH), GABA, and glutamate have all been shown to be important for respiratory control (Bonham, 1995; Chen et al., 1990; Nattie & Li, 2002; Nink et al., 1991a; Nink et al., 1991b; Severson et al., 2003; Taylor et al., 2005; Vonhof et al., 1991). Site-specific injections of these neurotransmitters in chemosensitive nuclei potently augment or suppress ventilation frequency (Chen et al., 1990; Li et al., 2006; Messier et al., 2002; Nink et al., 1991a; Nink et al., 1991b). Researchers have also site-specifically killed neurons containing receptors for some of these neurotransmitters and assayed to determine whether the animal's ventilatory response to CO_2 was the same or compromised (Hodges et al., 2004;

Nattie et al., 1991; Nattie & Li, 1994; Nattie & Li, 2002). Site specific lesions of neurons containing the neurokinin-1 receptor (NK1R), the natural receptor for SP, using a saporin-SP conjugate (SAP-SP) compromised the ventilatory response in rats challenged with CO_2 (Hodges et al., 2004; Nattie & Li, 2002; Wenninger et al., 2004). In these experiments SP guides the toxin saporin to neurokinin receptor positive neurons. Once substance P binds to the receptor the SAP-SP is internalized and the toxin kills the neurons. The technique has been shown to be very effective for site-specific lesioning of nuclei within the brainstem. Experiments have also been carried out to show the importance of neurons that produce the neurotransmitter serotonin in central CO_2 chemoreception (Hodges et al., 2004; Richerson et al., 2005; Severson et al., 2003; Taylor et al., 2005). The finding that neurotransmitters such as serotonin, substance-P and thyrotropin releasing hormone are involved in and are critical for the control of respiration suggests that they may play a role in the amplification of the CO_2/pH signal. This idea is further strengthened by the demonstration that the receptors for the neurotransmitters, SP, 5-HT, and TRH are G-protein coupled receptors (GPCR). Ligand binding to these receptors activates a guanine nucleotide binding protein (G-protein) which in turn leads to the activation of multiple second messenger cascades. One such activation cascade involves activation of phospholipase-C β that cleaves phosphatidylinositol bisphosphate (PIP_2) into inositol triphosphate (IP3) and diacylglycerol (DAG). The PIP_2 derivative, DAG, activates protein kinase C (PKC) and IP3 increases intracellular calcium which is also often necessary for PKC activation. The G-protein involved in this activation cascade is $G_{\alpha q}$. Interestingly, there are receptor

subtypes for SP, 5-HT, and TRH that are coupled to $G_{\alpha q}$. This $G_{\alpha q}$ signaling cascade may lead to the amplification of the signal as many intracellular messengers are activated following ligand binding to $G_{\alpha q}$ coupled receptors.

G-5. Potential chemoreceptor candidates

According to Jiang et al., 2001 there are at least four requirements for a molecule to be considered a possible central CO_2 chemoreceptor. Based on experimental observations the central CO_2 chemoreceptor molecule should: 1) be highly sensitive to CO_2/pH changes within the physiological range; 2) it should be able to detect CO_2/pH changes in both acidic and alkaline (hypercapnic or hypocapnic) directions; 3) it should be able to couple the variation in CO_2/pH to a change in neuronal membrane excitability (depolarization or hyperpolarization); and 4) it should be expressed in CO_2 chemosensitive sites within the brainstem. Of these four requirements the last one is arguably the most important for limiting the number of potential chemoreceptor candidates. However, based on the criteria above a number of molecules can be considered possible CO_2 chemoreceptors. Amongst the different membrane proteins ion channels receive the most consideration as central CO_2 chemoreceptors because, ion channels posess qualities necessary for central CO_2 chemoreception that are lacking in other membrane proteins, such as an ability to rapidly change cellular excitability. The list of ion channels considered potential chemoreceptor molecules include inward rectifier K^+ (Kir) channels, twik-related acid-sensitive K^+ (TASK) channels, gap junction channels, voltage activated K^+ channels, and several non-selective cation channels such as cyclic nucleotide gated (CNG) channels and transient receptor potential (TRP)

channels. Some of these channel families contain several potential candidates, making this list very long. None of the ion channels studied thus far have been shown to be the central CO_2 chemoreceptor. These channels however are all still candidates for different reasons. For example, some ion channels such as TASK channels are sensitive to CO_2/pH, but these channels are expressed abundantly throughout the brain suggesting a more universal role in neuronal functional than a specific role in central CO_2 chemoreception. The finding that a large number of ion channels can detect CO_2/pH has raised the question: Why are there so many potential CO_2/pH sensing molecules? Perhaps, there is more that one central CO_2 chemoreceptor molecule and potentially they work together to detect changes in CO_2. Indeed, we know that in addition to the requirement for high CO_2 sensitivity discussed in the previous section, the central chemoreceptor molecule should be able to detect a wide range of CO_2 changes. In humans the partial pressure of CO_2 (P_{CO2}) can range from ~40 mmHg to ~80 mmHg. To date no known molecule possess the ability to cover such a wide range of CO_2 changes. The use of multiple molecules to detect a wide range of stimuli can be found in other homeostatic systems. For example, temperature sensing and transduction has been shown to be carried out by multiple molecules many of which are transient receptor potential channels (Caterina et al., 1999; Jiang et al., 2005; Story et al., 2003; Watanabe et al., 2002; Xu et al, 2002). Perhaps, central CO_2 chemoreception has adopted a similar mechanism. This idea is becoming more and more popular with researchers in the field of central CO_2 chemoreception.

G-6. Kir channels as potential chemoreceptor molecules

Inward rectifier K^+ channels are key players in the maintenance of membrane excitability and the control of intracellular as well as extracellular K^+ homeostasis (Baukrowitz et al., 1999; Jan & Jan, 1997; Nichols & Lopatin, 1997; Oliver et al., 2000; Reimann & Ashcroft, 1999). In addition to satisfying criteria necessary for a central CO_2 chemoreceptor, the Kir channels demonstrate an additional characteristic that makes them strong candidates as sensing molecules, which is their involvement in setting the resting membrane potential (Baukrowitz et al., 1999; Nichols & Lopatin, 1997; Oliver et al., 2000). This characteristic allows these channels to directly alter cellular excitability. Unlike other K^+ channels, Kir channels conduct inward currents more readily than outward currents through a process known as "rectification". The property of inward rectification makes these Kir channels unique potassium channels (Fig. 4A). The K^+ channel family is one of the largest ion channel family. Within this super-family there are several sub-families. Currently, there are more than 70 cloned mammalian K^+ channels. Amongst the numerous K^+ channel sub-families the Kir channel family is the largest, containing the most members. In the Kir channel family there are seven sub-families, i.e., Kir1 (ROMK), Kir2 (IRK), Kir3 (GIRK), Kir4, Kir5, Kir6 and Kir7 (Fig. 4B). Totally, there are more than 15 functional Kir channels.

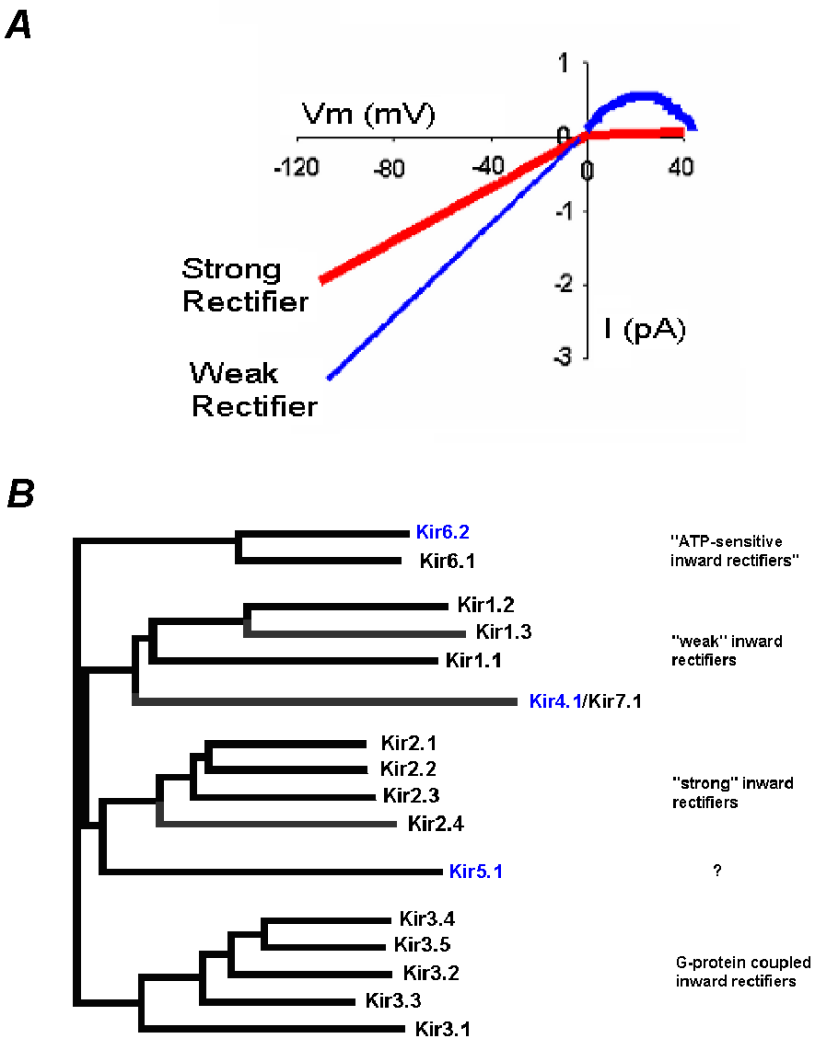

Fig. G-4. Diagram showing rectification in Kir channels and the Kir channel family tree. *A.* Current-voltage relationship observed in Kir channels. These are representative currents recorded from Kir channels in a high extracellular potassium environment. The red trace represents currents from a strong rectifier and the blue represents currents from a weak rectifier. Note that at positive membrane voltages the current changes direction (rectification). *B.* Phyllogenetic tree of Kir channels. The channels highlighted in blue are the channels discussed in this thesis. (Nichols & Lopatin, 1997)

Kir channels have a unique architecture. Each channel is composed of four subunits arranged in a tetrameric fashion (Fig. 5A, B). Each subunit is composed of two transmembrane spanning domains (TMD1, TMD2) that are joined by a pore loop and selectivity filter (H5) with intracellular N and C termini (Fig. 5C). The H5 (pore) contains a "TIGYG" motif that determines the selectivity for K^+. The N-termini in Kir channels are shorter (consisting of ~80 residues) than the C-termini (consisting of ~200 residues). Both termini have been shown to contain ligand binding and gating sites.

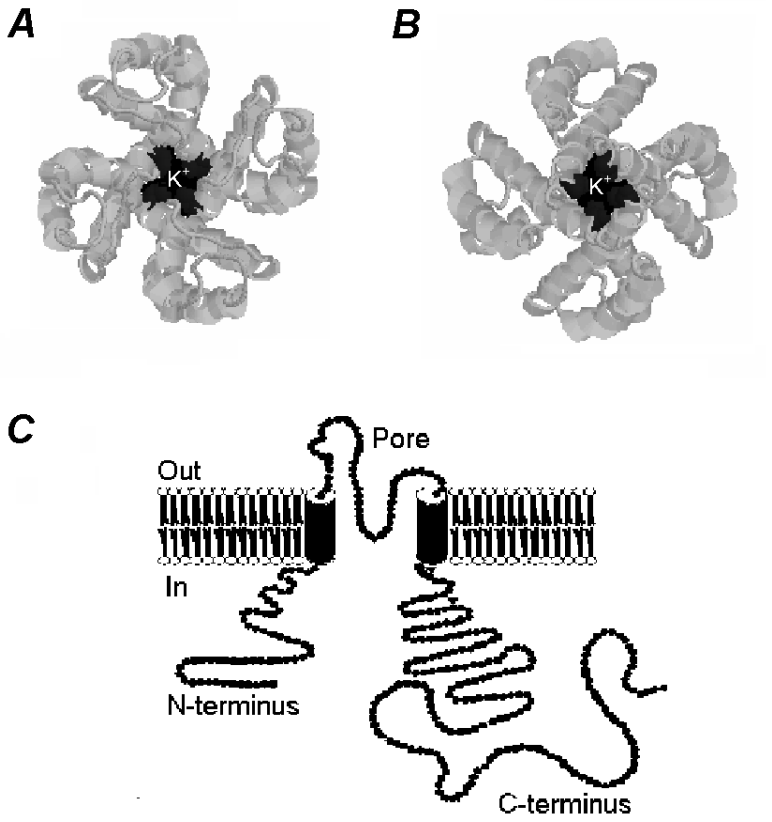

Fig. G-5. Kir channel structure. *A*, *B*. Structural representation of a typical Kir channel viewing from outside-in and from inside-out, respectively in a tetrameric arrangement. *C*. Diagram showing the architecture of one Kir channel subunit cross-sectioned through the plasma membrane. (Doyle et al., 1998)

Kir channels are functional in a number of specialized tissues such as the heart, brain, pancreas, skeletal muscle, testis, and kidney (Cuevas et al., 1991; Doi et al., 1996; Donley et al., 2005; Doring et al., 1998; Haller et al., 2001; Jiang et al., 2001; Karschin et al., 1998; Karschin & Karschin, 1997; Karschin et al., 1997; Lagrutta et al., 1996; Quayle et al., 1997; Salvatore et al., 1999; Vivaudou & Forestier, 1995; Wu et al., 2004). Although some Kir channels such as the Kir6.2 can be found in a variety of tissues, others such as the Kir1.1 and Kir7.1 are more localized to specific areas. The various Kir channels are regulated by a number of intracellular ligands such as ATP, PIP_2, proton, G-proteins, etc (Baukrowitz et al., 1999; Baukrowitz & Fakler, 2000; Cui et al., 2001; Doi et al., 1996; Jan & Jan, 1997; Matsuo et al., 2005; Nichols & Lopatin, 1997; Oliver et al., 2000; Quayle et al., 1997; Reimann & Ashcroft, 1999; Takano & Kuratomi, 2003). The ligand modulation of each Kir channel is specific for that channel. For example, only the Kir6 channels are sensitive to intracellular ATP. This property allows these Kir6x channels to couple the cellular metabolism to cellular excitability. The Kir6 family members are also the only Kir channels that associate with the sulphonylurea receptor (SUR) to form fully functional channels that are sensitive to ATP and ADP (Baukrowitz & Fakler 2000; Karschin et al., 1998; Karschin et al., 1997; Matsuo et al., 2005; Mikhailov et al., 2000; Moreau et al., 2005). Together the Kir6 and the SUR families form the K_{ATP} channel whose arrangement is based on a tetrameric structure with a 1:1 ratio of Kir to SUR. In the K_{ATP} channels the Kir6 subunits forms the center of the channel (pore) and the SUR subunits are regulatory subunits that surround the Kir6 subunits.

In addition to the homomeric channels, there are also several heteromeric Kir channels that exist as well. The heteromeric combinations increase the number of members in the Kir channel sub-family. One such interesting heteromeric channel is the Kir4.1-Kir5.1 channel. This channel is a unique Kir channel for several reasons. The Kir4.1-Kir5.1 channel is formed by the heteromultimerization of two inter-subfamily members (Kir4.1 and Kir5.1). In this channel there are two Kir4.1 subunits and two Kir5.1 subunits arranged in a "trans" configuration. The heteromultimerization of different proteins typically generates a new protein with unique properties and a specialized function. Indeed, this has been found to be the case for the Kir4.1-Kir5.1 channel. Although the Kir4.1 channel functions homomerically and exist in nature, its properties are very different than those of the heteromeric Kir4.1-Kir5.1. On the other hand, the Kir5.1 channel is the only Kir channel cloned with no identified homomeric function. The Kir5.1 is believed to only exist as a heteromer with members in the Kir4 sub-family. This is puzzling to researchers because as previously mentioned the Kir4.1-Kir5.1 heteromer has several different characteristics than the Kir4.1 suggesting that two Kir5.1 subunits are enough to function, however, four is not. This has led to intense investigation into the function of the Kir5.1 protein. Many researchers have tried to express this protein in vitro using heterologous systems. Unfortunately, detectable Kir currents are never identified although protein expression experiments show the presence of the Kir5.1 protein in the cells. Therefore, it is currently believed that this channel can only function as a heteromer with Kir4.1 or Kir4.2.

The heteromeric interaction of Kir4.1 and Kir5.1 produces a channel with distinct properties. The Kir4.1-Kir5.1 channel has increased pH sensitivity with a pKa at 7.35 (Yang et al., 2000). The channel also has distinct biophysical properties such as conductance, P_{open}, sensitivity to barium, and activation kinetics (Yang et al., 2000). The Kir4.1-Kir5.1 is considered a strong candidate sensing molecule for central CO_2 chemoreception because of its ability to satisfy the requirements of a central CO_2 chemoreceptor in addition to its fine tuned pH sensitivity (Cui et al., 2001; Xu et al., 2000; Yang et al., 2000). This channel is able to detect both hypocapnia and hypercapnia and couple this sensing to a change in membrane excitability (Cui et al., 2001). The role of the Kir4.1-Kir5.1 in central CO_2 chemoreception may be to detect changes in CO_2/pH and change the firing rate of respiratory neurons via membrane excitability. An increase in the firing rate of respiratory neurons from baseline is generated by a depolarization that causes the neurons to fire more action potentials, whereas a decrease in the firing rate of respiratory neurons is typically generated by hyperpolarization that can cause neurons to become silent firing fewer action potentials. Figure 6 show that the Kir4.1-Kir5.1 channel has a sigmoid response to pHi with a pKa at 7.35. This allows the channel to detect both acidic and alkaline pH levels with acidic pH levels inhibiting the channel and alkaline pH levels stimulating the channel, as such, the channel may be involved in both the augmentation and supression in the firing rate of respiratory neurons. Inhibition of the Kir4.1-Kir5.1 channel by slight acidosis may lead to augmentation of the firing frequency whereas stimulation of the channel by slight alkalization may lead to reduction of the firing frequency of respiratory neurons. Although previous in vitro studies with the

Kir4.1-Kir5.1 demonstrated its potential as a CO_2 chemoreceptor molecule, it's identity as a central CO_2 chemoreceptor molecule remains to be proven. This is mostly due to the lack of information regarding the expression level of this channel in the chemosensitive sites within the brainstem. Evidence for the expression of the heteromeric Kir4.1-Kir5.1 channel in brainstem neurons will strengthen its candidacy as a chemoreceptor molecule. However, a clear demonstration of the role played by this channel in central CO_2 chemoreception is necessary for the identification of this channel as one of the long searched for chemoreceptor molecules.

The Kir6.2 channel expressed with the SUR1 receptor has been shown to be expressed in several tissues including the brain. This KATP channel has been shown to be present in brainstem neurons at mRNA and protein levels (Haller et al., 2001; Karschin et al., 1998; Karschin et al., 1997). These important findings suggest that this channel may function in these neurons as the level of expression is not low. Several reports have suggested that during the process of central CO_2 chemoreception intracellular ATP levels decrease and appear to regulate an ATP sensitive K^+ channel (Gourine et al., 2003; Gourine, 2005; Haller et al., 2001). The level of intracellular ATP is critical for the regulation of the Kir6.2/SUR1 channel. An increase in intracellular ATP inhibits this channel whereas a decrease in ATP stimulates the channel activity. This channel contains ATP binding sites in the Kir6.2 and ATP/ADP binding sites in the SUR1 subunits. In the Kir6.2 the ATP binding sites are located in the N and C-termini where they form a three dimensional pocket for the binding of ATP (Cukras et al., 2002; Drain et al., 1998; Wu et al., 2002). Experiments performed on the Kir6.2 channel (in the

absence of the SUR1) demonstrated that the Kir6.2 channel is inhibited by high concentrations of ATP whereas the SUR1 is regulated by ATP and ADP.

Unlike the other Kir channels the Kir6.2 channel is activated by intracellular acidosis. When the channel current is plotted as a function of intracellular pH the channel shows a bell shaped response curve to acidosis (Fig. 6). Slight acidification activates the channel whereas strong acidification leads to channel inhibition. Alkalization also inhibits this channel. Independent of changes in intracellular ATP, acidification of a respiratory neuron may activate the Kir6.2 channel leading to a hyperpolarization of the cell. Although depolarization is seen in many chemosensitive neurons in response to acidosis, hyperpolarization of an inhibitory presynaptic motor neuron may release this neuron's inhibition and allow firing of the postsynaptic cell. However, when considering the function of the K_{ATP} channel the regulation by ATP has to be considered as ATP is a major modulator of the channel. In the situation where there is a change in intracellular ATP during acidosis, the pH sensitivity of the channel may be changed. Indeed, it has been shown that ATP and H^+ have allosteric effects on the Kir6.2/SUR1 channel. This characteristic gives this channel an advantage over other potential central CO_2 chemoreceptor molecules as the concentrations of ATP and H^+ that change during central CO_2 chemoreception may convert on the same molecule. However, the identification of this Kir6.2/SUR1 channel as a chemoreceptor molecule remains to be proven. Therefore, a clear demonstration of the role played by this channel is also necessary for the identification of this channel as one of the long searched chemoreceptor molecules.

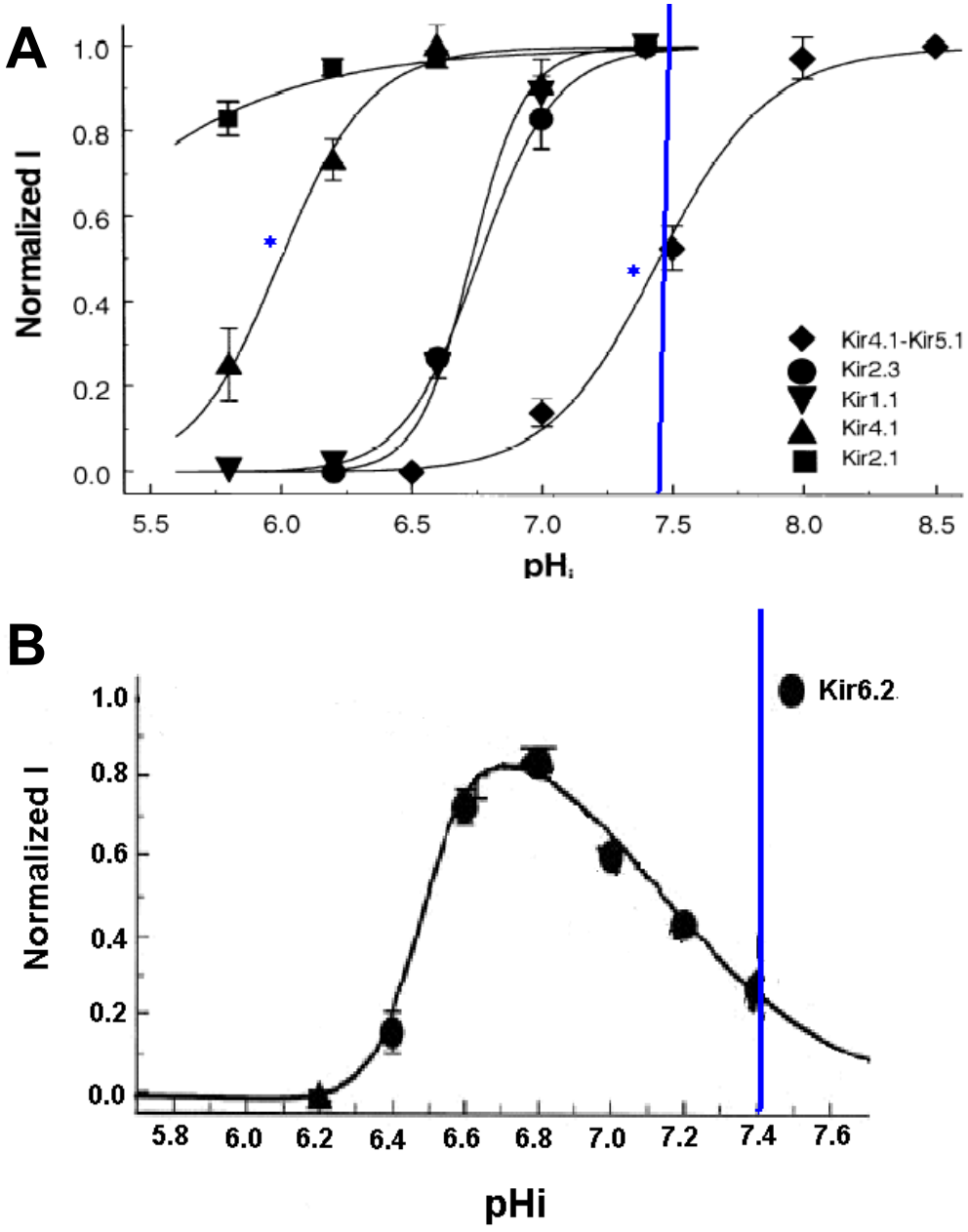

Fig. G-6. pH sensitivity of the various Kir channels. *A.* The channel current (I) is plotted as a function of intracellular pH. Most Kir channels are inhibited by intracellular acidosis. *B.* The Kir6.2 channel shows a bi-phasic response to intracellular acidification. The asterisks show the shift in the pH sensitivity of the Kir4.1 versus the Kir4.1-Kir5.1 channel. The blue bar represents an intracellular pH of 7.4 that is close to neutral. (Jiang et al., 2001; Xu et al., 2001)

G-7. The molecular basis for CO_2/pH sensing

The ability to detect pH is carried out by the titration of amino acids in the primary sequence of the proteins. There are only a few amino acids that are titratable (i.e. histidine, lysine, apartate, etc). Among the titratable amino acids only histidine is titratable at or near physiological levels. Although lysine has been demonstrated as a titratable residue in some pH sensing proteins, the titration of histidine appears to be much more common. The detection of elevated levels of protons resulting in the titration of amino acids is not sufficient for central CO_2 chemoreception. As discussed earlier, the central CO_2 chemoreceptor molecule has to have the ability to change cellular excitability. Therefore, following titration of the amino acid histidine, there has to be a coupling between the sensing and the effect. In ion channels this is done through a mechanism called "channel gating".

Gating refers to the opening and closure of ion channels. The mechanism for channel gating is poorly understood. The gating mechanism of a channel would allow for or reduce the flow of ions through the channel resulting in a change in cellular excitability. Ligand binding in ion channels leads to a change in the gating conformation of the channel through a "binding-gating" coupling mechanism. Therefore, the demonstration of the gating mechanism of a potential chemoreceptor candidate channel may lead to an understanding of the role played by this channel in central CO_2 chemoreception and how this molecule may lead to a change in cellular excitability.

Clearly, in order to demonstrate that a molecule is a central CO_2 chemoreceptor, experiments should be performed indicating that the whole body response to changes in

CO_2/pH is compromised in the absence of this molecule and is restored in its presence. This is usually done by the genetic manipulation of the gene of interest. However, before experiments can be performed involving genetic manipulations of a gene, there should be a clear demonstration of the basic properties of the gene product. In this way the removal of the gene and its by-product can be analyzed thoroughly. Therefore, the identification of Kir channels in chemosensitive brainstem neurons in addition to a demonstration of the modulation by neurotransmitters and CO_2 combined with an identification of the channel gating mechanism may correlate a particular protein such as a Kir channel with central CO_2 chemoreception and help to solidify the identification of the long sought after CO_2 chemoreceptor molecule.

H. SIGNIFICANCE

H-1. The problem and its clinical relevance

Since the early 1960's there have been tremendous efforts placed on identification of central CO_2 chemoreceptors. The widespread interests can be attributed to several medical complications associated with CO_2 detection. The ability to sense and regulate CO_2/pH has been found to be linked to diseases such as sleep apnea as well as sudden infant death syndrome (SIDS). Another specific disease that is caused by the central chemoreceptors inability to sense changes in CO_2 is Central Congenital Hypoventilation Syndrome (CCHS). CCHS is a human condition recognized within the first year of life in which central chemoreceptors are absent or malfunctional. These children breathe normally during the day. The problem arises at night when they are asleep. In order to survive during the night some sort of ventilation support is needed. Although there is a change in the response to hypoxia, the most dramatic and consistent abnormalities are the result of the loss of CO_2 chemosensitivity. There is a high incidence of death amongst children diagnosed with CCHS. In the normal population the increased respiratory drive response to the build up of CO_2 during a stoppage of ventilation of blockage of the lung airways is still poorly understood. The molecular mechanism for the detection of CO_2/pH under normal and pathophysiological conditions remains elusive. Therefore it is imperative to understand the molecular basis of central CO_2 chemoreception.

H-2. Why study the Kir4.1-Kir5.1 and Kir6.2+SUR1 channels?

While several Kir channels are recognized as potential chemoreceptors, the Kir4.1-Kir5.1 and Kir6.2+SUR1 channels are arguably the strongest candidates for central chemoreception. The Kir4.1-Kir5.1 is probably the strongest candidate amongst the Kir channels. This is mostly attributed to the fact that the Kir4.1-Kir5.1 channel satisfies the criteria required for a central CO_2 chemoreceptor molecule. The Kir4.1-Kir5.1, unlike any other Kir channels, has a pKa at 7.35 that allows it to detect both alkaline and acidic pH levels within the physiological range (Cui et al., 2001; Yang et al., 2000). This property is a result of the heteromultimerization of these two Kir channel subfamily members (Kir4.1, Kir5.1). However, the candidacy of the Kir4.1-Kir5.1 channel is weakened by the lack of information regarding its expression in chemosensitive brainstem nuclei. A demonstration of neuronal brainstem expression of the heteromeric Kir4.1-Kir5.1 channel may solidify a role of this channel in central CO_2 chemoreception.

Most of the focus placed on Kir6.2+SUR1 has been to understand its role in insulin secretion. However, immunocytochemistry and in situ hybridization studies have revealed high levels of expression of Kir6.2 and SUR1 in the brainstem (Haller et al., 2001; Karschin et al., 1998; Karschin et al., 1997). In addition to its expression in the brainstem, it is suggested that during the process of central CO_2 chemoreception intracellular ATP levels change and this change may regulate an ATP sensitive potassium channel (Gourine et al., 2003; Gourine, 2005).

Since both the Kir4.1-Kir5.1 and the Kir6.2+SUR1 channels are strong CO_2/pH chemoreceptor candidates, a clear demonstration of their function may answer questions lurking in the field of central CO_2 chemoreception and respiratory control. Although genetic manipulation will eventually solidify these channels as CO_2 chemoreceptors, prior experiments are necessary to strengthen their candidacy. In this thesis, a series of experiments was proposed to elucidate the role played by Kir channels (Kir4.1-Kir5.1, Kir6.2/SUR1) in central CO_2 chemoreception using a combined electrophysiological and molecular biological approach.

I. MATERIALS AND METHODS

I-1. *Xenopus* Oocyte Preparation and Injection

All experimental procedures were carried out in accordance with the Guidelines for the Care and Use of Laboratory Animals by the NIH and the Animal Welfare Assurance of Georgia State University (#A97008). Oocytes from female *Xenopus* laevis frogs (Xenopus One, Inc, Dexter, MI) were used in the present studies. Frogs were anesthetized by bathing them in 0.3% 3-aminobenzoic acid ethyl ester. After a few lobes of ovaries were removed through a small abdominal incision (~5 mm), the frog was allowed to recover from the anesthesia. The *Xenopus* oocytes were treated with 1 mg/ml of collagenase (Type IA, Sigma Chemicals, St. Louis, MO) in the OR2 solution containing (in mM): NaCl 82, KCl 2, $MgCl_2$ 1 and HEPES 5 (pH 7.4) for 60 min at room temperature. After five washes (10 min each) of the oocytes with the OR2 solution, cDNAs (25–50 ng or 5-10 femtomoles in 50 nl DD water) were injected into the oocytes. The oocytes were then incubated at 18 °C in the ND-96 solution containing (in mM): NaCl 96, KCl 2, $MgCl_2$ 1, $CaCl_2$ 1.8, HEPES 5, and sodium pyruvate 2.5 with 100 mg/l G418 sulfate (Medlatech, INC, Herndon, VA) and 50 mg/l tetracycline (Sigma Chemicals) added (pH 7.4).

I-2. Molecular Biology

Standard molecular biology techniques were used including site-directed mutagenesis, polymerase chain reaction (PCR), gene expression, and DNA sequencing. Rat Kir4.1 cDNA (GenBank #X83585) and rat Kir5.1 cDNA (GenBank #AF249676) are gifts from Dr. John Adelman at Oregon Health and Science University, Portland, OR. For

co-expression of Kir4.1 and Kir5.1, a tandem dimer of these two cDNAs was constructed using the overlapping extension technique, in which full length Kir4.1 and Kir5.1 sequences were obtained using *Pfu* DNA polymerase (Stratagene, La Jolla, CA) chain reaction (PCR). The PCR products were joined to each other at the 3' end of Kir4.1 and 5' end of Kir5.1. Mouse Kir6.2 (GenBank #D50581) was generously provided by Dr. S. Seino at Kobe University Graduate School of Medicine, Kobe, Japan. The Kir6.2 with a truncation of 36 AAs at the C-terminus end (Kir6.2ΔC36) expresses functional currents without the SUR subunit and retains ATP and pH sensitivities (Tucker et al., 1997; Xu et al., 2001). Rat Kir1.1 (GenBank #X72341) (from Dr. Steven Hebert, Yale University) and Mouse Kir2.1 (GenBank #X73052) (from Dr. Lily Jan, University of California at San Francisco) were also used in the present studies. Hamster SUR1 (GenBank#L40623) was a gift from Dr. L. Bryan at Baylor College of Medicine, Houston, TX. All of the above mentioned cDNAs were sub-cloned into the eukaryotic expression vector pcDNA3.1 (Invitrogen, Carlsbad, CA) and used for *Xenopus* oocyte expression without cRNA synthesis.

Rat neurokinin-1 receptor (NK1R) cDNA (Genbank #J05097) was generously provided by Dr. Shigetada Nakanishi at Kyoto University Faculty of medicine, Kyoto, Japan. Rat serotonin 2A receptor (5-HT2A) cDNA (Genbank #M30705) was generously provided by Dr. David Julius at the University of California at San Francisco, San Francisco, CA. Mouse thyrotropin-releasing hormone receptors R1 (mTRH-R1) (Genbank #M59811) and R2 (mTRH-R2) (Genbank #NM_133202) were generously provided by Dr. Marvin Gershengorn at the National Institutes of Health, Bethesda, MD.

Rat mu-opioid receptor cDNA (MOR) (Genbank #L22455) was generously provided by Dr. Stanley Watson at the University of Michigan, Ann Arbor, MI. All receptor cDNAs were sub-cloned into the eukaryotic expression vector pcDNA3.1 (Invitrogen, Carlsbad, CA) and used for *Xenopus* oocyte expression without cRNA synthesis.

Dynamin II (aa) wild-type and Dynamin II (aa) K44A are gifts from Dr. Mark McNiven at the Mayo Clinic. These two cDNAs were subcloned into the eukaryotic expression vector pEGFP-N1 creating an N-terminal GFP-Dynamin fusion and used directly for expression in *Xenopus* oocytes.

Site-specific mutations were made using a pfu DNA polymerase-based site-directed mutagenesis kit (Quickchange, Stratagene, La Jolla, CA). Orientation of the correct mutations and constructions were confirmed with DNA sequencing.

I-3. Expression and purification of MBP and C-terminal-MBP fusion proteins

The membrane and C-terminal cytoplasmic junction for the Kir4.1 (GenBank #X83585) and Kir5.1 (GenBank #X83581) was determined by ScanProsite. The C-terminal fragments were amplified by PCR and inserted into the pMALc2x vector (New England Biolabs) using EcoRI and XbaI. The PCR fragments contained these restriction enzyme sites as well as a stop codon to terminate transcription after the C-terminus. To express the maltose binding protein (MBP) alone a stop codon was introduced to prevent expression of part of the *LacZ* gene present in the pMALc2x vector. Correct constructions were confirmed with DNA sequencing.

Expression and purification of the fusion proteins were carried out in *Eschericia coli* BL21 competent cells. The cells were grown overnight at 37 ºC. The next morning the cultures were diluted in LB broth medium and grown to an A_{600} ~1 at 37 ºC. Protein induction was achieved by the addition of 1 mM isopropylthiogalactoside (IPTG) to the cultures which were then incubated at 25 ºC for 2 hours. The cells were harvested by centrifugation (4,000 x g, 15 min, 4 ºC). The bacterial pellet was washed with STE (150 mM NaCl; 10 mM Tris, pH 8.0; 1 mM EDTA) plus protease inhibitors (EDTA-free) (Roche Molecular Biochemicals) once and then resuspended in the same buffer. The cell membranes were lysed by the addition of lysozyme (100 µg/ml) added immediately following resuspension. The samples were incubated on ice for 15 min. Dithiothreitol (DTT) (5 mM) was added to the samples and the cell membranes were further lysed by sonication (4 x 20 s) followed by centrifugation (4,000 x g, 15 min, 4 ºC). The resulting supernatant was collected and Triton X-100 was added to a final concentration of 1%. The supernatant was then loaded onto amylose resin (New England Biolabs) pre-equilibrated with protein elution buffer (PEB) (50 mM Tris, pH 8.0; 1 mM EDTA) and incubated on ice for 45 minutes. The amylose resin was centrifuged and the supernatant was discarded. The resin was washed 7 times with 2 volumes of PEB. Elution of the maltose binding protein (MBP) and MBP fusion proteins was achieved by incubating the amylose resin with 1 volume of PEB containing 10 mM maltose. All fractions containing the fusion proteins were pooled and concentrated using centricon YM-10 centrifugal units (Millipore, Bedford, MA). Protein purity was determined by sodium dodecyl sulfate-polyacrylamide gel electrophoresis (SDS-PAGE) (10%) and subsequent

coomassie blue staining. The protein concentration was determined using a UV spectrophotometer at A_{280}.

I-4. In vitro kinase assay

One μg of purified proteins (Kir4.1-C-terminus-MBP, Kir5.1-C-terminus-MBP, MBP, Histone III-S) was added to a reaction mixture consisting of the catalytically active PKC subunit (20 ng) (BioMol, Plymouth Meeting, PA) 10 μCi of ^{32}P-γ-ATP (Perkin Elmer, Waltham, MA), Magnesium/ATP cocktail (75 mM $MgCl_2$ and 500 μM ATP in 20 mM MOPS, pH 7.2, 25 mM β-glycerol phosphate, 5 mM EGTA, 1 mM sodium orthovanadate and 1 mM dithiothreitol) and 5x reaction buffer (containing: 125 mM Tris-HCl, pH 7.5 and 0.1 mM EGTA) in a total volume of 25 μl. The samples were incubated at 30 ºC for 1 hour and 5x loading buffer was added to stop the reaction. The samples were then analyzed by running a symmetric 10% SDS-PAGE gel. The gel was cut down the middle and one half was stained with Coomassie brilliant blue solution and destained and the other half was dried and subjected to autoradiography. The autoradiograph was taken using the Fujifilm BAS 2500 phosphor imager and analyzed with the Multigauge software.

I-5. Transfection of HEK293 Cells

Human Embryonic Kidney cells (HEK293, CRL-1573, Batch #2187595, ATCC, Rockville, MD) were chosen to express the Kir4.1-Kir5.1, Kir1.1, and Kir2.1 channels. HEK293 Cells were cultured as a monolayer in MEM-E medium with 10% fetal bovine serum and penicillin/streptomycin added. The cells were incubated at 37 °C in the presence of 5% atmospheric CO_2 and split twice weekly.

The cells were transfected using Lipofectamine^{2000} (Invitrogen, Carlsbad, CA) with 5 μg wild-type Kir cDNA per petri dish (35 mm). To facilitate the identification of positively transfected cells, 0.5 μg of green fluorescent protein (GFP) cDNA (pEGFP-N2, Clontech, Palo Alto, CA) was added to the cDNA mixture. Cells were disassociated from the monolayer using 0.01% trypsin 24 hours post-transfection. A few drops of the cell suspension were added to a new petri dish. The cells were then incubated at 37 °C for 48 hrs before experiments.

I-6. Primary culture of brainstem neurons

The medulla oblongata and pons of fetal (P16-20) sprague dawley rat embryos were surgically removed and rapidly placed in ice cold Earle's Balanced Salt Solution (EBSS). The tissue was dissociated by treatment using a papain preparation kit (Worthington, Lakewood, NJ). The neurons were then plated on a polyethyleneimine, polyornithine, and laminin coated MEA dish which has 64 planar microelectrodes (ALA Scientific, Westbury, NY) containing dulbecco's modified minimum essential medium (Invitrogen-Gibco, Carlsbad, CA), with 5% horse serum (Invitrogen-Gibco), and 5% fetal calf serum (Invitrogen-Gibco) added. Two-thirds of the culture medium was replaced twice weekly. The neurons showed a similar morphology as in regular cell culture plates. The dissociated neurons were cultured at 37 ^{o}C in 5% CO_2/95% air at saturating humidity (Su & Jiang, 2006; Su et al., 2007).

I-7. Electrophysiology

Two-electrode voltage clamp (TEVC) was used to record whole-cell currents were studied on oocytes 2–4 days post cDNA injection using an amplifier (Geneclamp 500, Axon

Instruments Inc., Foster City, CA) at room temperature (~24 °C). The extracellular solution contained (in mM): KCl 90, $MgCl_2$ 3, and HEPES 5 (pH 7.4). The cells were impaled with recording pipettes filled with 3 M KCl. The potential leakage of KCl from the recording electrodes was not corrected because of the large volume of oocytes. One of the electrodes (1.0-3.0 MΩ) served as the voltage recording which was connected to the HS-2 x1L headstage (input resistance=10^{11} Ω), and the other (0.3-0.6 MΩ) was used for current recording connected to the HS-2 x10MG headstage (maximum current=130 μA). Oocytes were accepted for further experiments if they did not show evident leakage in membrane currents. Current records were low-pass filtered (Bessel, 4-pole filter, 3 dB at 5 kHz), digitized at 5 kHz (12-bit resolution) and stored on a computer disk for later analysis (pClamp6.0.3, Axon Instruments).

Patch clamp experiments for Kir4.1-Kir5.1 were performed at room temperature (~ 25 °C) using the Axo-patch 200B amplifier (Axon Instruments). In brief, the vitelline membranes were mechanically removed after exposing the oocytes to a hypertonic solution (400 mOsm). The stripped oocytes were placed in a petri dish containing the regular bath solution (see below). Fire-polished patch pipettes (2-4 MΩ) were made of 1.2 mm borosilicate glass capillaries (Sutter Instruments, Novato, CA). The pipette tip was ~2 μm. The bath solution (FVPP) contained (in mM): 40 KCl, 75 potassium gluconate, 5 potassium fluoride, 0.1 sodium vanadate, 10 potassium pyrophosphate, 1 ethylene glycol-bis-β-aminoethylether-N,N,N',N'-tetraacetic acid (EGTA), 0.2 adenosine diphosphate (ADP), 10 piperazine-N,N'-bis-2-ethanesulfonic acid (PIPES), 10 glucose, and 0.1 spermine (pH=7.4). The pipette was filled with the same FVPP solution used in the bath or a solution

containing: 40 KCl, 110 potassium gluconate, 0.2 ADP, 1 EGTA, 10 N-2-hydroxyethyl-piperazine-N'-2-ethanesulfonic acid (HEPES), 10 glucose, 2 $MgCl_2$ (pH 7.4). Single channel currents were recorded from cell-attached patches. Current records were low-pass filtered (2,000 Hz, Bessel, 4-pole filter, -3 dB), digitized (10 kHz, 12-bit resolution), and stored on computer disk for later analysis using the pClamp 9 software. Junction potentials between bath and pipette solutions were appropriately nulled before seal formation. The open-state probability (NP_o) was calculated by first measuring the time, t_j, spent at current levels corresponding to j=0, 1, 2,...N channels open. The P_{open} was then obtained as $P_{open} = (\sum^{N}_{j=1} t_j\, j)/TN$, where N is the number of channels active in the patch and T is the duration of recordings. P_{open} values were calculated from one or a few stretches of data having a duration of 20 s each.

Single-electrode whole-cell voltage-clamp was performed using the HEK293 cell line (American Type Culture Collection, Manassas, VA) at room temperature as described previously (Li et al., 2004; Wu et al., 2002a; Zhu et al., 1998). In brief, fire-polished patch pipettes were made from 1.2 mm borosilicate capillary glass (Sutter Instruments, Novato, CA). Tight seals (>1 gigaohm before breaking into the whole-cell mode) were obtained with the transfected cells. The patch electrodes had an open tip resistance of 0.5-1.0 MΩ. The series resistance during recording varied from 5 to 10 MΩ and was not compensated. Recordings were terminated whenever significant increase (>20%) in series resistance occurred. Current records were low-pass filtered (2 kHz, Bessel, 4-pole filter, -3 dB), digitized (20 kHz, 16-bit resolution), and stored on computer disk for later analysis using the pCLAMP 9 software (Axon Instruments Inc, Foster City, CA). Recordings were

performed using solutions containing equal concentrations of K^+ applied to the bath and recording pipettes. This solution contained (in mM): KCl 40, potassium gluconate 110, ADP 0.2, EGTA 1, Hepes 10, glucose 10 and $MgCl_2$ 2 (pH 7.4). 100 nM thymeleatoxin dissolved in DMSO and the same concentration of DMSO alone was applied to the bath solution.

Patch clamp experiments for Kir6.2 were performed at room temperature (about 25 °C) as described previously (Xu et al., 2001; Wu et al., 2002a; Wu et al., 2002b). In brief, fire-polished patch pipettes were made from 1.2 mm borosilicate glass capillaries using a Sutter P-97 puller (Sutter Instrument, Novato, CA). Giant inside-out patches were employed to study macroscopic currents in a cell-free condition using recording pipettes of 0.5–1.0MΩ and an Axo-patch 200B amplifier (Axon Instruments, Foster City, CA). The current records were low-pass filtered (Bessel, 4-pole filter, -3 dB at 2 kHz), digitized with pClamp 9 software (Axon Instruments), and stored on computer disk for later data analysis. Patch clamp recording solutions contained equal concentrations of K^+ applied to the bath and recording pipettes. The solution contained (in mM): 10 KCl, 105 potassium gluconate, 5 KF, 5 potassium pyrophosphate, 0.1 sodium vanadate, 5 EGTA, 5 glucose, and 10 HEPES (pH = 7.4) (Xu et al., 2001; Wu et al., 2002a; Wu et al., 2002b). Pyrophosphate and vanadate are known to alleviate channel rundown in the Kir6.2. In several control experiments, we did not find any evident difference in current profile and channel responses to pH and ATP from those recorded in the absence of pyrophosphate and vanadate. The open-state probability (P_o) was calculated by measuring the time, t_j, spent at current levels corresponding to j = 0,1,2,⋯⋯N channels open, based on all

evident openings during the entire period of record (Wu et al., 2002b). The P_o was then obtained as $P_o = (\sum^{N}_{j=1} t_j\, j)/TN$, where N is the number of channels active in the patch and T is the duration of recordings. Open and closed times were measured from records in which only a single channel was active. In the some patches, the second active channel appeared during recording. The data from such patches were used for the open-time and closed-time analysis only if the P_o for the second openings was not larger than 0.002. The open-time and closed-time distributions were fitted using the Marquardt-LSQ method in the Pstat6 software (Axon Instruments Inc.) (Wu et al., 2002b). Open/closed events < 200μs were ignored.

A parallel perfusion system was used to deliver perfusates with different concentrations of ATP (K^+ Salt) at a rate of ~1 ml/min with no dead space (Xu et al., 2001; Wu et al., 2002a). All solutions with ATP were prepared immediately before experiments and were used for less than 4 hours. The ATP-current relationship was expressed with the Hill equation: $y = 1 / (1 + ([ATP] / IC_{50})^h)$, where [ATP] = ATP concentration, and IC_{50} = the [ATP] at midpoint channel inhibition.

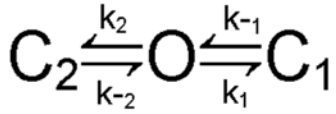

Kir6.2ΔC36 (no ATP)

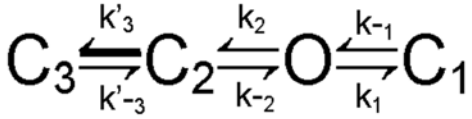

Kir6.2ΔC36 (ATP)

Scheme 1

Our data was fitted to the kinetic scheme 1 in which O is the open state, C1 represents the short-lived closure, and C2 refers to the long-lived closed state in the absence of ATP. A third long-lived close state (C3) appears in the presence of ATP for the Kir6.2ΔC36. In the scheme the bold arrows indicate the transitions that are more favored and the dashed arrow refers to transitions that are lessened. The rate constants for Kir6.2ΔC36 were calculated from our single channel data based on the following equations (equations 1-6) (Colquhoun & Hawkes, 1990; Trapp et al., 1998):

$$\tau_{c1} = \frac{1}{k_{-1}} \quad (1),$$

$$\tau_{c2} = \frac{1}{k_{-2}} \quad (2),$$

$$\tau_{o} = \frac{1}{k_{1} + k_{2}} \quad (3),$$

$$P_{OB} = \frac{1}{1 + \frac{k_{1}}{k_{-1}} + \frac{k_{2}}{k_{-2}}} \quad (4),$$

$$\tau_{c3'} = \frac{1}{k'_{-3}} \quad (5),$$

$$\tau_{c2'} = \frac{1}{k_{-2} + k'_{3}[ATP]} \quad (6),$$

$$P_{OB} = \frac{1}{1 + \frac{k_1}{k_{-1}} + \frac{k_2}{k_{-2}} + \frac{k_2 k_3}{k_{-2} k_{-3}}} \quad (7),$$

$$\frac{Nc_3}{Nc_1} = \frac{k_3 k_2}{k_1 k_{-2}} \quad (8),$$

$$\tau_{c2} = \frac{1}{k_{-2} + k_3} \quad (9),$$

$$\tau_{c3} = \frac{1}{k_{-3}} \quad (10),$$

where τc1 is the time constant for short closures, τc2 for long closures, τc3 for the additional long closures in the presence of ATP, and τo is the time constant for openings. P_{OB} is the open state probability in the absence of ATP. In the F168G mutant, an additional closed state appeared in the absence of ATP. Thus, additional equations (equations 7-10) were used to calculate the rate constant kinetics (Colquhoun & Hawkes, 1990; Trapp et al., 1998). Under this condition τc3 is the additional long closed time constant, Nc3 and Nc1 are the number of C3 and C1 events. Notice that the equations used to calculate the F168G mutant are very similar to those used to calculate the kinetics of Kir6.2ΔC36. The difference is that the k_3 and k_{-3} in the F168G mutant represents the rate constant kinetics of the closed time in the baseline level (in the absence of ATP), which requires additional calculations.

I-8. Recording of Neuronal Activity Using Multi-Electrode Arrays

Extracellular recordings were carried out in the DMEM medium using a preamplifier (MCS MEA1060, Reutingen, Germany) 10-60 days post culture at 37 ºC. The spikes were digitized at 40 kHz with a 64-channel A-D converter and the MEA workstation software (Plexon inc. Dallas, TX). Single units were identified using the Offline Sorter software (Plexon Inc.) based on the Principal Component Analysis method (Horn & Friedman, 2003), with which the likelihood to achieve pure single unit recording is greatly improved over the traditional window discriminators. Single-unit recordings were also determined by the absence of action potentials in the initial period (5-100ms) of the inter-spike histogram.

I-9. CO_2 Exposure

For acidification experiments with CO_2, the oocytes were placed in a semi-closed recording chamber (BSC-HT, Medical System, Greenvale, NY, USA), on a supporting nylon mesh, where perfusion solution 90 K^+ (90mM NaCl, 3mM $MgCl_2$, and HEPES (pH 7.4) bathed both the top and bottom surfaces of the oocytes. The perfusate and superfusion gas (15% CO_2) entered the chamber from the inlet at one end and flowed out through the other end. At the top of the chamber, enough space was provided for the gases to escape and also for the recording microelectrodes to be injected into the oocytes. During baseline-control recording, the chamber was ventilated with atmospheric air. Exposure of the oocytes to CO_2 was carried out by exposing the oocytes to a gas mixture containing CO_2 at 15% balanced with 21% O_2 and N_2. The oocytes were exposed to this

mixture for ~4-8 minutes or until the current reached a steady state. The high solubility of CO_2 resulted in very rapid changes in intracellular and extracellular pH levels. The pH level was stabilized within 4 min (Xu et al., 2001; Yang et al., 2000; Zhu et al., 2000).

Intracellular acidification alone of oocytes was carried out by using 90mM $KHCO_3$ to replace all KCl (90 mM) in the extracellular solution, so that the K^+ concentration remained the same in these experiments. This solution was titrated to pH 7.4 immediately before use to selectively acidify the cytosol of the oocytes to pH 6.6.

I-10. Chemical Administration and Exposure

4-α-Phorbol 12-myristate 13-acetate (PMA) and 4α-phorbol-12,13-didecanoate (4α-PDD) were purchased from Calbiochem (La Jolla, CA). 1-Oleoyl-2-acetyl-*sn*-glycerol (OAG), thymeleatoxin, chelerythrine chloride and calphostin-C were purchased from Sigma (St Louis, MO). Genistein and wortmannin were purchased from Tocris (Ellisville, MO). Substance-P (SP) (acetate salt), Spantide I, L-703,606, 4-Iodo-2, 5-dimethoxyamphetamine (DOI), serotonin (5-HT), thyrotropin releasing hormone (TRH), and [D-Ala^2, N-Me-Phe^4, Gly^5-ol]-Enkephalin (DAMGO) were also purchased from sigma. Spiperone and Ketanserin Tartate were purchased from Tocris (Ellisville, MO). PMA, OAG, thymeleatoxin, genistein, wortmannin, chelerythrine, calphostin-C, spiperone and 4α-PDD were dissolved in dimethylsulfoxide (DMSO) as stocks and mixed with a recording solution reaching a final concentration as indicated in the results. The final DMSO concentration was ≤0.1%. Other chemicals were dissolved in double-distilled water or experimental solutions. Exposures to these chemicals were done after baseline currents were stabilized.

I-11. Data Analysis

Data are presented as means ± S.E. (standard error). Student t test or single-factor ANOVA was used. Differences of chemical effects before versus during chemical exposures were considered to be statistically significant if $P \leq 0.05$.

I-12. HEK293 Cell Culture Immunocytochemistry

For single-label immunohistochemistry of Kir4.1 and Kir5.1 the cultured HEK293 cells transfected 3 days prior with Kir4.1-Kir5.1 dimer cDNA were fixed with 4% paraformaldehyde in Phosphate Buffered Saline (PBS) (0.01 M, pH 7.4) for 30 min. The cells were washed three times with PBS and then blocked for 30 min in PBS containing: 1% bovine serum albumin (BSA), 10% normal serum (NS), and 0.3% Triton X-100. The cultures were then incubated overnight at 4 °C in primary antibodies of rabbit anti-Kir4.1 (1:400) (Alomone Labs, Jerusalem, Israel) or goat anti-Kir5.1 (1:400) (Santa Cruz Biotechnology, Santa Cruz, CA), diluted in Antibody Dilution Solution (ADS), containing: 0.1% gelatin, 0.1% NaN_3, and 0.3% Triton X-100 in PBS. Both antibodies were used to detect antigen of human, rat, and mouse origin. After washing three times with ADS, the cultured cells were then incubated with biotinylated goat anti-rabbit IgG (Kir4.1) or biotinylated donkey anti-goat (Kir5.1) (Jackson Immuno Research, West Grove, PA) diluted to 1:1000 in ADS for 2 hr at 25 °C. The cells were rinsed with ADS and then incubated at 25 °C with a 546 fluorophore conjugated streptavidin (Molecular Probes, Eugene, OR) diluted to 1:1000. The fluorescence reaction was visualized using a Zeiss axioscope 200 fluorescence microscope (Zeiss, Oberkochen, Germany). Pictures were taken using the software AxioVision AC 4.1 (Zeiss, Oberkochen, Germany).

Subsequently, fluorescence imaging was performed with a confocal microscope (LSM 510) (Zeiss, Jena, Germany). The confocal images were taken using a 40x oil immersion objective lens.

I-13. Brainstem Neuron Culture Immunocytochemistry

Brainstem neurons were fixed with 4% paraformaldehyde in phosphate buffered saline (PBS, 0.1 M, pH 7.4) for 30 min. The cells were washed three times with PBS and then blocked for 30 min in PBS containing 1% bovine serum albumin (BSA), 10% normal donkey serum (NDS) or 10% normal goat serum (NGS), and 0.3% Triton X-100. The cells were then incubated overnight with the primary antibodies: rabbit polyclonal anti-Kir4.1 (1:1000) (Alomone Lab, Israel), goat polyclonal anti-Kir5.1 (1:500), (Santa Cruz Biotech, Santa Cruz, CA), and mouse monoclonal anti-MAP2 (1:400, Sigma, St. Louis, MO) diluted in antibody dilution solution (ADS), containing 0.1% gelatin, 0.1% NaN_3, and 0.3% Triton X-100 in PBS. After washing five times with ADS (5 min each), the cultured cells were incubated at 25 °C with the secondary antibodies for 2 hrs: AlexaFluor488-conjugated donkey anti-rabbit IgG for demonstration of Kir4.1 (1:1000) (Molecular Probes, Eugene, OR), AlexaFluor594-conjugated donkey anti-goat IgG for Kir5.1 (1:1000) (Molecular Probes, Eugene, OR), and AMCA (7-amino-4-methylcoumarin-3-acetic acid) conjugated donkey anti-mouse IgG (1:100, Jackson ImmunoRes, West Grove, PA) for MAP2. In control experiments, the primary antibodies were omitted for Kir5.1 and MAP2 or pre-absorbed with a 3-fold excess of the epitope for Kir4.1 (Alomone Lab). All of these control experiments showed negative stainings. The fluorescence reaction was first visualized using a Zeiss axioscope 200 fluorescence

microscope (Zeiss, Oberkochen, Germany). Subsequently, fluorescence imaging was performed with a confocal microscope (LSM 510) (Zeiss, Jena, Germany). The confocal images were taken using a 20x and 40x objective lenses.

I-14. Brainstem Tissue Slice Immunocytochemistry

All experimental procedures were carried out in accordance with the Guidelines for the Care and Use of Laboratory Animals by the NIH and Georgia State University. Male Sprague-Dawley rats (200-250 g) were deeply anesthetized by inhalation with halothane and perfused transcardially with 0.9% saline followed by 4% (wt/vol) paraformaldehyde in 0.1 M PBS (pH 7.4).The brains were rapidly dissected, post-fixed in the same solution at 4 °C for 3 hrs, and transferred to 30% (wt/vol) sucrose in PB at 4 °C overnight. The brains were then mounted onto a tissue cutting block and frozen in optimum cutting temperature (OCT) compound (VWR, West Chester, PA). Transverse sections (10 μm, 20 μm and 40 μm) were cut on a cryostat (Leica, Wetzlar, Germany) and placed in PBS (free-floating for 40 μm sections) or mounted on a slide (fixed for 10 μm, 20 μm sections). The sections were washed five times with PBS for 5 min each and pre-treated with PBS containing: 1% bovine serum albumin (BSA), 10% normal serum (NS), and 0.3% Triton X-100 at 25 °C for 30 min to reduce nonspecific immunostaining. The sections were then incubated in the primary antibodies [Kir4.1 (1:400) (Alomone Labs, Jerusalem, Israel); Kir5.1(1:200) (Santa Cruz Biotechnology, Santa Cruz, CA); Tyrosine Hydroxylase (TH) (1:5000) (Sigma-Aldrich, St. Louis, MO); NK1R (1:3000) (Sigma-Aldrich, St. Louis, MO); and 5-HT2AR (1:500) (Immunostar Inc, Hudson, WI)] diluted with ADS at 4 °C for 48 hrs. The sections were then washed five times with ADS

at 25 °C for 5 min each and incubated with the corresponding secondary antibody (Jackson Immuno Research, West Grove, PA) diluted to 1:1000 in ADS for 2 hrs at 25 °C. In the case where ABC was used the sections were subsequently rinsed with ADS and then incubated at 25 °C with a 546 fluorophore conjugated streptavidin (Molecular Probes, Eugene, OR) diluted to 1:1000. The fluorescence reaction was visualized using a Zeiss axioscope 200 fluorescence microscope (Zeiss, Oberkochen, Germany). Pictures were taken using the software AxioVision AC 4.1 (Zeiss, Oberkochen, Germany). Confocal images were obtained with a LSM510 confocal imaging system (Zeiss, Oberkochen, Germany) and manipulated with Adobe Photoshop 5.5 software (Adobe Systems, Mountain View, CA).

Diaminobenzidine (DAB) with enhanced nickel staining was used to increase the sensitivity of the antibody staining. Ni-DAB immunocytochemistry was performed on free-floating and fixed sections similarly as described above. Briefly, sections were washed 3 times with 0.05 M Tris Buffered Saline (TBS) and then exposed to 0.5% H_2O_2 for 30 min. The sections were then washed 3 times again with 0.05 M TBS and pre incubated for 30 min at 25 °C in the corresponding blocking solution (see above section). Following blocking the sections were incubated for 48 hours at 4 °C with specific primary antibodies against (Kir4.1, Kir5.1, and TH) diluted in ADS made with TBS. The sections were washed five times with ADS for 5 min each and subsequently exposed to ADS containing the horse radish peroxidase (HRP) conjugated secondary antibody at 25 °C overnight. The sections were washed again 5 times for 5 min each and then soaked in ADS containing an HRP-conjugated streptavidin for 4 hours at 25 °C. The sections were

washed with TBS and exposed to DAB and nickel ammonium sulfate in the presence of glucose oxidase. The floating sections were subsequently mounted onto clean slides and allowed to dry. After drying the sections were dehydrated by exposure to increasing concentrations of ethanol. The sections were made transparent with Xylene and then cover slipped in the presence permount. The Ni-DAB reaction was visualized using a Zeiss axioscope 200 microscope as well as a bright-field microscope and digit-imaged. Protein expression was judged according to the relative optical intensity of the stain.

J. EXPERIMENTAL DESIGN AND RESULTS

I. IDENTIFICATION OF THE HETEROMERIC KIR4.1-KIR5.1 CHANNEL IN BRAINSTEM NEURONS*

Manuscript in preparation:

Asheebo Rojas, Junda Su, Xiaoli Zhang, Ming Lee, Morium Chowdhury & Chun Jiang. Identification of the Heteromeric Kir4.1-Kir5.1 channel in brainstem neurons.

*In this part, Dr. Junda Su and Ms. Xiaoli Zhang helped me to perform immunocytochemistry on brainstem sections. Dr. Junda su performed 20 % of the DAB immunocytochemistry on sections taken from the LC and the ventralateral medulla. Ms. Xiaoli Zhang performed 10 % of the fluorescence immunocytochemistry on sections taken from the LC. Mr. Ming Lee helped me by obtaining and preparing the 10 μM adjacent sections from the LC. All of the adjacent sections were obtained by Mr. Ming Lee. Ms. Morium Chowdhury assisted me with 40 % of the animal perfusions and she prepared solutions in addition to mounting the brainstem sections onto the slides. All of their help is greatly appreciated.

Ia. INTRODUCTION

The candidacy of the Kir4.1-Kir5.1 channel as a central CO_2 chemoreceptor molecule is strengthened by demonstrating expression of the channel in brainstem chemosensitive neurons where it is co-expressed with receptors for neurotransmitters that are critical for respiratory control. Recently, a study using in situ hybridization demonstrated the presence of mRNAs of both Kir4.1 and Kir5.1 in chemosensitive neurons of the brainstem (Wu et al., 2004). However, in situ hybridization results showing the presence of mRNAs are suggestive. Although mRNAs are present in neurons, the channel may not exist at the protein level. Therefore, we have conducted the present study to demonstrate the presence of the Kir4.1-Kir5.1 channel in brainstem neurons. The locus coeruleus (LC) nucleus is chosen as the primary site of interest as this nucleus is highly sensitive to changes in pH/CO_2, it is easy to identify, and also mRNAs for both Kir4.1 and Kir5.1 are found in LC neurons. We also conducted experiments to demonstrate that the Kir4.1-Kir5.1 channel is co-expressed with the NK1 recepter, the natural receptor for SP. Here we present evidence showing expression of the Kir4.1, Kir5.1, and NK1R subunits in the locus coeruleus, and the Kir4.1 and Kir5.1 in the hypoglossal and trigeminal motor nuclei.

Ib. RESULTS

Ib-1. *Specificity of the Kir4.1 and Kir5.1 antibodies*

The Kir4.1 and Kir5.1 antibodies are both commercially available. We first performed control experiments to demonstrate the specificity and efficiency of these antibodies in our system. The specificity of the Kir4.1 and Kir5.1 antibodies was demonstrated using HEK293 cells. HEK293 cells were transfected with the Kir4.1-Kir5.1 dimer cDNA along with GFP cDNA as described in the methods

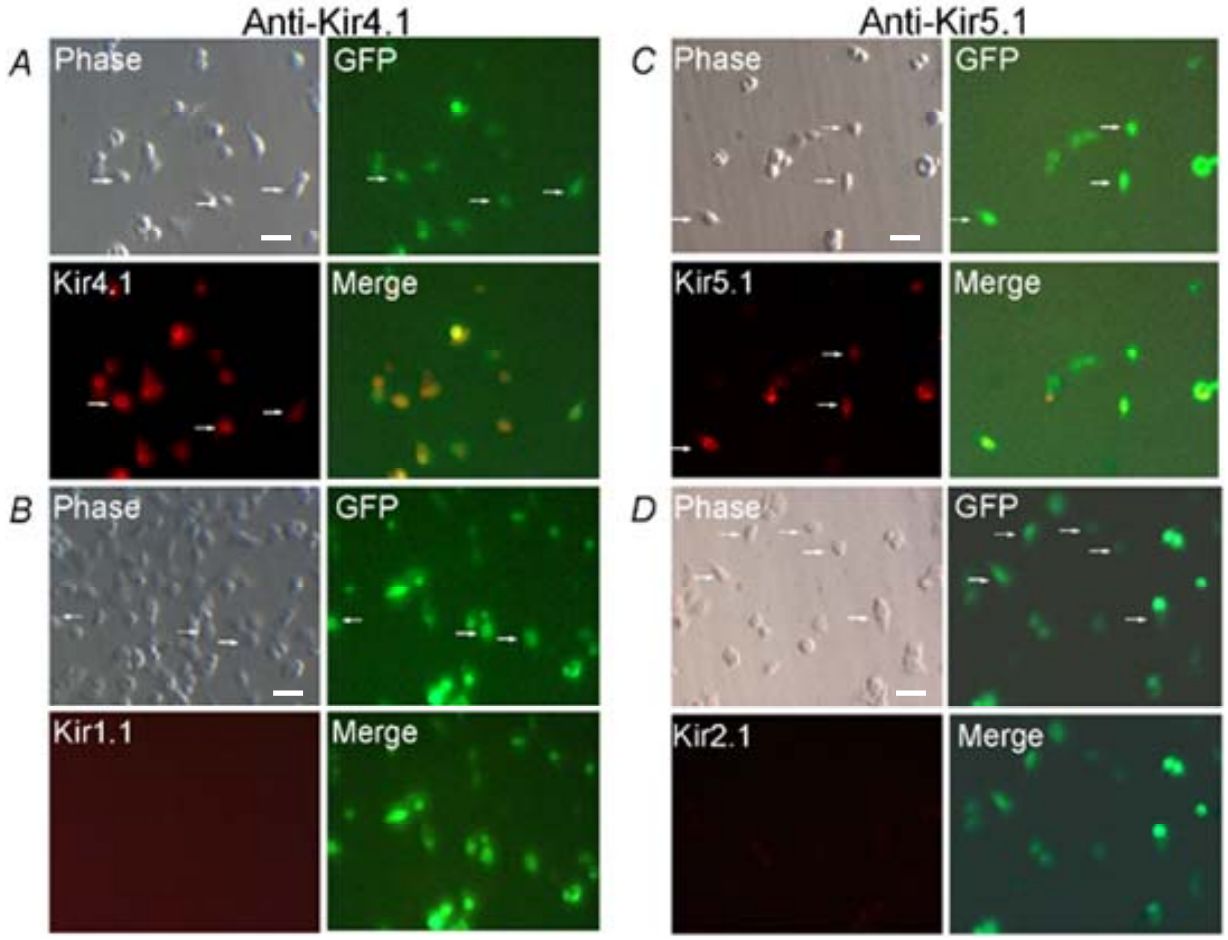

Fig I-1. Specificity and efficiency of the Kir4.1 and Kir5.1 antibodies. *A*. The Kir4.1 and Kir5.1 antibodies are highly effective. HEK293 cells were transfected with the Kir4.1-Kir5.1 cDNA along with the GFP cDNA. Immunocytochemistry was performed on these cells. Strong labellings were seen when cells expressing the Kir4.1-Kir5.1 were stained with the anti-Kir4.1 (A) and anti-Kir5.1 (C). No labellings were seen when cells expressing the Kir1.1 (B) and Kir2.1 (D) were stained with the anti-Kir4.1 and anti-Kir5.1, respectively. GFP was used as an indicator of transfection efficiency. The arrows represent typical and healthy HEK293 cells. Bar=50 μm.

sections. GFP was used as an indicator of transfection efficiency. Positive immunoassays were identified for both Kir4.1 and Kir5.1 when the HEK293 cells were incubated with the Kir4.1 and Kir5.1 antibodies as described in the methods section, suggesting that the antibodies can efficiently label the Kir4.1 and Kir5.1 proteins (Fig. 1 A, C). Similar experiments were repeated using two other Kir channels that share high homology to Kir4.1 and Kir5.1 to demonstrate the specificity of the antibodies. The Kir1.1 was used to demonstrate the specificity of the Kir4.1 antibody as the Kir1.1 shares the highest homology to Kir4.1. The Kir1.1 also shares the highest identity with the Kir4.1 in the epitope region that was used to generate the Kir4.1 antibody used here. When cells transfected with Kir1.1 were exposed to the Kir4.1 antibody no positive immunostains were detected although the GFP fluorescence suggests that the Kir1.1 channel was expressed (Fig. 1B). The same experiment was carried out using Kir2.1 to demonstrate specificity of the Kir5.1 antibody. The Kir2.1 channel shows the highest homology to the Kir5.1 and the highest idenitity in the epitope region of Kir5.1 used to generate the antibody. Cells transfected the Kir2.1 cDNA failed to reveal positive immunostains after incubation with the Kir5.1 antibody although GFP fluorescence indicated that the Kir2.1 channel was expressed (Fig. 1D). Experiments were also conducted with the homomeric Kir4.1 and Kir5.1 and positive immunostains were also detected (data not shown). Taken together, these results suggests that the Kir4.1 and Kir5.1 antibodies are specific and can be used to detect the presence of the Kir4.1 and Kir5.1 subunits in the heteromeric Kir4.1-Kir5.1 channel.

Ib-2. ***Expression of Kir4.1 and Kir5.1 in hypoglossal and trigeminal motor neurons***

Recently, tremendous efforts have been placed on detecting the tissue specific expression of various Kir channels. Although these efforts have led to the identification of many Kir channels in various tissues, there still remains debate as to the cellular expression of certain Kir channels. For example, the Kir4.1 and Kir5.1 has been shown to be highly expressed in brain tissue (Hibino et al., 2004; Ma et al., 1998; Poopalasundaram et al., 2000), however, it is not known whether these channels are expressed in neurons, in glia, or in both. There is overwhelming evidence showing that the Kir4.1 and Kir5.1 channels are expressed in glial cells within various regions of the brain (Hibino et al., 2004; Higashi et al., 2001; Horio 2001), suggesting that these channels may not function in neurons. However, recently a study using in situ hybridization demonstrated the presence of mRNA for both Kir4.1 and Kir5.1 in many brainstem neurons, suggesting that these channels may be expressed in neurons in addition to glial cells (Wu et al., 2004). To strengthen this conclusion we used immunocytochemistry to detect the Kir4.1 and Kir5.1 proteins in brainstem motor neurons, which are large and easily identifiable. Also, motor neuron clusters are not easily contaminated by neurons from adjacent nuclei. DAB immunocytochemistry was performed on brainstem sections as indicated in the methods section. Positive immunostains were detected for both Kir4.1 and Kir5.1 in hypoglossal motor neurons at the level of the medulla (Fig. 2).

Immunoassay experiments were also performed to detect Kir4.1-Kir5.1 expression in motor neurons at the level of the pons. Using DAB immunocytochemistry,

positive immunostains were detected for both Kir4.1 and Kir5.1 in trigeminal motor neurons (Fig. 3). These results suggest that the Kir4.1 and Kir5.1 channels are not only localized to glia, but are also expressed in neurons.

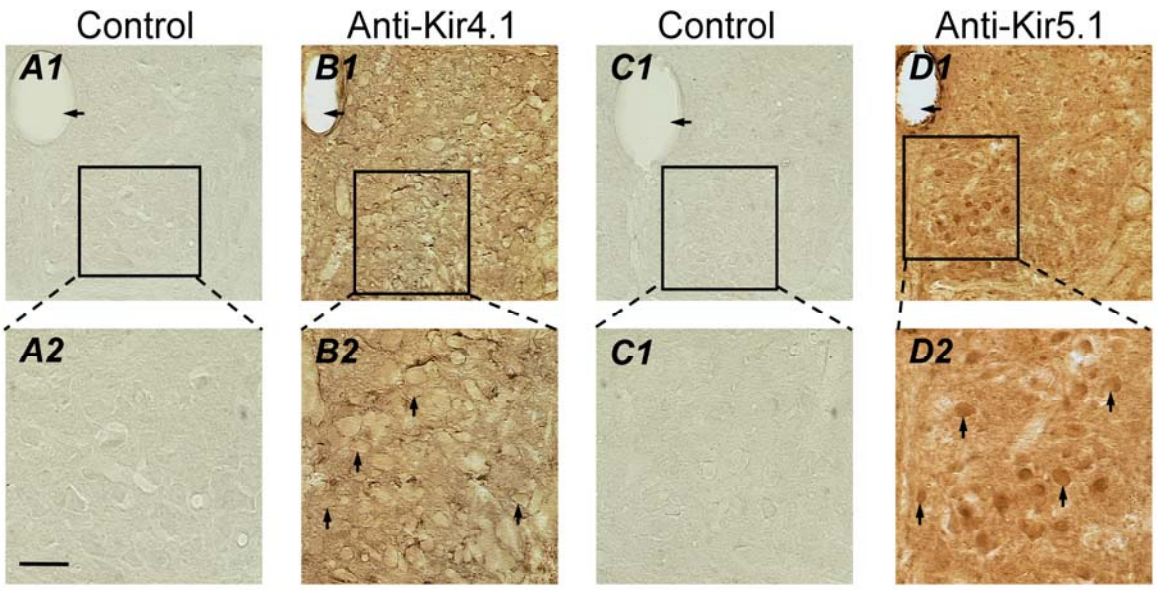

Fig I-2. Detection of Kir4.1 and Kir5.1 in hypoglossal motor neurons. DAB immunocytochemistry was performed on medullary sections (40 μm) obtained from rats. Strong staining was seen in the hypoglossal motor neurons for Kir4.1 (B1) and Kir5.1 (D1) at 10x magnification. Higher magnification (20x) revealed expression of both Kir4.1 (B2) and Kir5.1 (D2). For the controls the medullary sections were treated in a similar manner as the experimental sections except the control sections were not exposed to the primary antibody. In both cases no DAB staining was detected in the absence of the primary antibody at low and high magnifications (A1, A2, C1, C2). The horizontal arrow in A1-D1 represents the central canal. Vertical arrows in B2 and D2 represent typical hypoglossal motor neurons expressing Kir4.1 and Kir5.1. Bar=100 μm.

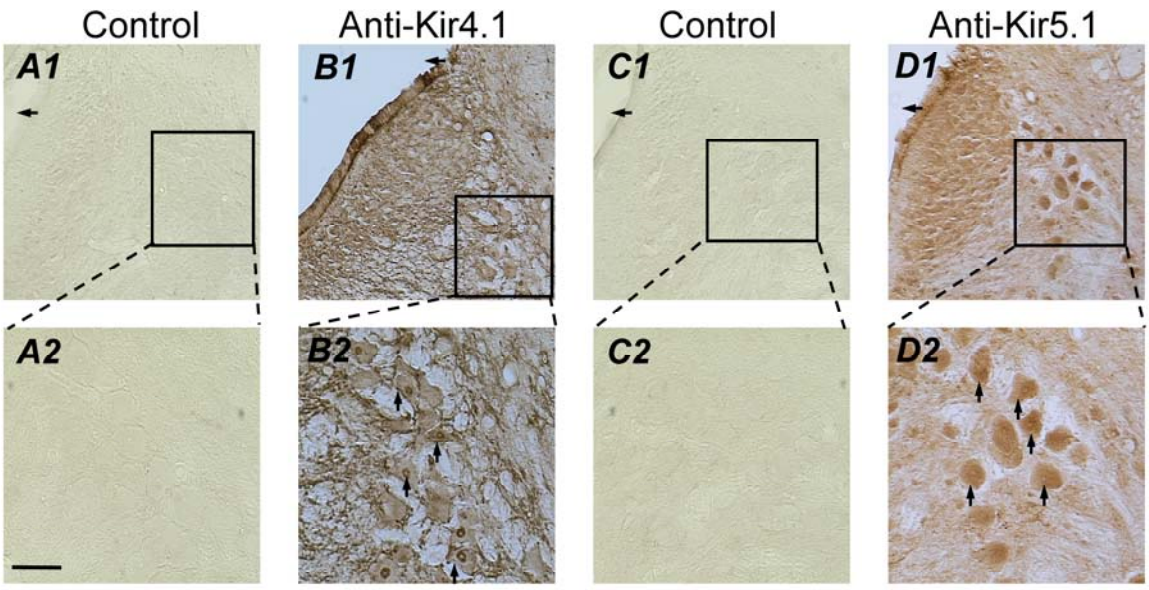

Fig I-3. Expression of Kir4.1 and Kir5.1 in trigeminal motor neurons. Labelling of Kir4.1 and Kir5.1 proteins in trigeminal motor neurons of rats. DAB immunocytochemistry was performed on brainstem (pons) sections (40 μm) at the area of the trigeminal motor neurons. At 10x these neurons were differentially stained with some showing strong labelling for Kir4.1 (B1) and Kir5.1 (D1). Higher magnification (20x) revealed expression of both Kir4.1 (B2) and Kir5.1 (D2). For the controls the pontine sections were treated in a similar manner as the experimental sections except the control sections were not exposed to the primary antibody. In both cases no DAB staining was detected in the absence of the primary antibody at low and high magnifications (A1, A2, C1, C2). The horizontal arrow in A1-D1 represents the 4th ventricle. Vertical arrows in B2 and D2 represent typical trigeminal motor neurons expressing Kir channels. Bar=100 μm.

Ib-3. ***Co-expression of Kir4.1 and Kir5.1 in Locus Coeruleus neurons of rats***

There are several primary chemosensitive sites within the brainstem. We focused our attention on the locus coeruleus (LC), because it is known to be highly chemosensitive (Elam et al., 1981; Haxhiu et al., 1996; Oyamada et al., 1998; Oyamada et al., 1999; Pineda & Aghajanian, 1997). The ventilatory response to CO_2 was significantly reduced in rats that had specific lesioning of LC neurons (Li & Nattie, 2006). According to the study carried out by Wu et al., Kir4.1 and Kir5.1 mRNA is highly abundant in the LC. In addition to this, the LC is an easily identifiable nucleus in the brainstem with nearby markers such as the fourth ventricle and the trigeminal motor nucleus. The neurons of the LC are densely packed and they are almost uniform in size. Since the LC is the major norepinephrine producing site in the brain, the presence of enzymes necessary for the production of NE is a useful tool used to identify the locus coeruleus.

We performed DAB immunocytochemistry on 40 μm brainstem sections taken at the level of the pons as described in the materials and methods section. Positive immunostains were identified for both Kir4.1 and Kir5.1 in the area of the LC (Fig. 4). As a positive control we assayed for expression of both channels in the trigeminal motor neurons in the same animals, as these motor neurons contain both Kir4.1 and Kir5.1 as previously mentioned. Negative staining in the areas ventrolateral and dorsolateral to the trigeminal motor neurons again demonstrated the specificity of the antibodies (Fig. 4).

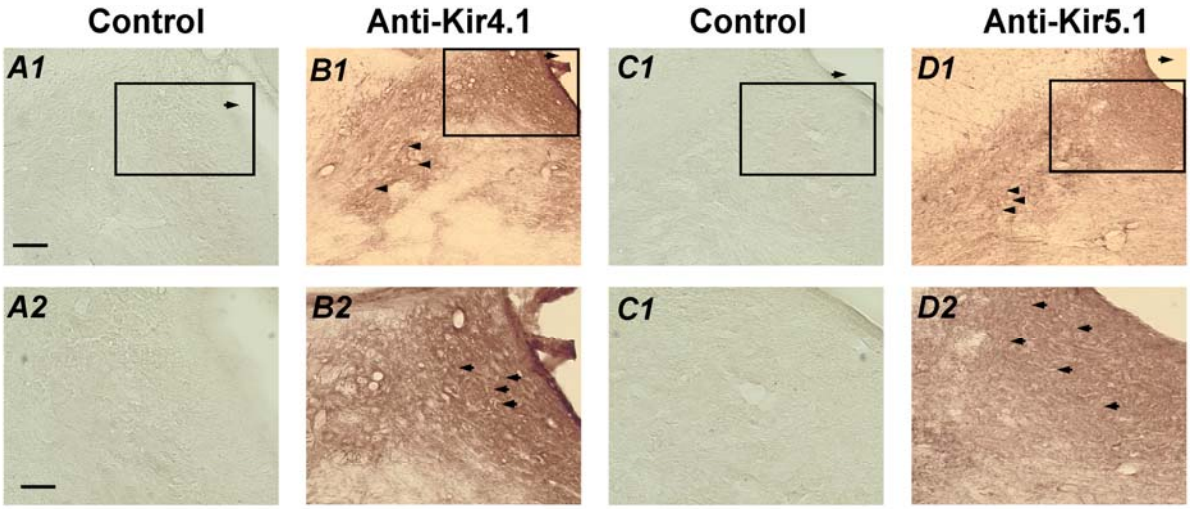

Fig I-4. The Kir4.1 and Kir5.1 expression in LC area. DAB immunocytochemistry was performed on pontine sections (20 μm) at the region of the LC. At 10x strong staining was seen in the LC nucleus for Kir4.1 (B1) and Kir5.1 (D1). The staining was more apparent at a higher magnification (20x) for Kir4.1 (B2) and Kir5.1 (D2). For the controls the pontine sections were treated in a similar manner as the experimental sections except the control sections were not exposed to the primary antibody. In both cases no DAB staining was detected in the absence of the primary antibody at low and high magnifications (A1, A2, C1, C2). The horizontal arrows in A1-D1 represent the 4^{th} ventricle. The arrow heads in B1 and D1represent trigeminal motor neurons expressing Kir4.1 and Kir5.1. The horizontal arrows in B2 and D2 represent typical neurons expressing Kir channels. Bar=100 μm.

We took advantage of the fact that LC neurons, that have a diameter ranging from 15-25 μM, produce norepinephrine to demonstrate the expression of the Kir4.1 and Kir5.1 subunits in the same individual LC neurons. The enzyme tyrosine hydroxylase (TH) is the rate limiting enzyme for the production of the catecholamines dopamine and norepinephrine. Therefore, immunoassaying for TH would allow for the identification of LC neurons. Brainstem sections were obtained at the level of the LC in the pons. Groups of adjacent 10 μm sections were obtained using a cryostat. Each group consisted of three consecutive sections that were used to stain for the presence of Kir4.1, Kir5.1 and TH. Using the DAB procedure described in the methods section we identified positive immunostains for Kir4.1, Kir5.1, and TH in the LC (Fig. 5). Such a high magnification allowed for the positive detection of individual neurons identified by the presence of TH co-expressing the Kir4.1 and Kir5.1 (Fig. 5).

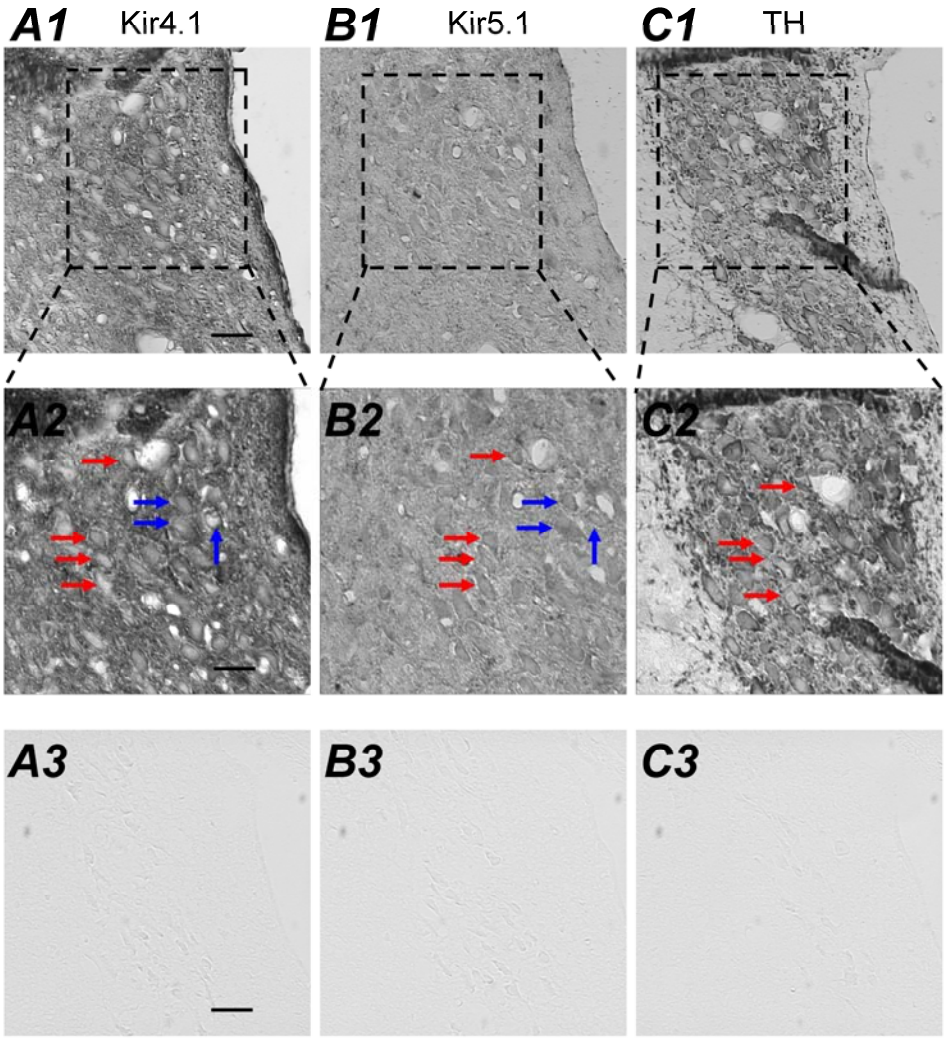

Fig I-5. Expression of Kir4.1 and Kir5.1 in individual LC neurons. DAB immunocytochemistry was performed on three adjacent pontine sections (10 µm) at the region of the LC. At 20x strong staining was seen in the LC nucleus for Kir4.1 (A1), Kir5.1 (B1), and TH (C1). The staining was more apparent at a higher magnification (40x) (A2-C2). For the controls the pontine sections were treated in a similar manner as the experimental sections except the control sections were not exposed to the primary antibody. In each case no DAB staining was detected in the absence of the primary antibody at a high magnification (A3-C3). The red horizontal arrows represent the same LC neurons with positive labelling for Kir4.1, Kir5.1, and TH. The blue horizontal arrows represent the same LC neurons with positive labelling for Kir4.1 and Kir5.1. Bar=50 µm.

To confirm the co-existence of the Kir4.1 and Kir5.1 in LC neurons we decided to use triple fluorescence immunocytochemistry. Brainstem sections (20 μm) were obtained at the level of the LC in the pons and fixed on glass slides. These sections were incubated with anti-Kir4.1, anti-Kir5.1 and anti-TH. To simplify the antibody staining and reduce the amount of background signal we decided to use fluorescent conjugated secondary IgG antibodies for detection instead of the ABC method. Kir4.1 was labeled with a 488-IgG fluorophore (green) (Fig. 6A); Kir5.1 with a 594-IgG fluorophore (red) (Fig. 6B); and TH with an AMCA-IgG (blue) (Fig. 6C). Using these three fluorophores we assayed for positive immunostains for all three antigens in the same neurons. Indeed, all three proteins were identified in the LC (Fig 6). High magnification confocal images allowed us to view the expression at the single cell level. When viewed at a higher magnification (40x) we were able to identify co-existence of both Kir4.1 and Kir5.1 in the same TH positive neurons (Fig. 6). Taken together, these results suggest that the Kir4.1 and Kir5.1 proteins co-exist in locus coeruleus neurons and the heteromeric channel may also exist here.

Ib-4. ***Detection of the NK1R in the LC of Rats***

The neuromodulators substance-P (SP) and serotonin (5-HT) have been shown to regulate the control of respiration (Moss et al., 1986; Nattie et al., 2004). The receptors for these neurotransmitters are G protein coupled receptors (GPCRs). Chemosensitive neurons co-expressing these receptors and the Kir4.1-Kir5.1 channel may be modulated by these neurotransmitters. Therefore, we immunoassayed for the presence of the neurokinin-1 receptor (NK1R) and the serotonin 2A receptor subtypes (5-HT2AR) in the

LC of rats. Using double fluorescence immunocytochemistry against TH (used to identify the LC) and the NK1R, we detected positive expression of the NK1R in a positive TH cluster of cells (Fig. 7A), suggesting that there may be a coupling of function between the Kir4.1-Kir5.1 channel and the NK1R as has been demonstrated

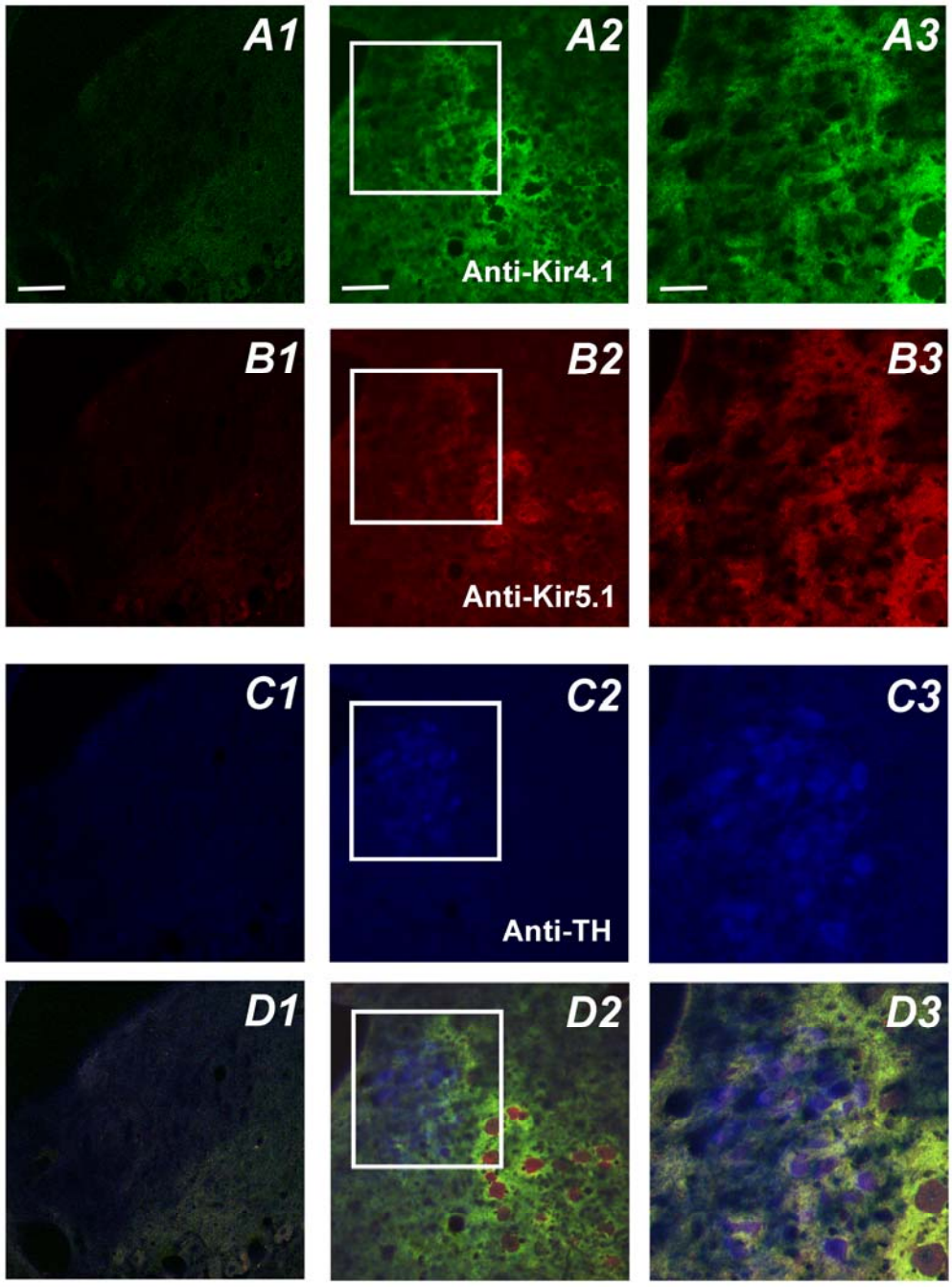
A1
A2
Anti-Kir4.1
A3
B1
B2
Anti-Kir5.1
B3
C1
C2
Anti-TH
C3
D1
D2
D3

Fig I-6. Triple labelling of Kir4.1, Kir5.1 and TH in LC neurons. Fluorescence immunocytochemistry was performed on brainstem sections (20 μm) at the region of the LC. Strong staining was seen in LC neurons for Kir4.1 (A2), Kir5.1 (B2), and TH (C2) at 20x magnification using a confocal microscope. Higher magnification (40x) revealed expression of Kir4.1 (A3) and Kir5.1 (B3) and TH (C3) in the LC. Panels D1-D3 show the overlay of A, B, and C. The overlay shows the co-localization of Kir4.1, Kir5.1 and TH in the same individual LC neurons. For the controls the pontine sections were treated in a similar manner as the experimental sections except the control sections were not exposed to the primary antibody. In each case no fluorescence staining was detected in the absence of the primary antibody at a high magnification (A1, B1, C1).The box represents the area that was magnified to 40x. Bar=40 μm.

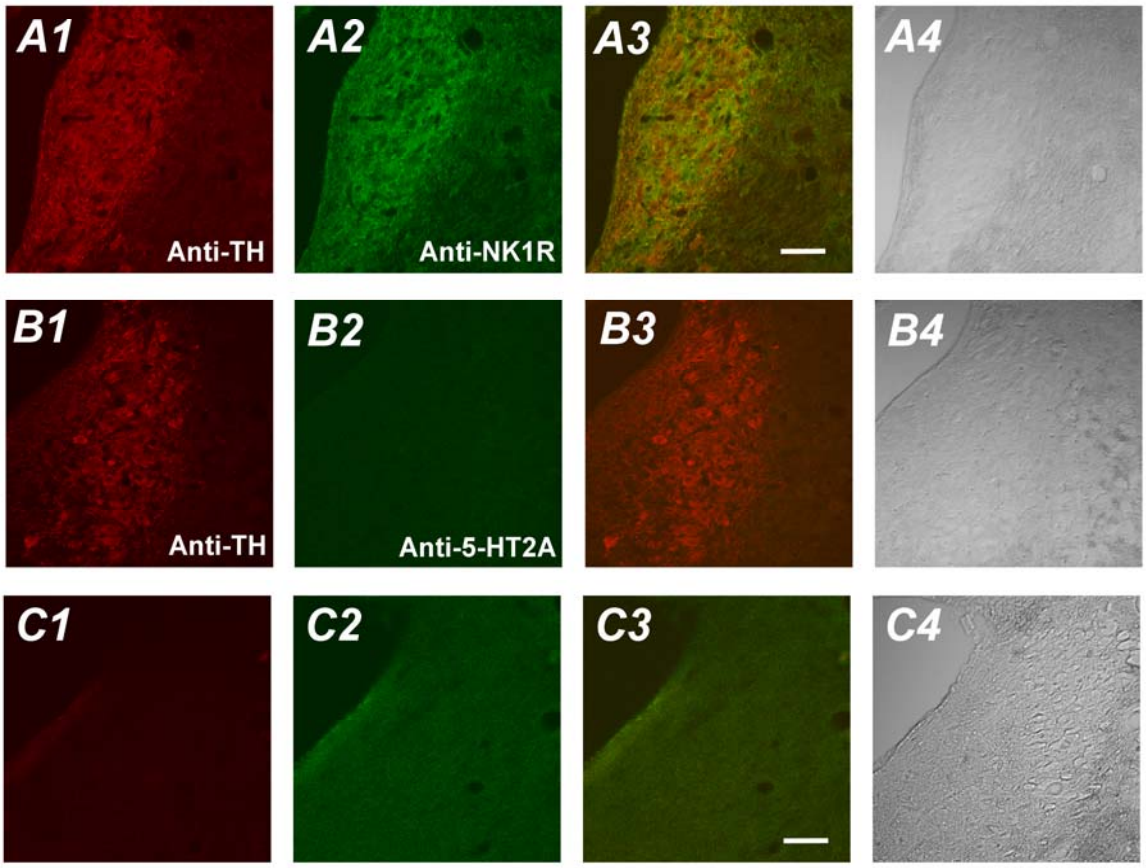

Fig I-7. Expression of the NK1R in the LC. Fluorescence immunocytochemistry was performed ponto-medullary sections (20 µm) at the region of the LC. Strong staining was seen in LC neurons for TH (A1) and the NK1R (A2) at 20x magnification using a confocal microscope. The overlay shows that the NK1R is expressed in the same TH positive neurons (A3). A4 shows the phase contrast. The same experiment was repeated for the 5-HT2A receptor. Although there were positive labellings for TH (LC neurons) (B1), no labellings were seen for the 5-HT2A (B2). The overlay shows that the 5-HT2A is not expressed in the same TH positive neurons (B3). B4 shows the phase contrast. For the controls the pontine sections were treated in a similar manner as the experimental sections except the control sections were not exposed to the primary antibody. In each case no fluorescence staining was detected in the absence of the primary antibody at a high magnification (C1-C3). Bar=40 µm.

for G-protein coupled inward rectifier K^+ (GIRK) channels. The same experiment was carried out for the 5-HT2A receptor. Unfortunately we failed to detect positive immunostains for the 5-HT2A in the LC of rats (Fig. 7B).

Ib-5. ***Expression of Kir4.1, Kir5.1 and NK1R in the LC of mice***

All of the previous experiments were carried out using Sprague Dawley rats. We recently obtained a strain of transgenic mice that expresses GFP in the 98 % of LC neurons (van den Pol et al., 2002). Therefore, we decided to take advantage of these transgenic (GFP expressing) LC mice to immunoassay for the co-existence of the Kir4.1 and Kir5.1 proteins in the locus coeruleus. In this way we could assay for expression of Kir4.1 and Kir5.1 without having to perform triple labelling. This also made identification of the LC easier. Single staining fluorescence immunocytochemistry showed the presence of the Kir4.1 and Kir5.1 in LC neurons of the GFP-transgenic mice (Fig. 8D-I). We immunoassayed for the neurokinin-1 receptor (NK1R) in these mice and similar to the results obtained with rats we also found expression of this receptor in the LC of mice (Fig. 8J-L).

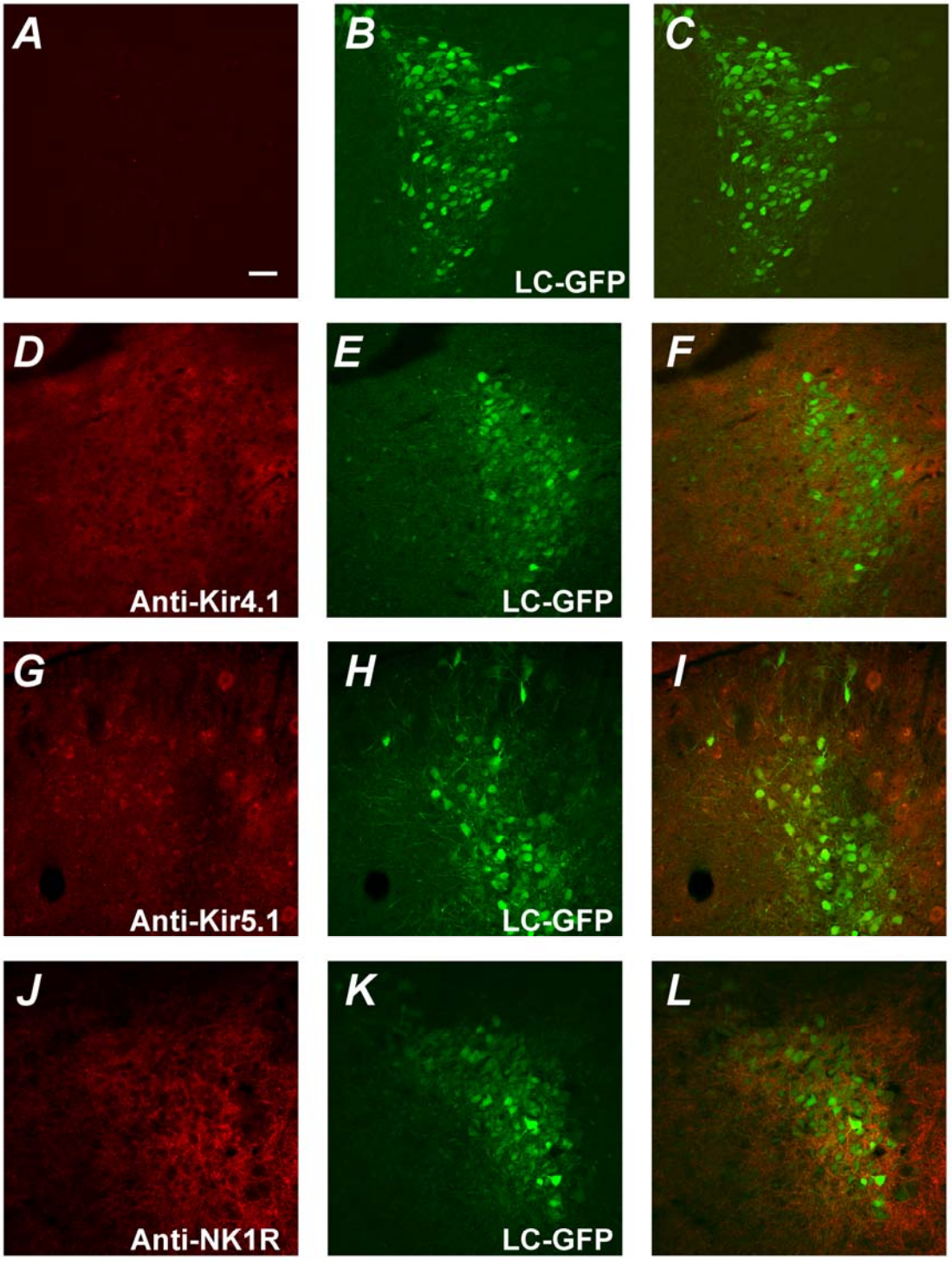
A
B
LC-GFP
C
D
Anti-Kir4.1
E
LC-GFP
F
G
Anti-Kir5.1
H
LC-GFP
I
J
Anti-NK1R
K
LC-GFP
L

Fig I-8. Expression of the Kir4.1, Kir5.1 and NK1R in the LC of mice. Fluorescence immunocytochemistry was performed on brainstem sections (20 μm) at the region of the LC. These mice express GFP in LC neurons as shown by panels B, E, H, and K. Strong staining was seen in LC neurons of these mice for Kir4.1 (D) Kir5.1 (G) and the NK1R (J) at 20x magnification using a confocal microscope. The overlay shows that the Kir4.1, Kir5.1 and NK1R are expressed in GFP positive LC neurons (F, I, L). For the controls the pontine sections were treated in a similar manner as the experimental sections except the control sections were not exposed to the primary antibody. In each case no fluorescence staining was detected in the absence of the primary antibody at a high magnification (A1). Note that the trigeminal motor neurons were positively labeled for Kir4.1 and Kir5.1 as previously mentioned. Bar=40 μm.

I-c. DISCUSSION

In the present study we have presented evidence for the expression of the Kir4.1 and Kir5.1 proteins in neurons. Our results show that hypoglossal motor neurons and trigeminal motor neurons contain both Kir4.1 and Kir5.1 subunits. There appeared to be a difference in the expression pattern of these two subunits. The Kir4.1 subunit appeared to express predominantly on the surface of these motor neurons, whereas the Kir5.1 channel was express throughout the cell. However, both subunits were detected on the surface of several motor neurons suggesting that the heteromeric Kir4.1-Kir5.1 channel may be expressed there. The expression of the heteromeric channel on the surface of these motor neurons may be important physiologically. Both hypoglossal motor neurons and trigeminal motor neurons are chemosensitive (Komai et al., 1993; Necakov et al., 2002). Perhaps, the Kir4.1-Kir5.1 channel plays a role in the CO_2 chemoreception of these motor neurons.

We also showed evidence for the detection of both the Kir4.1 and Kir5.1 subunits in the same TH positive neurons using two different methods (DAB staining in adjacent sections and triple fluorescence immunoassaying in the same sections). Although the DAB method is more sensitive than fluorescence we were able to detect significant levels of expression using triple labelling with fluorescence suggesting that the heteromeric Kir4.1-Kir5.1 channel may function in these LC neurons.

This demonstration of the presence of the heteromeric Kir4.1-Kir5.1 channel in chemosensitive brainstem nuclei strengthens the candidacy of this channel as a central CO_2 chemoreceptor molecule. However, further functional studies with the Kir4.1-

Kir5.1 in brainstem chemosensitive nuclei must be performed to solidify the roles of this channel in central CO_2 chemoreception. Now that we know the channel is expressed in brainstem neurons the next step is to demonstrate the role played by the channel in these brainstem neurons during central CO_2 chemoreception. Ultimately, the aim is to prove that the heteromeric Kir4.1-Kir5.1 channel is one of the central CO_2 chemoreceptor molecules that have eluded researchers for more than 50 years.

I-d. SUMMARY AND CONCLUSION

Using immunocytochemistry we present evidence for the co-expression of the Kir4.1 and Kir5.1 proteins in the hypoglossal nucleus, the trigeminal motor nucleus, and the locus coeruleus (LC). Both Kir4.1 and Kir5.1 subunits were present in these nuclei, suggesting that the heteromeric channel may be expressed in these cells. We also show that the Kir4.1 and Kir5.1 subunits are located in the same tyrosine hydroxylase containing cells suggesting expression of the Kir4.1-Kir5.1 channel in the LC. The Kir4.1-Kir5.1 channel along with the NK1 receptor was also detected in LC neurons. Unfortunately, we were unable to obtain positive immunoassays for the 5-HT2A receptor in the LC. Taken together these results suggest that the Kir4.1-Kir5.1 channel is indeed expressed in chemosensitive neurons and the channel may be regulated by neurotransmitters involved in the control of respiration.

II. MODULATION OF THE HETEROMERIC KIR4.1-KIR5.1 CHANNEL BY MULTIPLE NEUROTRANSMITTERS VIA $G_{\alpha q}$-COUPLED RECEPTORS*

Manuscript in press:

Asheebo Rojas, Junda Su, Liang Yang, Ming Lee, Ningren Cui, Xiaoli Zhang, Dyanna Fountain & Chun Jiang. Modulation of the Heteromeric Kir4.1-Kir5.1 Channel by Multiple Neurotransmitters via $G_{\alpha q}$-coupled Receptors. *J Cell Physiol* (2007).

*In this part, Dr. Junda Su prepared 80 % of the neuronal cultures for MEA recording and together Dr. Junda Su and I recorded the neuronal activity from the dishes. Dr. Liang Yang performed all of the offline data analysis for the MEA experiments. Dr. Ningren Cui taught me to do whole cell recording and performed 20 % of all cDNA injections and recordings. Mr. Ming Lee and Ms. Xiaoli Zhang performed 20 % of the immunocytochemistry on the cultured neurons. Ms. Dyanna Fountain constructed 30 % of the mutations on the Kir4.1-Kir5.1 channel and prepared cDNAs for injection. I greatly appreciate all of their help.

IIa. INTRODUCTION

It is known that the brainstem control of respiration relies on several neurotransmitters including serotonin (5-HT), substance-P (SP) and thyrotropin releasing hormone (TRH) (Cream et al., 1997; Dekin et al., 1985; Moss et al., 1986; Mutolo et al., 1999; Nattie et al., 2004; Nink et al., 1991; Pete et al., 2002; Richerson, 2004; Richerson et al., 2005; Schulz et al., 1996; Severson et al., 2003; Taylor et al., 2005; Wang et al., 2001). Site-specific injections of these neurotransmitters can potently stimulate ventilation. Systemic CO_2 response is reduced by selective disruption of serotonergic neurons and neurons expressing the neurokinin-1 receptor (NK1R) (Hodges et al., 2004; Nattie & Li, 2002; Wenninger et al., 2004a; Wenninger et al., 2004b). Receptors for these neurotransmitters have been identified in the ventral and dorsal respiratory groups (VRG, DRG). Midline raphe neurons that are known to be CO_2 chemosensitive and project to the DRG and VRG also contain these neurotransmitters, suggesting that they may modulate the neuronal response to hypercapnia (Richerson, 2004; Richerson et al., 2005; Severson et al., 2003). Therefore, we tested whether the Kir4.1-Kir5.1 channel is a downstream target of these neurotransmitters as this channel is expressed CO_2 chemosensitive neurons.

IIb. RESULTS

IIb-1. *Inhibition of the Kir4.1-Kir5.1 channel by SP, 5-HT, and TRH*

The NK1 receptor cDNA was co-injected into *Xenopus* oocytes together with the Kir4.1-Kir5.1 tandem dimer cDNA. Inward rectifying currents were recorded from the oocytes 2-3 days post injection using two-electrode voltage clamp with the bath solution containing 90 mM K^+. Typical Kir4.1-Kir5.1 currents were revealed: small outward currents and large inward currents with slow activation at highly negative membrane potentials (Fig. 1A, B, C). Following stabilization of the baseline, the Kir4.1-Kir5.1 currents were inhibited by an exposure to 1 μM SP applied to the bath (Fig. 1A). Similar experiments were done by expressing the Kir4.1-Kir5.1 with the 5-HT2A or mTRH-R1 receptor. The currents were inhibited by 40 μM 5-HT and 100 μM TRH, respectively (Fig. 1B, C).

The current-voltage (I-V) relationship was examined for the neurotransmitter effects. Currents were recorded at baseline as well as at the peak plateau effect after exposure to 1 μM SP, 40 μM 5-HT, and 100 μM TRH, respectively. Both currents were then normalized to -160 mV and plotted against the membrane potential. The I-V plot indicated that current inhibition occurred at all negative membrane potentials and did not show evident voltage-dependence (Fig. 1D, E, F). Recordings using a ramp protocol showed that the Kir4.1-Kir5.1 channel was inhibited by SP, 5-HT, and TRH in both negative and positive membrane potentials without a change in rectification (Fig. 1G, H, I).

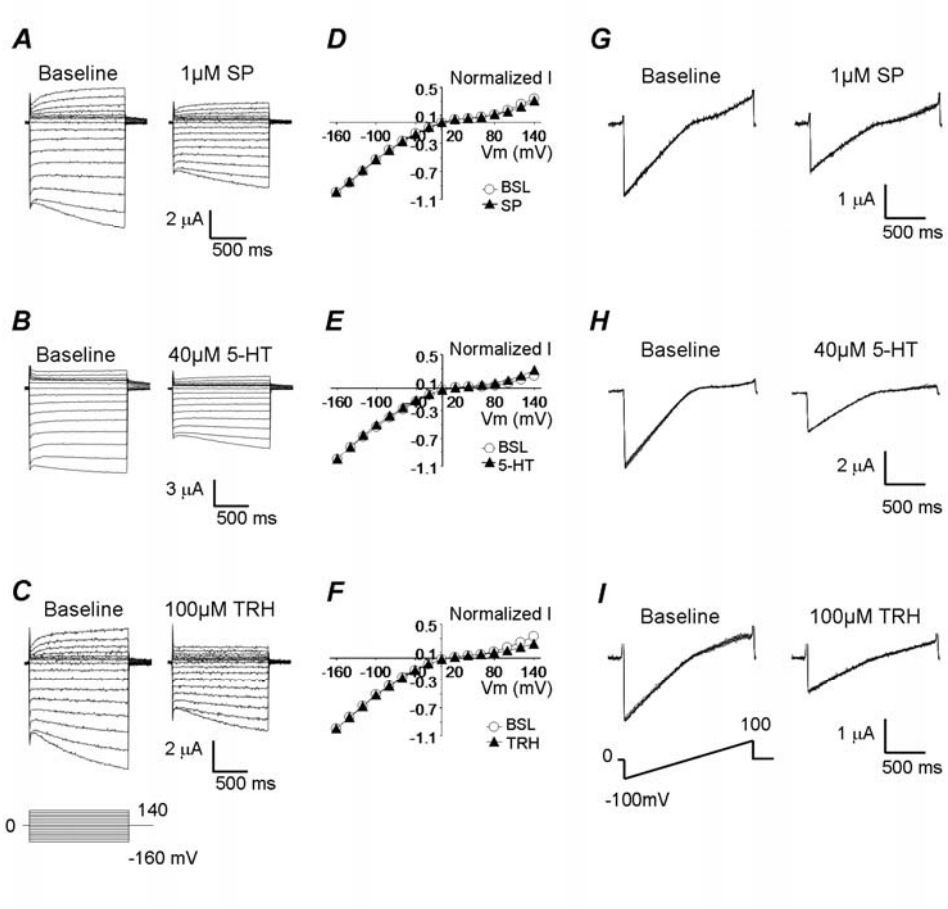

Fig II-1. Kir4.1-Kir5.1 channel is inhibited by SP, 5-HT, and TRH. *A, B, C*. Using TEVC whole-cell Kir4.1-Kir5.1 currents were recorded from an oocyte 3 days post-injection of the Kir4.1-Kir5.1 dimer cDNA along with the NK1R, 5-HT2A, and mTRH-R1 receptor cDNAs. With 90 mM K^+ in the extracellular solution inward rectifying currents were recorded at baseline. Membrane potential (V_m) was held at 0 mV. A series of command pulse potentials from –160 mV to 140 mV with a 20-mV increment was applied to the cell. Note that in highly negative membrane potentials, there was slow activation of the currents. Exposure by bath application to 1 μM SP, 40 μM 5-HT, and 100 μM TRH inhibited the currents by 36, 34, and 30%, respectively. *D, E, F*. When baseline and peak PMA affected currents were scaled to the same magnitude at -160 mV, the I/V relationship of the currents recorded under these two conditions were superimposed, suggesting that the effects were voltage-independent. *G, H, I*. Using TEVC whole-cell Kir4.1-Kir5.1 currents were recorded from an oocyte 3 days post-injection of the Kir4.1-Kir5.1 dimer cDNA along with the NK1R, 5-HT2A, and mTRH-R1 receptor cDNAs. With 90 mM K^+ in the extracellular solution inward rectifying currents were recorded at baseline. Membrane potential (V_m) was held at 0 mV with -100 mV and 100 mV applied to the cell using a

ramp protocol. Exposure to 1 μM SP, 40 μM 5-HT, and 100 μM TRH inhibited the currents in a similar manner as in A, B, C.

The response to SP, DOI (a potent 5-HT2A agonist), and TRH showed clear dose dependence. The maximum inhibition by SP (44.6±4.6% (n=9) occurred with 50 μM SP (Fig. 2A). Channel inhibition (8.7±1.2%, n=4) was seen with SP concentrations as low as 1 nM. Similarly, 160 μM DOI produced the maximum inhibition of the Kir4.1-Kir5.1 currents by 56.1±6.8% (n=4), while significant channel inhibition was seen with 10 μM DOI (21.9±7.5%, n=7) (Fig. 2B). Dose-dependent inhibition was also observed with TRH (Fig. 2C). The concentrations represented by the gray bars in Figure 2 were used in subsequent experiments as these concentrations are within the physiological range and have been used before (Bajic et al., 2002; Cream et al., 1997; Koike-Tani et al., 2005; Lei et al., 2001; Mao et al., 2004; Mutolo et al., 1999).

Specificity of the neurotransmitter effects was examined using specific antagonists. Pre-incubation of oocytes expressing the Kir4.1-Kir5.1+NK1R with 10 μM spantide I, a competitive peptide antagonist for SP, markedly attenuated the effect of 1 μM SP (Fig. 2D). Higher concentrations of spantide I (30 μM) more potently attenuated the effect of 1 μM SP by over 60% (15.9±4.6% inhibition, n=4) (Fig. 2D). Similar attenuation was seen with 10 μM L-703,606, a non-competitive receptor blocker (23.7±3.0%, n=4) (Fig. 2D). Pre-incubation of oocytes expressing the Kir4.1-Kir5.1+5-HT2A with 40 μM ketanserin or 40 μM spiperone, two 5-HT2A receptor antagonists, almost completely abolished the effect of 40 μM DOI that inhibited the currents by 5.3±4.5% (n=6) and 8.9±3.1% (n=5), respectively (Fig. 2E). Since there is no commercially available antagonist for the mTRH-R1 receptor, we used the mTRH-R2

receptor to demonstrate the specificity as it is less sensitive to TRH than the mTRH-R1 receptor. Indeed,

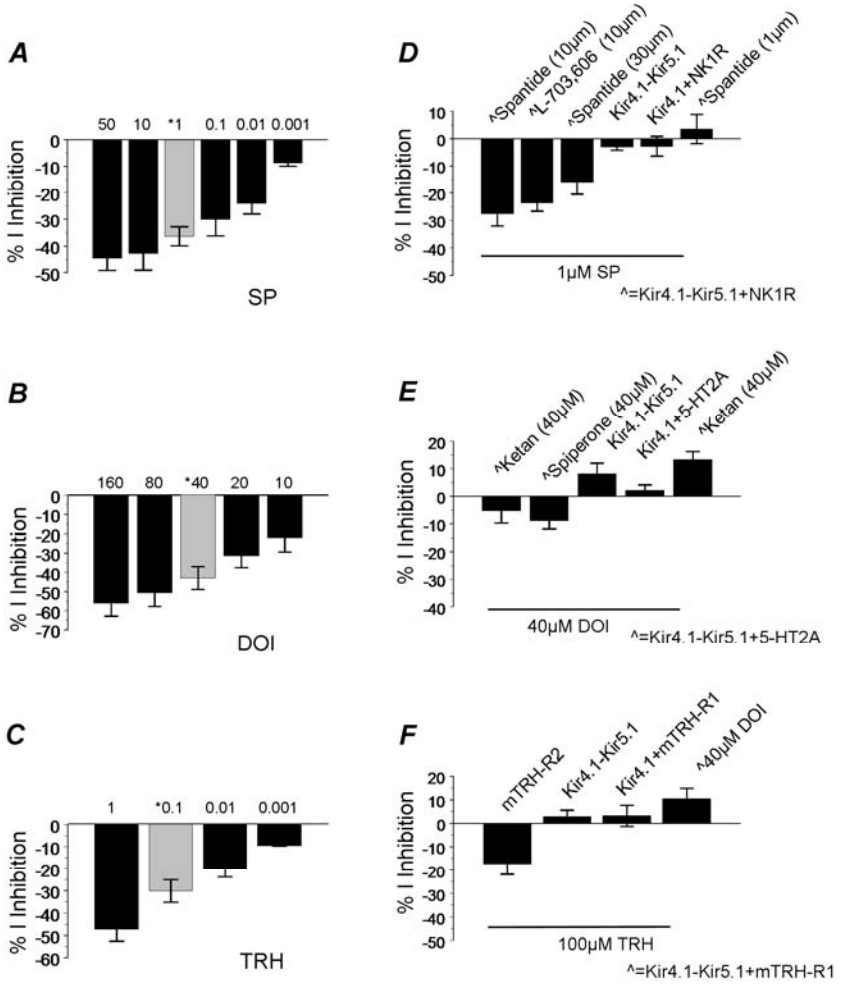

Fig II-2. Specificity and concentration-dependence of the neurotransmitter effect. *A, B, C*. The effect of SP, DOI, and TRH on the Kir4.1-Kir5.1 channel was clearly concentration-dependent (n≥4). The Kir4.1-Kir5.1 channel was inhibited by low concentrations of each agonist. Exposure to higher concentrations of the agonists resulted in greater channel inhibition. The gray bars represent the concentrations used for further experiments. The concentrations in A and B are μM. The concentrations in C are mM. *D, E, F*. Specificity for the receptor-mediated channel inhibition was studied. The channel inhibition was attenuated in the presence of specific antagonists of the neurotransmitters or receptors. The Kir4.1-Kir5.1 channel expressed without receptors failed to be inhibited by the neurotransmitters. Also, SP, DOI, and TRH failed to inhibit the homomeric Kir4.1 channel expressed with the respective receptors. n≥4 for each experiment.

100 μM TRH inhibited the Kir4.1-Kir5.1+mTRH-R1 to a greater degree than the Kir4.1-Kir5.1+mTRH-R2 (Fig. 2F).

Injection of the Kir4.1 cDNA along with the NK1R, 5-HT2A, or mTRH-R1 expressed typical Kir4.1 currents. Strikingly, the homomeric Kir4.1 channel was not capable of being inhibited by SP, DOI, or TRH (Fig. 2D, E, F). Furthermore, the Kir4.1-Kir5.1 channel expressed without exogenous receptors failed to be inhibited by SP, DOI and TRH (Fig. 2D, E, F). Taken together these results strongly suggest that inhibition of Kir4.1-Kir5.1 currents by SP, DOI, and TRH is specific depending on their receptors and requiring the expression of both Kir4.1 and Kir5.1 subunits.

Although the exposure was carried out by application of the neurotransmitters to the bath solution, the time-dependent inhibition occurred rapidly. The inhibition started within the first minute and reached a maximal effect in ~15 min (Fig. 3A, B). At the maximal effect, 37.8% of the inward rectifying currents were inhibited by 1 μM SP. The effect of DOI on the Kir4.1-Kir5.1 currents was also time dependent. The inhibition occurred rapidly, starting within the first minute after exposure to the chemicals and reaching a maximal effect in ~10 min (Fig. 3C, D). In the presence of 100 μM TRH the Kir4.1-Kir5.1 currents were inhibited by 29% with a rapid onset and reaching a maximal effect in ~10 min (Fig. 3E, F). Thereafter, all neurotransmitter experiments were done with a 10-20 min exposure.

The Kir4.1-Kir5.1 co-expressed with the mu-opioid receptor (MOR) failed to be regulated by 1 μM DAMGO, an enkephalin analog and potent activator of the MOR (Fig.

3G, H). Since the MOR is also a GPCR, this result suggests that the Kir4.1-Kir5.1 channel may not interact with G-proteins directly.

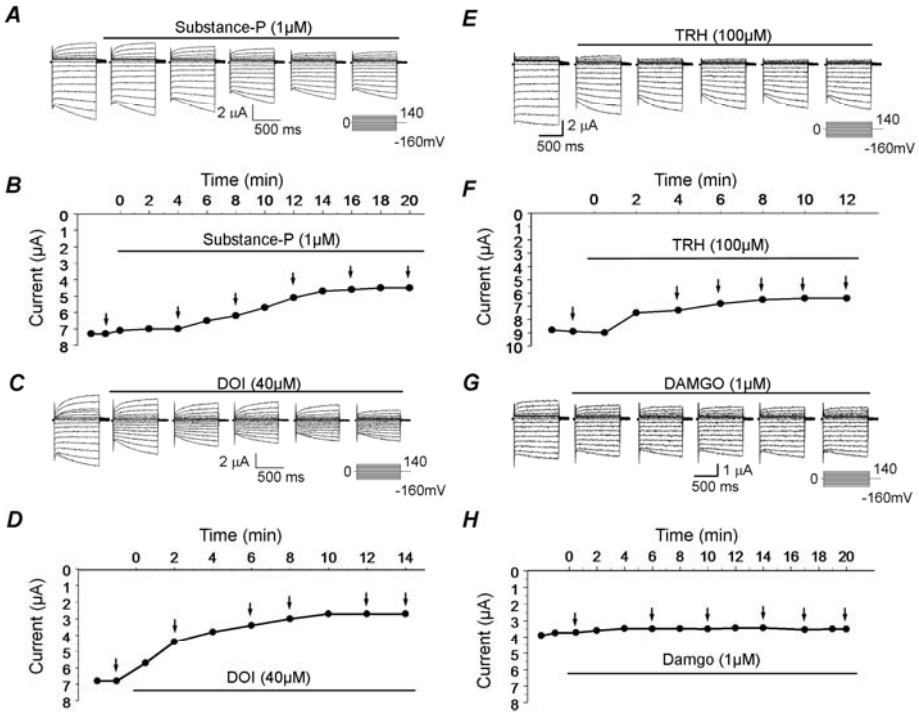

Fig II-3. Time-dependent effects. *A*. Using TEVC whole-cell Kir4.1-Kir5.1 currents were recorded from an oocyte 3 days post-injection of the Kir4.1-Kir5.1 dimer cDNA along with the NK1R receptor cDNA. With 90 mM K^+ in the extracellular solution inward rectifying currents were recorded at baseline. Membrane potential (V_m) was held at 0 mV. A series of command pulse potentials from –160 mV to 140 mV with a 20-mV increment was applied to the cell. Exposure to 1μM SP inhibited the channel currents by ~36%. *B*. The time profile showed that the current amplitude decreased rapidly when SP was present in the bath solution, and reached maximum inhibition in ~15 min. *C*. Whole cell currents were recorded from an oocytes 3 days post injection of the Kir4.1-Kir5.1 tandem-dimer along with the 5-HT2A as described in A. *D*. The time profile shows that DOI decreased the current amplitude rapidly when applied to the bath solution. The maximum inhibition was reached in ~10 min. *E*. Whole cell currents were recorded from an oocytes 3 days post injection of the Kir4.1-Kir5.1 tandem-dimer along with the mTRH-R1 as described in A. *F*. The time profile shows that TRH decreased the current amplitude rapidly when applied to the bath solution. The maximum inhibition was reached in ~10 min. *G*. Using TEVC whole-cell Kir4.1-Kir5.1 currents were recorded from an oocyte 3 days post-injection of the Kir4.1-Kir5.1 dimer cDNA along with the mu-opioid receptor (MOR) cDNA as described in A. Exposure to 1 μM DAMGO failed to affect the channel currents *H*. The time profile shows that the current amplitude did not change when DAMGO was present in the bath solution.

IIb-2. ***PKC involvement in the modulation of the Kir4.1-Kir5.1 channel by the neurotransmitters***

The NK1, 5-HT2A, and TRH-R1 are G-protein coupled receptors (GPCRs). These receptors share a common cascade following ligand binding involving activations of $G_{\alpha q}$, phospholipase C and protein kinase C (PKC). The latter has been shown to phosphorylate several Kir channels and regulate their activity (Fakler et al., 1994; Henry et al., 1996; Light et al., 2000; Zhu et al., 1999). For instance, we have previously shown that protein kinase C (PKC) phosphorylation underscores the inhibition of GIRK channels by SP (Mao et al., 2004). Therefore, we conducted experiments to determine whether PKC was involved in the Kir4.1-Kir5.1 channel inhibition by SP, DOI, and TRH as both the Kir4.1 and Kir5.1 subunits contain putative PKC phosphorylation sites. Pre-incubation of oocytes expressing Kir4.1-Kir5.1+NK1R, Kir4.1-Kir5.1+5-HT2A, or Kir4.1-Kir5.1+mTRH-R1 with the specific PKC inhibitor chelerythrine showed a clear attenuation of the SP, DOI, and TRH effects (Fig. 4A, B, C). Calphostin-C, another specific and potent PKC inhibitor, showed strong attenuations of the channel inhibition to 6.7±2.8% (n=6), 3.4±10.8% (n=6), and 11±4.0% (n=8) by SP, DOI, and TRH, respectively (Fig. 4A, B, C).

Exposure of oocytes expressing Kir4.1-Kir5.1+NK1R to 15 nM PMA, a specific and potent PKC activator, inhibited Kir4.1-Kir5.1 currents by 39.8±5.5% (n=5). The same degree of inhibition was also seen in the absence of the NK1R suggesting that the effect is not mediated by receptor phosphorylation (data not shown). The inhibition by 1 μM SP was significantly lessened when the oocytes were prior exposed to PMA (Fig.

4D). Similar effects were observed for DOI and TRH (Fig. 4E, F). The attenuation of PKC activation was also observed when the order of the neurotransmitter and PMA exposure was reversed, suggesting that the effects of the neurotransmitters and PMA are mediated via a common mechanism (Fig. 4G, H, I).

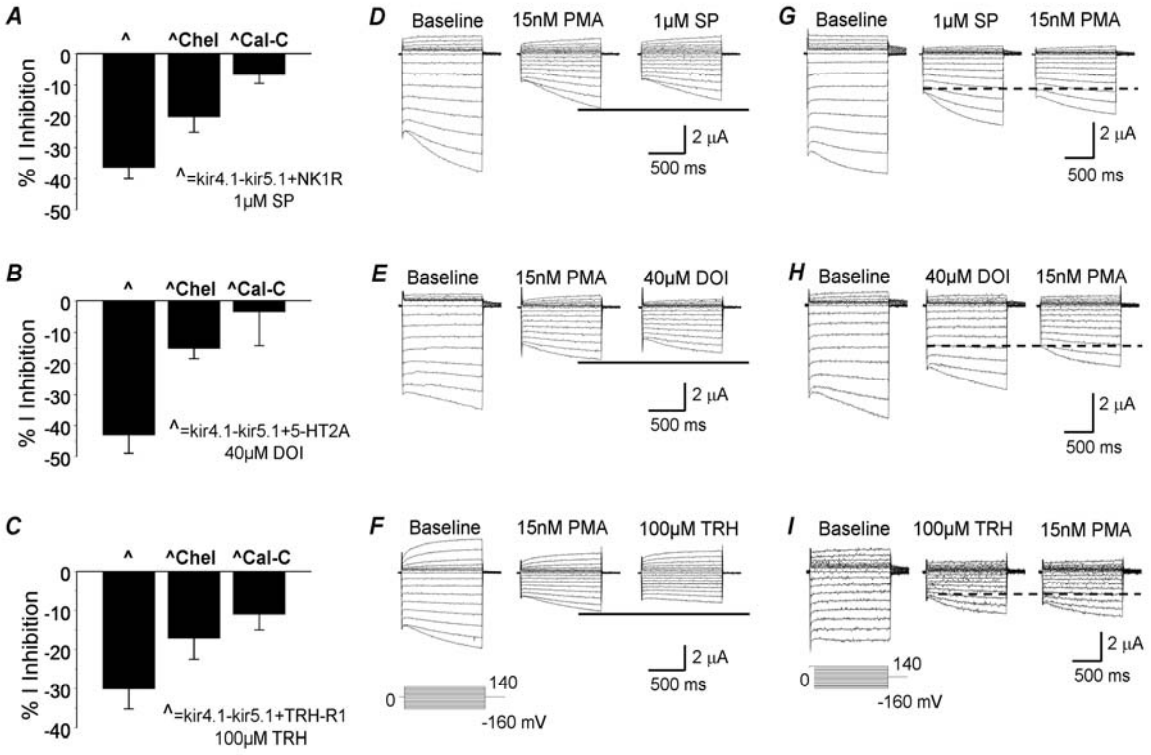

Fig II-4. Involvement of PKC in the Kir4.1-Kir5.1 inhibition by SP, DOI and TRH. *A*, *B*, *C*. Currents were recorded from an oocyte in the same condition as in Figure 1A. Prior to exposure to SP, DOI or TRH the cells were incubated with PKC inhibitors. Pre-incubation of oocytes with specific PKC inhibitors (50 μM chelerythrine or 3 μM calphostin-C) strongly attenuated the effect of SP, DOI, and TRH (n≥4). *D*, *E*, *F*. Currents were recorded from an oocyte in the same condition as in Figure 1A. Following exposure to 15 nM PMA for ~30 minutes the cells were subsequently treated with 1 μM SP or 40 μM DOI. Prior exposure to PMA resulted in a much lower channel response to the neurotransmitters. Instead of 36% current inhibition for SP and 43% current inhibition for DOI, the Kir4.1-Kir5.1 currents were barely inhibited (>10%).*G*, *H*, *I*. Currents were recorded from an oocyte in the same condition as in Figure 1A. Following exposure to SP, DOI or TRH the cells were subsequently treated with 15 nM PMA. Prior exposure to the neurotransmitters resulted in a reduced response to PMA. Instead of 40% current inhibition as indicated by the dashed lines, the Kir4.1-Kir5.1 currents were inhibited by 0~20%.

IIb-3. ***Effects of SP on single-channel properties***

To identify the exact channel mechanism leading to a decrease in the whole cell currents, the effect of SP on the single-channel biophysical properties was studied in cell-attached patches with 145 mM K^+ applied to the extracellular solution at a membrane potential of -80 mV. Inward rectifying currents with a single-channel conductance of ~40 pS (Pessia et al., 1996; Tanemoto et al., 2000; Tanemoto et al., 2004) showing long-lasting openings and closures were recorded from oocytes expressing the Kir4.1-Kir5.1+NK1R (Fig. 5). These currents were inhibited with an exposure to 1 μM SP (Fig. 5A, B). Macroscopic currents also showed a clear inhibition by application of SP to the bath solution (Fig. 5C). The current inhibition was mainly produced by a suppression of the channel open-state probability (NP_o). Plotting the baseline NP_o versus SP NP_o shows a clear reduction in the NP_o (0.43±0.11 at baseline vs. 0.06±0.01 with SP, n=7), while the single-channel conductance did not show any significant changes (Fig. 5D).

IIb-4. ***Relationship with CO_2/pH Sensitivity***

We have previously shown that the Kir4.1-Kir5.1 channel is strongly inhibited by intracellular acidosis (Cui et al., 2001; Xu et al., 2000a; Yang et al., 2000). To understand whether the neural modulation affects the channel sensitivity to pH, the Kir4.1-Kir5.1 channel was co-expressed in *Xenopus* oocytes with the NK1R or 5-HT2A. Following stabilization the cells were perfused with 1 μM SP or 40 μM DOI until the plateau effect was reached. Subsequently, the cells were exposed to 90 mM $KHCO_3$ that has been shown to reduce intracellular pH (pH_i) to ~6.6. Intracellular acidosis inhibited the Kir4.1-Kir5.1 channel expressed without receptors by 58.2±2.4% (n=8), by 60.8±1.5% (n=9) in

the presence of the NK1R and by 55.0±3.7% (n=5) with the 5-HT2A receptor, respectively. No significant difference was found, suggesting that the presence of the receptors do not interfere with the channel sensitivity to CO_2. Following SP and DOI

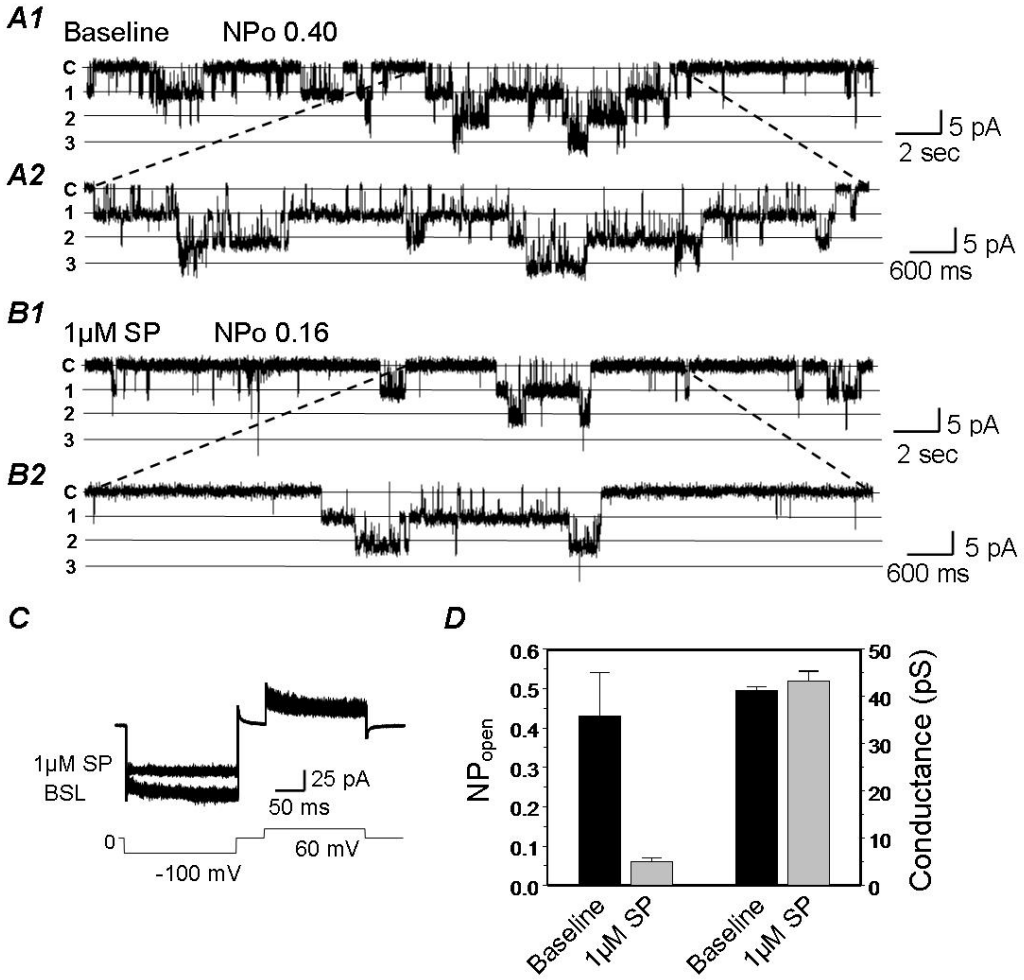

Fig II-5. Effects of SP on the single channel activity of Kir4.1-Kir5.1. *A*. Single Kir4.1-Kir5.1 currents were recorded from an oocyte in a cell-attached patch configuration with 145 mM K^+ in the patch pipette. At V_m of -80 mV, two active channels are seen at pH 7.4. *B*. Following stabilization, exposure to 1 μM SP reduced the channel activity mainly by a decrease in the NPo. Labels on the left: c, closure; 1, the first opening; 2, the second opening; etc. Labels on the top represent NPo at baseline and NPo at SP exposure level. *C*. Reduction of the macroscopic inward currents can be seen in the cell-attached patch configuration. *D*. Bargraph showing that 1 μM SP drastically reduced the NPo, but only slightly affected the single-channel conductance (n≥6).

exposure all of the oocytes tested were further inhibited by intracellular acidosis in the presence of the neurotransmitters (Fig. 6A, D), and recovered with washout. The time course showed that following SP and DOI inhibition, the channel was rapidly inhibited by intracellular acidosis to the same degree as in the absence of the neurotransmitters (Fig. 6B, E), suggesting that the neurotransmitters and CO_2 inhibit the channel through independent mechanisms. Also both CO_2 and neurotransmitters have a partial additive effect leading to a stronger channel inhibition when both are present ($P<0.05$, $n\geq4$; Fig. 6C, F). The same experiments were repeated with 15% CO_2 and similar results were obtained (Fig. 6C, F).

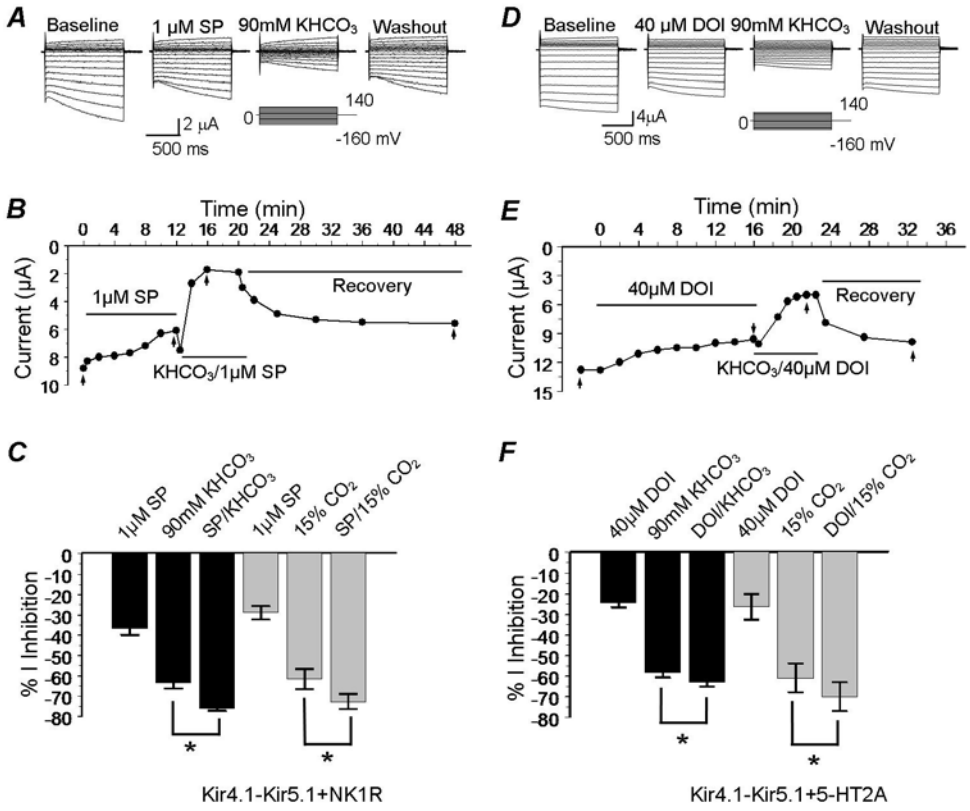

Fig II-6. Independent regulation of the Kir4.1-Kir5.1 channel by neurotransmitters and pHi. *A, B.* Using TEVC whole-cell Kir4.1-Kir5.1 currents were recorded from an oocyte 3 days post-injection of the Kir4.1-Kir5.1 dimer cDNA along with the NK1R. With 90 mM K^+ in the extracellular solution inward rectifying currents were recorded at baseline. Membrane potential (V_m) was held at 0 mV. A series of command pulse potentials from –160 mV to 140 mV with a 20-mV increment was applied to the cell. Following exposure to 1 μM SP, the cells were perfused with 90 mM $KHCO_3$ (pHi≈6.6). Such an exposure resulted in a further inhibition of the Kir4.1-Kir5.1 currents to the degree identical to that of $KHCO_3$ exposure alone, suggesting that the two channel inhibitors are independent of each other. Washout allowed the currents to recover to the level prior to $KHCO_3$ exposure. *C*. The percent effect shows that exposure to SP/$KHCO_3$ gives a larger inhibition of the Kir4.1-Kir5.1 currents than either modulator alone. *D, E*. Using TEVC whole-cell Kir4.1-Kir5.1 currents were recorded from an oocyte 3 days post-injection of the Kir4.1-Kir5.1 dimer cDNA along with the 5-HT2A in a similar manner as in A. Following exposure to 40 μM DOI, the cells were perfused with 90 mM $KHCO_3$ (pHi≈6.6). Such an exposure resulted in a further inhibition of the Kir4.1-Kir5.1 currents. Washout allowed the currents to recover to the level prior to $KHCO_3$ exposure. *F*. The percent effect shows that exposure to DOI/$KHCO_3$ gives a larger inhibition of the Kir4.1-Kir5.1 currents than either

modulator alone. Both sets of experiments were repeated with 15% CO_2 represented by the gray bars. n≥4 for each experiment. The SP and DOI effects are relatively slow and long-lasting, while the effect of 90 mM $KHCO_3$ is rapid and fully reversible. The asterisk represents the comparable difference between $KHCO_3$ and neurotransmitter+$KHCO_3$ as well as the comparible difference between 15% CO_2 and the neurotransmitter+15% CO_2. Differences were considered to be statistically significant if $P \leq 0.05$. The arrows in B and E represent the time points shown in panels A and D.

IIb-5. ***Modulation of brainstem neurons by neurotransmitters***

To demonstrate the modulation of brainstem neurons by the neurotransmitters SP and 5-HT we took advantage of multi-electrode array (MEA) technology. Neurons were isolated from the brainstem of fetal rats and cultured on MEA dishes as detailed in the methods section (Su & Jiang, 2006; Su et al., 2007). Extracellular recordings were carried out in the DMEM medium at 37 ºC. Single-unit recordings were identified using the Offline Sorter software based on the principal component analysis methods (Horn & Friedman, 2003). Single-unit recordings were also determined by the absence of action potentials in the initial period (5-100ms) of the inter-spike histogram. Most spikes showed a negative-positive waveform with a duration > 1 ms, suggesting that they were recorded from the soma (Gustafsson & Jankowska, 1976; Jiang & Lipski, 1990). Neuronal responses to CO_2, SP and DOI were studied. Changes in neuronal firing rate were determined with a change in CO_2 from 5% (basal level) to 9.2% (hypercapnia). The CO_2-augmented units whose firing rate increased during acidosis (Fig. 7A, E) were chosen for further study, although neurons that were inhibited by CO_2 or showed no response were also observed (Su and Jiang, 2006; Su et al., 2007). Following washout of the CO_2, the cells were exposed to SP and DOI that augmented reversibly the firing frequency of a group of neurons (Fig. 7B, C, F, G). To determine whether PKC played a role, 100 nM calphostin-C was applied to the MEA dish for 1 hour prior to application of SP and DOI. Action potentials were recorded before and after application of calphostin-C. In the presence of calphostin-C, SP and DOI only modestly augmented the firing rate (Fig. 7D, H). Statistical analysis showed that the difference in the effects of SP and DOI

before versus after calphostin C treatment was significantly different ($P<0.01$ for both SP and DOI) (Fig. 7D, H).

Immunocytochemistry showed that both Kir4.1 and Kir5.1 subunits were co-localized in cultured brainstem neurons that also displayed positive immunoreactivity of the microtubule-associate protein 2 (MAP2) (Fig. 8). Control experiments were performed with HEK293 cells, demonstrating the specificity of the anti-Kir4.1 and anti-Kir5.1 antibodies (shown in prior part).

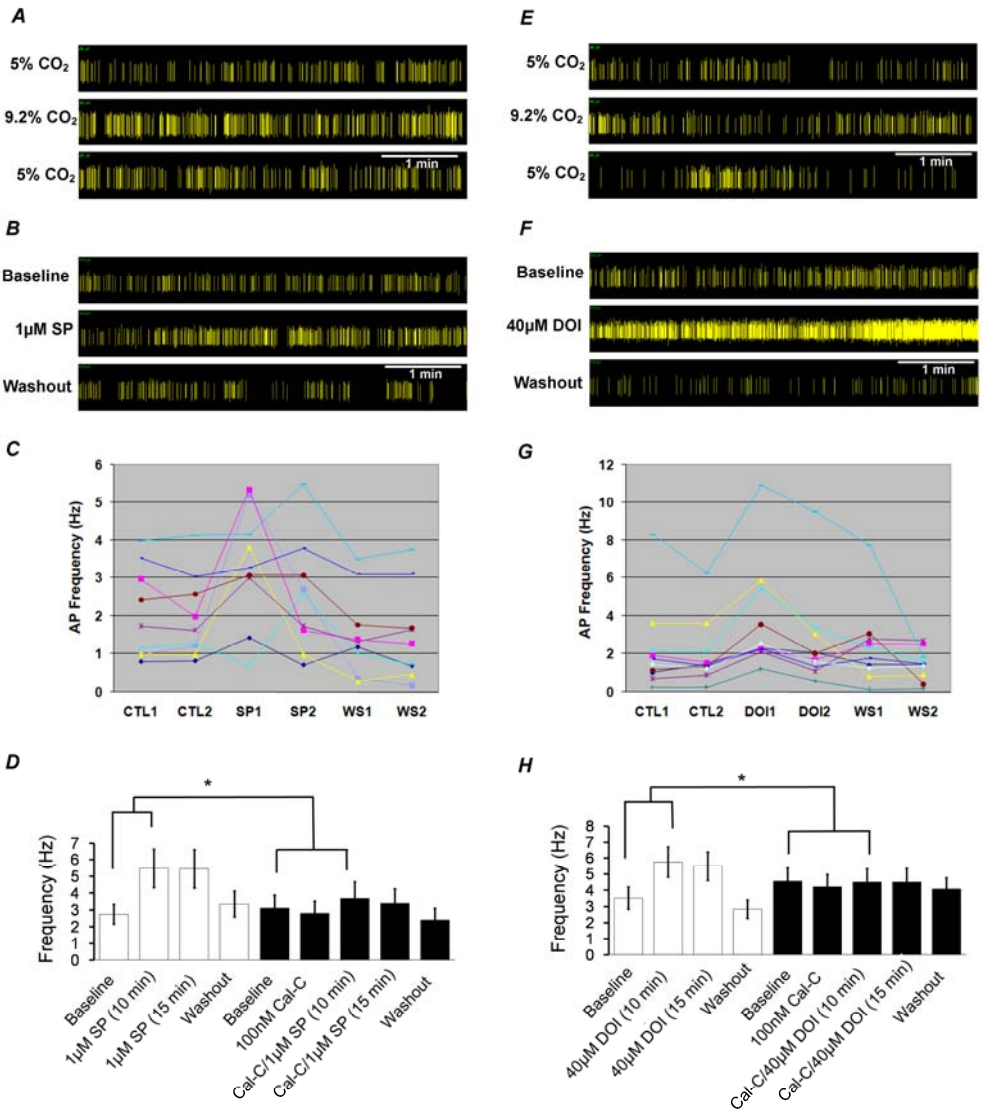

Fig II-7. Modulation of brainstem neurons by neurotransmitters. *A*. A single unit was recorded from a 14-day brainstem neuronal culture using the multiple electrode arrays technique in 5% CO_2. The spikes had a negative-positive waveform with a duration >1 ms, and the 2D cluster plot and the interspike interval (ISI) histogram indicated single-unit recording. Increasing CO_2 to 9.2% augmented the firing frequency shown in a period of 5 min. *B*. The same unit recorded in A was stimulated during exposure to 1 μM SP. *C*. The effect of SP on the average firing frequency from a 5 min recording. SP1=the first recording taken following SP application. SP2=the second recording taken following SP application. Nine units were stimulated during SP exposure. Washout led to complete recovery. *D*. Following pre-incubation with 100 nM calphostin-C (cal-

C) for 1 hour the stimulatory effect of SP was greatly reduced. *E*. A single unit was recorded from a 14-day brainstem neuronal culture using the multiple electrode arrays technique in 5% CO_2. The spikes had a negative-positive waveform with a duration >1 ms, and the 2D cluster plot and the interspike interval (ISI) histogram indicated single-unit recording. Increasing CO_2 to 9.2% augmented the firing frequency shown in a period of 5 min. *F*. The same unit recorded in E was strongly stimulated during exposure to 40 μM DOI. *G*. The effect of DOI on the average firing frequency from a 5 min recording. Ten units were stimulated during DOI exposure. Washout led to complete recovery. DOI1=the first recording taken following DOI application. DOI2=the second recording taken following DOI application. *H*. Following pre-incubation with 100 nM calphostin-C for 1 hour the stimulatory effect of DOI was greatly reduced. CTL=control, SP=substance P, DOI=4-Iodo-2, 5-dimethoxyamphetamine, WS=washout.

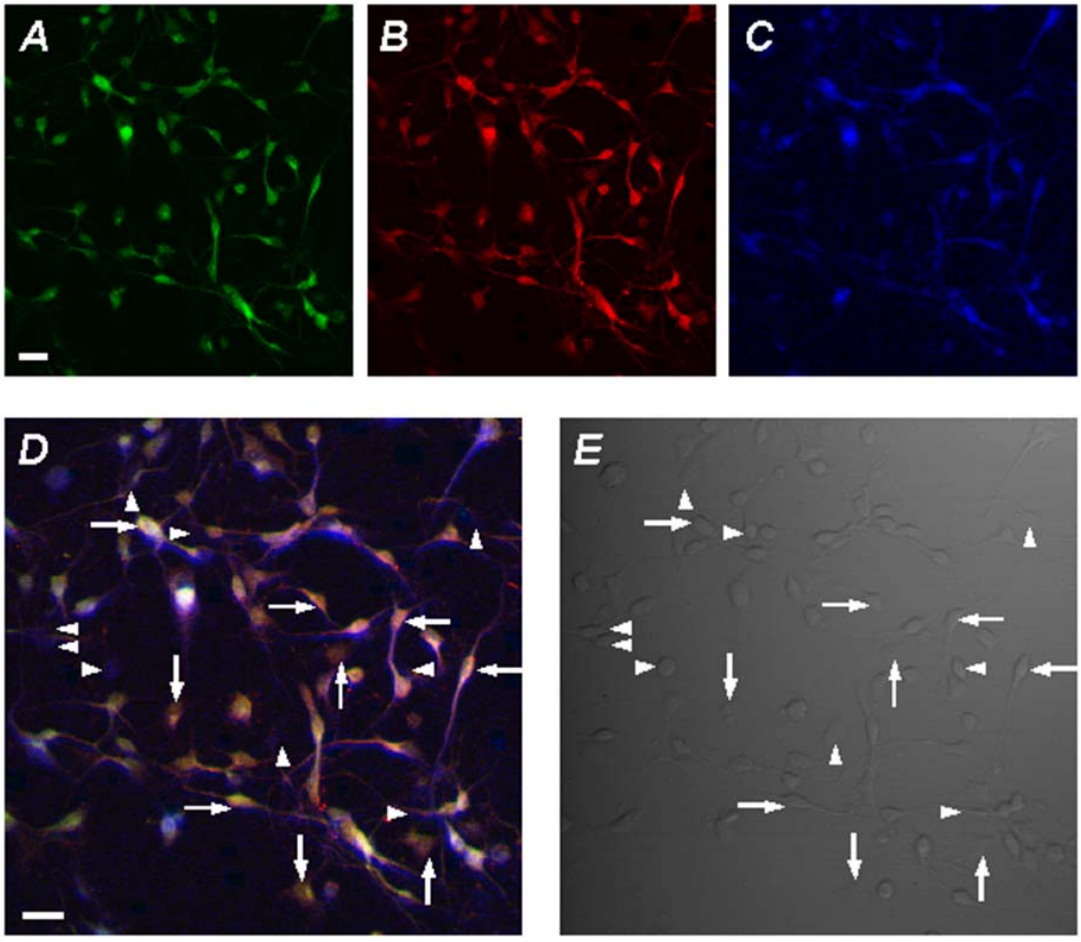

Fig II-8. Expression of Kir4.1-Kir5.1 in brainstem neurons. *A.* Immunocytochemistry was performed on cultured brainstem neurons. *A.* Shows positive immunoassaying for Kir4.1. *B.* Shows positive immunoassaying for Kir5.1. *C.* Blue fluorescence indicates the presence of the neuronal marker microtubule associated protein 2 (MAP2). *D.* Overlay of A, B, C. The horizontal arrows represent typical neurons expressing the Kir4.1 and Kir5.1 subunits. Vertical arrows represent typical glia cells expressing Kir4.1 and Kir5.1. Horizontal arrowheads indicate neurons void of Kir4.1 and Kir5.1. The vertical arrowheads indicate glia void of Kir4.1 and Kir5.1. *E.* Shows the phase contrast (note that majority of cells are neurons). Bar=20 μm.

IIb-6. ***Amplification of CO_2 chemosensitivity by synaptic transmission***

The high sensitivity of central chemoreceptors may be attributed to a potential amplification mechanism in the neuronal network. If this is the case, blockade of presynaptic input should reduce neuronal CO_2 chemosensitivity. We thereby performed studies to test this hypothesis. Since several groups of serotonin producing neurons in the brainstem are CO_2 chemosensitive (Wang et al. 1998; Severson et al. 2003), we used 20 μM ketanserin to block 5-HT2A receptors known to play an important role in respiratory control (Richerson 2004; Tryba et al. 2006). Ketanserin markedly diminished neuronal responses to hypercapnia from 4.88 ± 0.84 Hz to 3.07 ± 0.69 Hz ($P<0.001$, n=28, paired t test) (Fig. 9, Fig. 10A). Amongst 29 CO_2-stimulated units in 3 MEA dishes, only 2 cells lost their CO_2 sensitivity completely. The CO_2 chemosensitivity of such a small number of cells was interpreted to be derived solely from presynaptic input. The other 27 units remained to be stimulated by hypercapnia to various degrees. Of these 27 units, 20 showed significant reduction in their CO_2 sensitivity, suggesting that the CO_2 chemosensitivity of most neurons is determined by both pre- and postsynaptic mechanisms. The CO_2 chemosensitivity of the remaining 7 units was either retained (n=2) or slightly enhanced (n=5) with ketanserin, suggesting that their CO_2 chemosensitivity is independent of serotonergic input or slightly inhibited by serotonergic input.

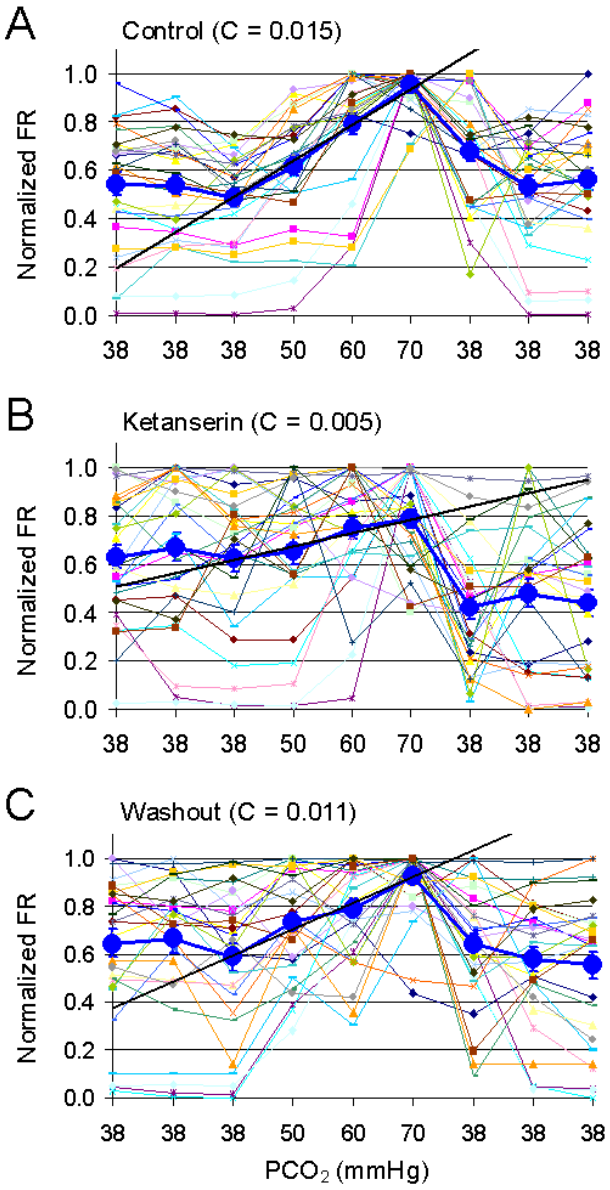

Fig II-9. Neuronal FR before, during and after ketanserin during CO_2 exposure. Neuronal FR was studied before, during and after ketanserin (20μM) exposure in two MEA dishes. Neuronal FR was normalized to the peak frequency, and plotted against P_{CO2} levels. Ketanserin drastically attenuated neuronal response to hypercapnia (0.62 ± 0.06 to 0.79 ± 0.04, $P<0.05$, n=28, ANOVA). C is the slope of the bold black line and it represents the sensitivity index that was determined: $\Delta FR / \Delta P_{CO2}$, where ΔFR is the percentage change in the firing rate and ΔP_{CO2} is the change in P_{CO2} (mm Hg). The value C = 0.0067 corresponds to a 0.67% change in FR per mm Hg P_{CO2}.

Another group of candidate CO_2 chemoreceptors are glutamatergic neurons, especially those in the retrotrapezoid nucleus that are activated by glutamate (Mulkey et al. 2004). We found that neuronal CO_2 sensitivity was significantly inhibited from 2.41 ± 0.57 Hz to 1.40 ± 0.44 Hz ($P<0.001$, n=28, paired t test) in the presence of 10μM CNQX, a non-NMDA receptor antagonist (23 reduced, 2 enhanced, and 4 lost response out of 29 units in 4 MEAs) (Fig. 10B). Similar effect was found with blockade of NK1 receptors (from 1.57 ± 0.40 Hz to 0.85 ± 0.25 Hz; $P<0.01$, n=21, paired t test) in the presence of 100μM spantide (of 22 units in 3 MEAs, CO_2 sensitivity was reduced in 17 units, enhanced in 3, and lost in 2) (Fig. 10C). In contrast, blockade of purinergic P2x receptors that have been suggested to be involved in CO_2 chemosensitivity (Thomas et al. 1999; Gourine et al. 2005) with 10μM PPADS did not show any significant effect (from 2.24 ± 0.79 Hz to 2.66 ± 0.92 Hz; $P>0.05$, n=36) (Fig. 10D), suggesting that the enhancement of CO_2 chemosensitivity is rather specific to certain synaptic connections.

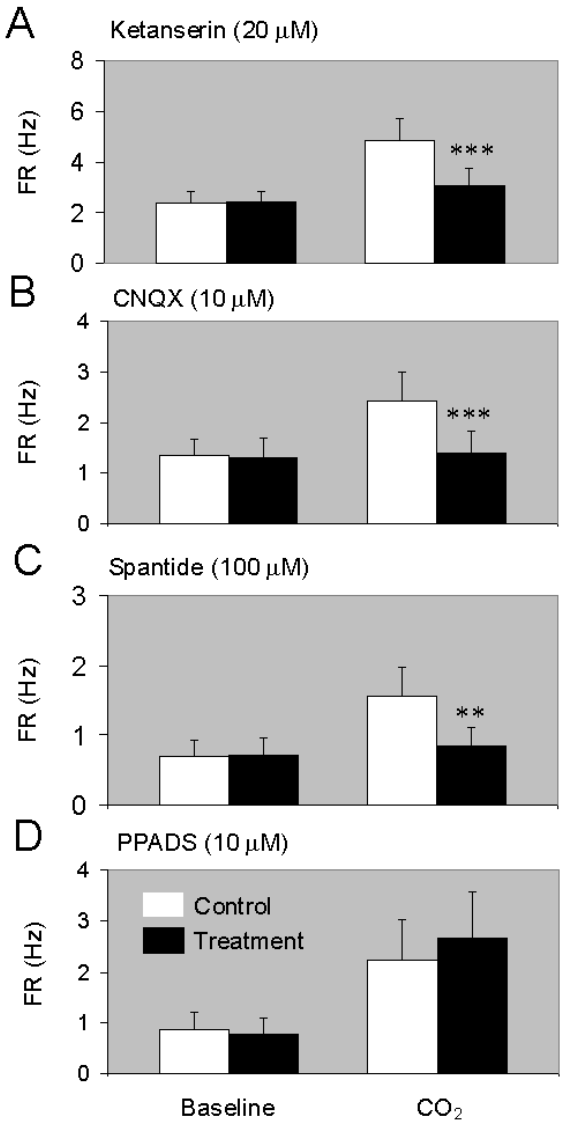

Fig II-10. A. Average FR with and without ketanserin during CO_2 exposure. When the average FR was compared with and without ketanserin, significant reductions in the FR were seen during CO_2 (70 mm Hg) exposure ($P<0.001$, n=28 from 3 MEAs, paired t test). B,C. Similar attenuations of the hypercapnic response were observed with CNQX ($P<0.001$, n=28 from 4 MEAs, paired t test) and spantide ($P<0.01$, n=21 from 3 MEAs, paired t test). D. PPADS, a P2x receptor blocker, did not have significant effect ($P>0.05$, n=36 from 3 MEAs, paired t test). Note that the units studied did not show significant differences in their baseline FR with and without the blockers (A-D).

IIc. DISCUSSION

In the present study, we have demonstrated a novel property of the Kir4.1-Kir5.1 channel but not the Kir4.1, i.e., the capability to be modulated by several neurotransmitters. This finding provides more evidence for the functional significance of the heteromultimerization.

The Kir4.1 and Kir5.1 subunits are expressed in brainstem neurons. The mRNAs of both Kir subunits have been detected in various nuclei within the brainstem (Wu et al., 2004). Several studies have demonstrated specific expression of Kir4.1 and Kir5.1 at the protein and mRNA level in oligodendrocytes and astrocytes in the CNS (Hibino et al., 1999; Hibino et al., 2004; Higashi et al., 2001). Here, we have shown expression of both the Kir4.1 and Kir5.1 proteins in cultured brainstem neurons. Although direct evidence demonstrating the involvement of this channel in central CO_2 chemoreception is lacking the co-expression of the Kir4.1 and Kir5.1 subunits in the same neurons strongly suggests that the heteromeric Kir4.1-Kir5.1 channel may form in brainstem neurons.

Several neurotransmitters are particularly important for the brainstem control of respiration including substance-P, serotonin, and thyrotropin releasing hormone. These neuromodulators have been shown to regulate central respiratory activity *in vitro* and *in vivo* (Cream et al., 1997; Dekin et al., 1995; Hodges et al., 2004; Moss et al., 1986; Mutolo et al., 1997; Nattie & Li, 2002; Nattie et al., 2004; Nink et al., 1991; Pete et al., 2002; Richerson, 2004; Richerson et al., 2005; Schulz et al., 1996; Severson et al., 2003; Taylor et al., 2005; Wang et al., 2001; Wenninger et al., 2004a; Wenninger et al., 2004b). In the present study, we have shown evidence for the inhibition of the heteromeric

Kir4.1-Kir5.1 channel by these neurotransmitters. Exposures to SP, 5-HT, and TRH resulted in inhibition of the Kir4.1-Kir5.1 channel currents when the channel was expressed with the corresponding receptors in *Xenopus* oocytes. The neurotransmitter effects were reversible, specific and dependent on ligand concentrations. The current inhibition is voltage-independent and is mediated by selective inhibition of Po with no effect on single-channel conductance.

We previously showed that PKC underscored the inhibition of GIRK channels by substance-P (Mao et al., 2004). Therefore, we assayed for the involvement of PKC in the inhibition of the heteromeric Kir4.1-Kir5.1 channel by SP, DOI and TRH. Our results suggest that PKC activation also underscores the inhibition of the Kir4.1-Kir5.1 channel by these neurotransmitters. In cultured brainstem neurons, inhibition of PKC led to a dramatic attenuation of the augmentation of the firing frequency in neurons by SP and DOI, suggesting that PKC activation also underscores the SP and DOI dependent increase in the firing rate of the cultured brainstem neurons.

The modulation of the Kir4.1-Kir5.1 channel by SP, 5-HT, and TRH does not compromise the channel sensitivity to pH, as we have shown that the application of both modulators combined had a greater inhibitory effect on the channel than either modulator alone. This is important physiologically as we know that during central CO_2 chemoreception, there is an amplification of the CO_2 signal.

The neural modulation described in the present study seems to enable the Kir4.1-Kir5.1 channel to function as a distinct member in the Kir channel family. It is known that GIRK channels play a role in neurotransmission (Jan & Jan, 1997; Luscher et al.,

1997; Yamada et al., 1998). A common characteristic of these channels is that their activity is controlled by neurotransmitters and hormones. Clearly such a property is shared by the Kir4.1-Kir5.1 channel, as shown in our current studies.

The neural modulation shown in the present study does not occur in the homomeric Kir4.1 channel and relies on the Kir5.1 that is known to form heteromeric channels only with Kir4x (Casamassima et al., 2003; Konstas et al., 2003; Pessia et al., 2001; Tanemoto et al., 2000). Thus, the expression of the Kir4.1 in cells allows two functional properties that both can control membrane potential and cellular excitability with one of them regulated by extracellular messengers. All of these functional properties therefore allow diverse cellular responses that appear to fit well to the diverse cellular functions in the brainstem and other systems.

Previous studies have demonstrated the presence of CO_2 chemosensitivity in both pre- and postsynaptic neurons (Kawai et al 1996; Kawai et al., 2006; Richerson 1995; Stunden et al 2001; Takakura 2006), which we inferred may allow an amplification of P_{CO2} signals detected by each cell. Consistent with this scenario, our results indicate that CO_2 chemosensitivity is significantly reduced when 5-HT2A, NK1 or non-NMDA receptors are blocked, all of which are receptors for neurotransmitters that play an important role in the modulation of central respiratory activity and CO_2 chemosensitivity (Feldman et al, 2003; Richerson 2004; Guyenet 2005). Blockade of the P2x receptor, however, did not produce evident attenuation of the CO_2 chemosensitivity, consistent with two recent studies showing lack of effect on the CO_2 chemosensitivity by P2x receptor blockade (Lorier et al., 2004; Mulkey et al. 2006).

IId. SUMMARY AND CONCLUSION

The heteromeric Kir4.1-Kir5.1 channel is a candidate sensing molecule for CO_2 central chemoreception. Since CO_2 central chemoreception is subject to neural modulations, we performed studies to test the hypothesis that the Kir4.1-Kir5.1 channel is modulated by the neurotransmitters critical for respiratory control, including serotonin (5-HT), substance-P (SP), and thyrotropin releasing hormone (TRH). The heteromeric Kir4.1-Kir5.1 channel was strongly inhibited by SP, TRH, and 5-HT when expressed in *Xenopus* oocytes, whereas these neurotransmitters had no effect on the homomeric Kir4.1 channel. Such an inhibition was dose-dependent and relied on specific $G_{\alpha q}$-protein-coupled receptors and protein kinase C (PKC). No direct interaction of the channel with G-proteins was found. Channel sensitivity to CO_2/pH was not compromised with the inhibition by these neurotransmitters, as the channel remained to be inhibited by acidic pH following an exposure to the neurotransmitters. The firing rate of CO_2-sensitive brainstem neurons cultured in microelectrode arrays was augmented by SP or a 5-HT2A receptor agonist, which was blocked by PKC inhibitors suggesting that PKC underscores the inhibitory effect of SP and 5-HT in cultured brainstem neurons as well. Immunostaining showed that both Kir4.1 and Kir5.1 proteins were co-localized in the cultured brainstem neurons. These results therefore indicate that the heteromeric Kir4.1-Kir5.1 channel is modulated by the neurotransmitters critical for respiratory control, suggesting a novel neuromodulatory mechanism for the chemosensitivity of brainstem neurons to elevated P_{CO2} and acidic pH. The CO_2 chemosensitivity was reduced but not eliminated by blockade of presynaptic input from serotonin, substance P or glutamate neurons, indicating that both

pre- and postsynaptic neurons contribute to the CO_2 chemosensitivity. This strongly suggests that the high sensitivity may be achieved by cellular mechanisms via synaptic amplification in cultured brainstem neurons.

III. PROTEIN KINASE C DEPENDENT INHIBITION OF THE HETEROMERIC KIR4.1-KIR5.1 CHANNEL*

Manuscript in press:

Asheebo Rojas, Ningren Cui, Junda Su, Liang Yang, Jean-Pierre Muhumuza, and Chun Jiang. Protein Kinase C Dependent Inhibition of the Heteromeric Kir4.1-Kir5.1 Channel. *BBA-Biomembranes* (2007).

*In this part, Dr. Junda Su performed 20% of the cDNA injections. Dr. Ningren Cui performed 30 % of the whole cell recordings. Dr. Liang Yang and Mr. Jean-Pierre Muhumuza (combined) created 40% of the mutations on the Kir4.1-Kir5.1 and did Mini and Midi preparations. All of their help is greatly appreciated.

IIIa. INTRODUCTION

It is known that the central CO_2 chemoreception and K^+ transport in renal epithelium are regulated by neurotransmitters, hormones and pharmacological agents through specific intracellular signaling systems (Feldman et al., 2003; Germann & Stanfield, 2005; Richerson, 2004). Therefore, it is possible that the heteromeric Kir4.1-Kir5.1 channel is regulated by certain second messenger systems. Such a modulation may enable cells expressing the Kir4.1-Kir5.1 channel to respond to P_{CO2} and pH changes according to systemic needs. One common intracellular signaling system activated by neurotransmitter and hormone is mediated by protein kinase C (PKC). Indeed, a number of consensus sequences of potential PKC phosphorylation sites exist in the Kir4.1 and Kir5.1 subunits. Supporting the idea of PKC phosphorylation are also previous reports indicating that other Kir channels such as Kir3.1-Kir3.4, Kir2.2, Kir2.3, and Kir6.2 are modulated by PKC with several phosphorylation sites identified in these channel proteins (Fakler et al., 1994; Henry et al., 1996; Light et al., 2000; Lin et al., 2000; Mao et al., 2004; Stevens et al., 1999; Vorobiov et al., 1998; Zhang et al., 2004; Zhu et al., 1999; Zitron et al., 2004). Therefore, we performed experiments to test the possibility that PKC regulates the Kir4.1-Kir5.1 channel. Our results showed that the Kir4.1-Kir5.1 channel was strongly inhibited by the activation of PKC.

IIIb. RESULTS

IIIb-1. *Inhibition of the Heteromeric Kir4.1-Kir5.1 Channel by PMA*

In two-electrode voltage clamp, inward rectifying K^+ currents were recorded from *Xenopus* oocytes 2-3 days post injection of the Kir4.1-Kir5.1 cDNA using a bath solution containing 90 mM K^+. Typical Kir4.1-Kir5.1 currents were revealed: small outward currents and large inward currents with slow activation at highly negative membrane potentials (Fig. 1A). Following stabilization of the baseline currents, PMA, a specific and potent PKC activator, was added to the bath solution. The PMA exposure resulted in a strong inhibition of the Kir4.1-Kir5.1 currents. Higher concentrations of PMA resulted in a more rapid inhibition of the Kir4.1-Kir5.1 currents (Fig. 2E). This inhibition was dose-dependent (Fig. 3A, B): Evident channel inhibition was seen with PMA concentrations as low as 5 nM; maximum effect occurred with 1 μM PMA at which the Kir4.1-Kir5.1 currents were inhibited by 93.3±1.4% (n=4); and 15 nM PMA inhibited the Kir4.1-Kir5.1 currents by 41.4±2.2% (n=13). In comparison, the homomeric Kir4.1 channel showed no response to 15 nM PMA (Fig. 1B), and was slightly inhibited (8.4±8.6%, n=5) by 100 nM PMA. Numerous attempts were made to express the homomeric Kir5.1 channel. Unfortunately, we were unable to detect inward rectifying K^+ currents that were sensitive to micromolar concentrations of barium in *Xenopus* oocytes and HEK293 cells. Therefore, we were unable to determine the effect of PMA on the Kir5.1 channel.

The voltage dependence was analyzed using the current-voltage (I-V) plot. The currents recorded at -160 mV were normalized to the same level for both baseline and PMA treatment. When plotted in the I-V curve, the curve of the PMA treatment

overlapped that obtained from the baseline suggesting that the inhibition of the Kir4.1-Kir5.1 currents by PMA is voltage independent (Fig. 1C). The same analysis on the Kir4.1 showed an identical effect (Fig. 1D).

When the time course of the Kir4.1-Kir5.1 channel inhibition by 15 nM PMA was plotted, the inhibition started 2 min after exposure to PMA and reached the maximum in ~30 min (Fig. 1E). Thus, all PMA experiments were done with a PMA exposure of 20-40 min.

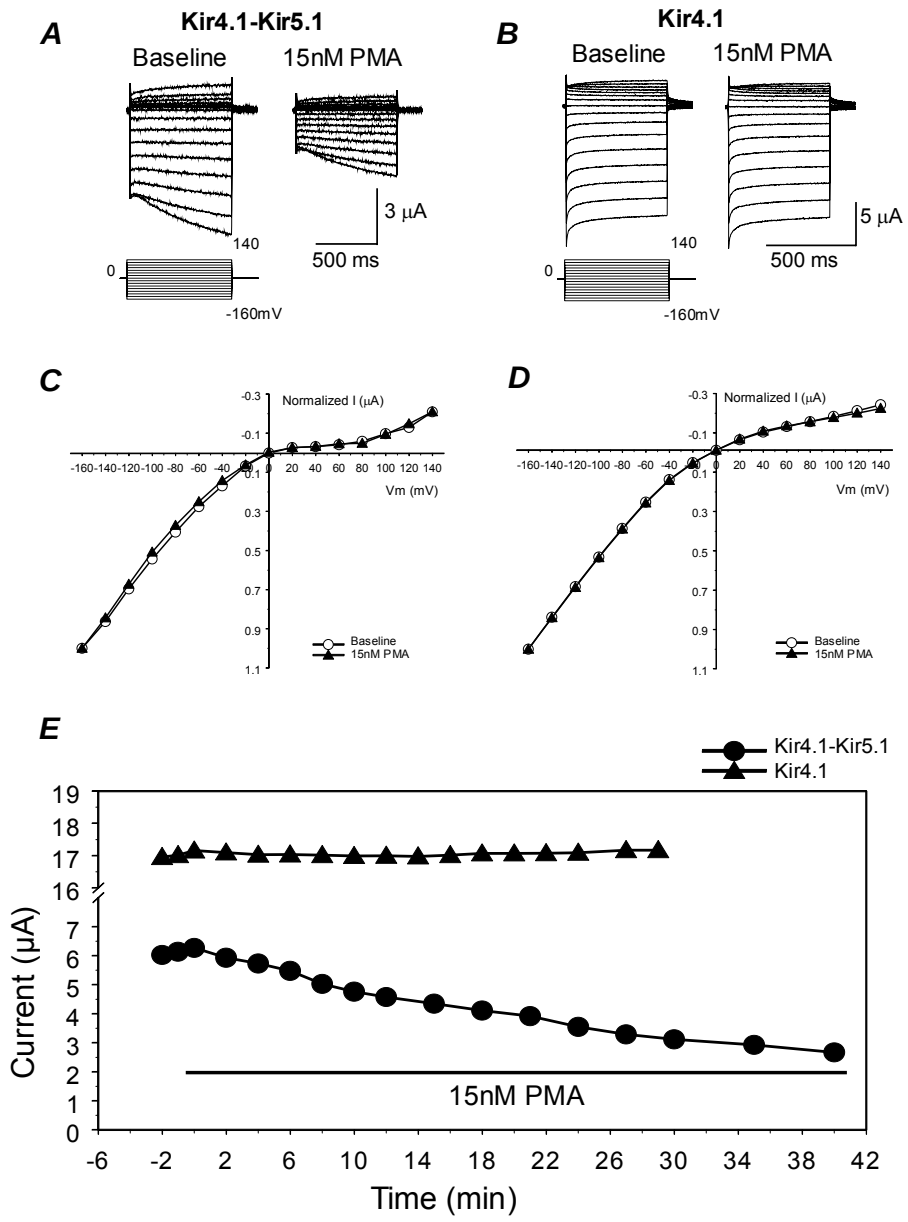

Fig III-1. The Kir4.1-Kir5.1 channel but not homomeric Kir4.1 is sensitive to PMA. *A*. Using TEVC whole-cell Kir4.1-Kir5.1 currents were recorded from an oocyte 3 days post-injection of the Kir4.1-Kir5.1 dimer cDNA. With 90 mM K^+ in the extracellular solution inward rectifying currents were recorded at baseline. Membrane potential (V_m) was held at 0 mV. A series of command pulse potentials from –160 mV to 140 mV with a 20-mV increment was applied to the cell. Note that in highly negative membrane potentials, there was slow activation of the currents. Exposure to 15 nM PMA (a specific and potent PKC activator) inhibited the Kir4.1-Kir5.1 currents by 40%. *B*. The same experiment was carried out with the homomeric Kir4.1. Exposure to 15 nM PMA failed to inhibit this channel. *C, D*. When baseline and peak PMA affected

currents were scaled to the same magnitude at -160 mV, the I/V relationship of the currents recorded under these two conditions were superimposed, suggesting that the effects were voltage-independent. *E.* The time profile showed that the Kir4.1-Kir5.1 current amplitude decreased rapidly when PMA was present in the bath solution, and reached maximum inhibition in ~35 min. The Kir4.1 currents remained constant for 30 minutes during exposure to PMA.

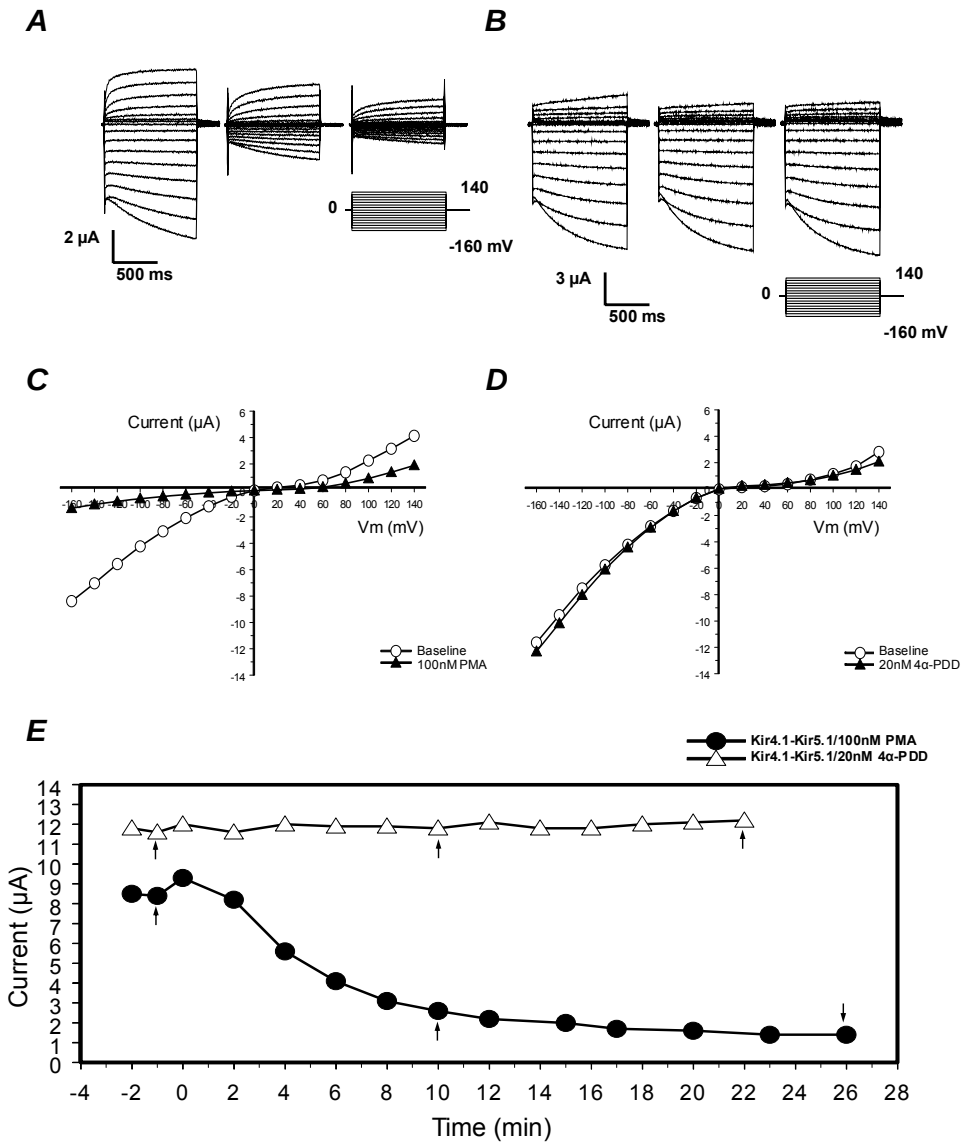

Fig III-2. *A*. Inhibtion of Kir4.1-Kir5.1 by PMA and not 4α-PDD. Using TEVC whole-cell Kir4.1-Kir5.1 currents were recorded from an oocyte 3 days post-injection of the Kir4.1-Kir5.1 dimer cDNA. With 90 mM K^+ in the extracellular solution inward rectifying currents were recorded at baseline. Membrane potential (V_m) was held at 0 mV. A series of command pulse potentials from –160 mV to 140 mV with a 20-mV increment was applied to the cell. Exposure to 100 nM PMA strongly inhibited the Kir4.1-Kir5.1 currents. *B*. The same experiment was carried out using the 4α-PDD (an inactive analogue of PMA) instead of PMA. Exposure to 20 nM 4α-PDD failed to inhibit the Kir4.1-Kir5.1 channel. *C, D*. Shows the I-V curve relationships for the experiments carried out in A and B. *E*. The time profile shows that the Kir4.1-Kir5.1 current

amplitude decreased rapidly when PMA was present in the bath solution at a high concentration (100 nM), and reached maximum inhibition in ~25 min.

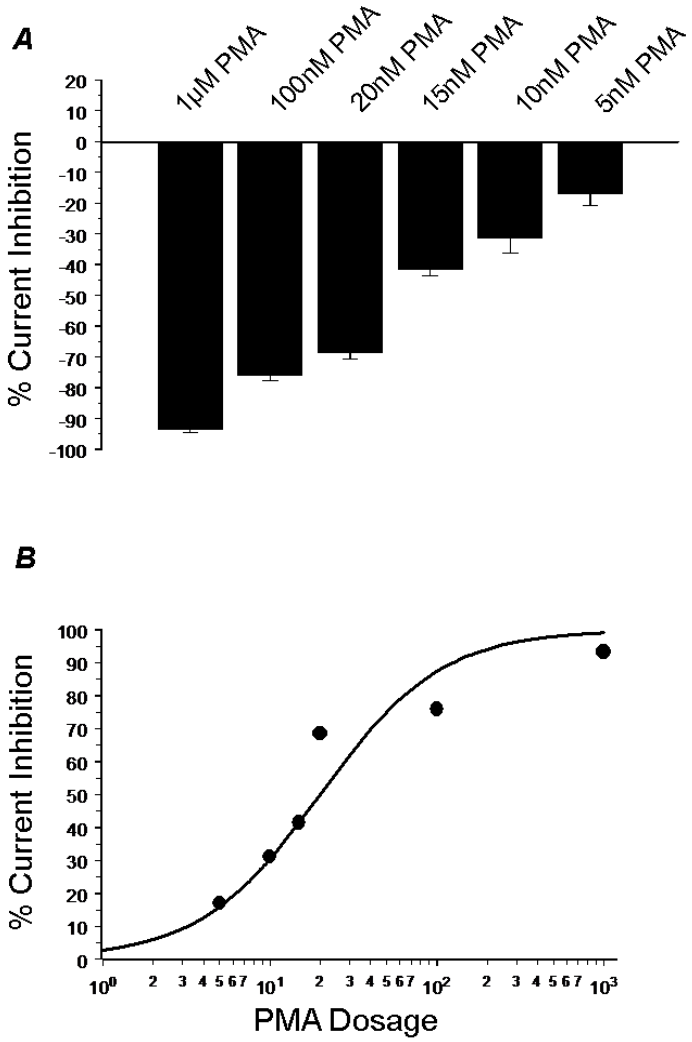

Fig III-3. Concentration-dependent response of PMA. *A*. The effect of PMA on the Kir4.1-Kir5.1 channel was clearly concentration-dependent. The Kir4.1-Kir5.1 channel was inhibited by very low concentrations of PMA. Exposure to 5 nM PMA suppressed Kir4.1-Kir5.1 channels by 16.9±3.8% (n=5). 1 μM PMA maximally inhibited the Kir4.1-Kir5.1 currents by 93.3±1.4% (n=4). n≥4 for each concentration tested. *B*. The concentration-dependent response fits a sigmoid curve. This curve was used to more accurately obtain the IC_{50} concentration which was 15 nM PMA.

IIIb-2. ***Involvement of PKC***

To demonstrate that PKC activation underscores the PMA inhibition of Kir4.1-Kir5.1, we took advantage of several other specific kinase activators and inhibitors. Exposure of the oocytes to phorbol ester (OAG), another PKC activator, resulted in a similar inhibition as PMA (Fig 4A, F). Thymeleatoxin (100 nM), that selectively activates the conventional PKC isoforms (α, β, & γ), brought about an inhibition of the Kir4.1-Kir5.1 channel (47.8±2.5%, n=5) to the same degree as PMA ($P>0.05$), suggesting that at least one of the conventional PKC isoforms is involved (Fig. 4B, F). In contrast, the homomeric Kir4.1 was not inhibited by OAG and thymeleatoxin, consistent with the results from PMA (Fig. 4D-F). An inactive analogue of PMA (4α-PDD, 15 and 20 nM) failed to inhibit the Kir4.1-Kir5.1 channel (Fig. 4F; Fig. 2B, D, E).

The cAMP dependent protein kinase A (PKA) has been shown to modulate Kir channels (Light et al., 2000; Lin et al., 2000; Wischmeyer & Karschin, 1996; Zitron et al., 2004). We therefore used forskolin that activates the enzyme adenylyl cyclase leading to increases in the cAMP concentration and activation of PKA. With 100 μM forskolin, oocytes expressing the Kir4.1-Kir5.1 channel showed a modest inhibition of the Kir4.1-Kir5.1 currents (10.2±3.3%, n=8; Fig. 4F), suggesting that the PMA-induced channel inhibition is not a result of PKA activation.

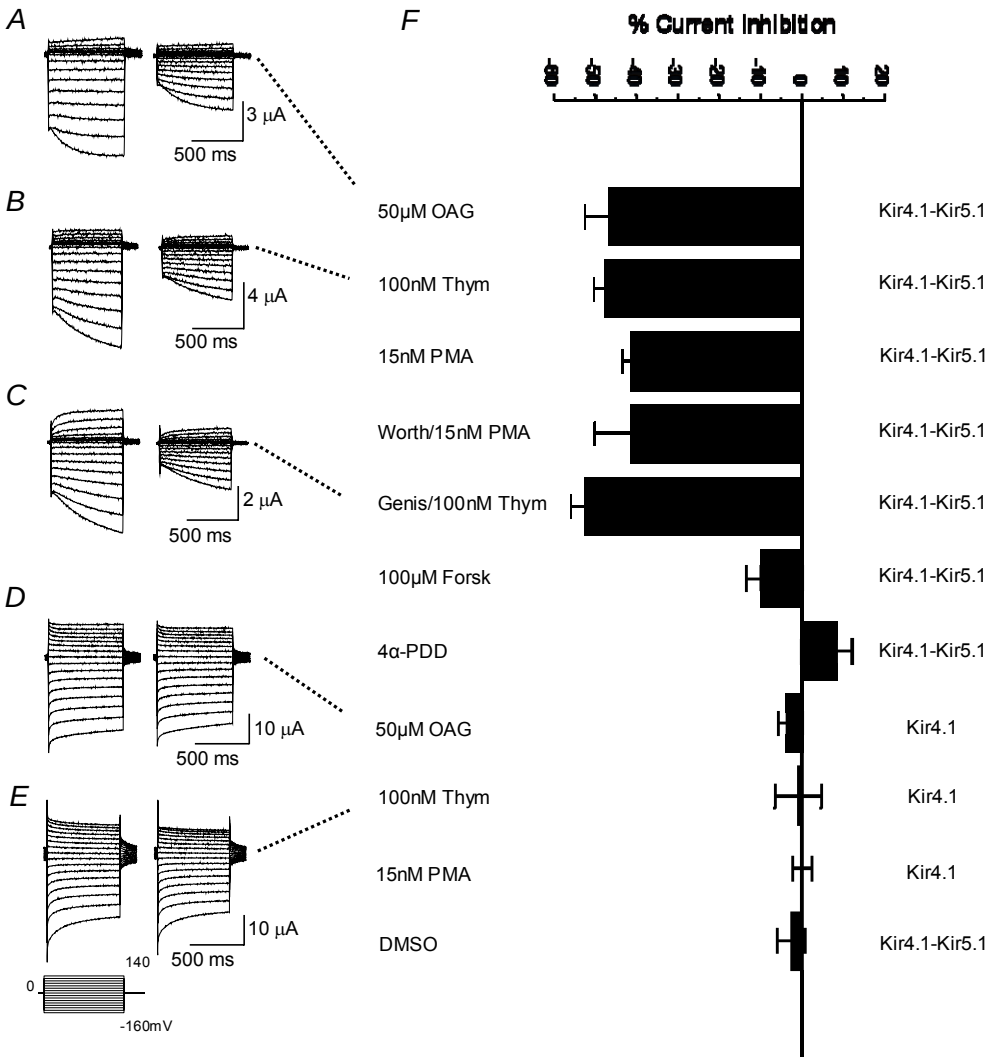

Fig III-4. PKC activation inhibits the Kir4.1-Kir5.1channel. *A*. Currents were recorded from an oocyte in the same condition as in Figure 1A. These currents were strongly inhibited (46.3%) by exposure to 50 μM OAG (another potent activator of PKC). *B*. Exposure of an oocyte expressing the Kir4.1-Kir5.1 channel to 100 nM thymeleatoxin (activator of the conventional PKC isoforms α, β, γ) resulted in a similar inhibition (48.9%). *C*. Currents were recorded from an oocyte in the same condition as in 3B. Prior to application of 100 nM thymeleatoxin the cell was pre-incubated with 100 μM Genistein (a potent and general tyrosine kinase inhibitor) for 1 hour. Blocking activation of tyrosine kinases failed to reduce the inhibition by thymeleatoxin. *D, E*. The same

experiments in 3A and 3B were carried out on oocytes expressing the homomeric Kir4.1 channel. This channel was barely inhibited by 50 μM OAG and 100 nM thymeleatoxin 8.9%, 6.8%, respectively. *F*. The effect of PMA appears to be via activation of PKC as Forskolin (a PKA activator) shows very little inhibition. Also, neither DMSO alone nor 4α-PDD (an inactive analog of PMA) had a significant effect. n≥4 for each experiment.

Specific PKC inhibitors were studied, in which oocytes were pre-incubated in chelerythrine or calphostin-C prior to PMA application to the recording solution. The pre-incubation of cells with 3 μM calphostin-C for 2 hours resulted in a complete elimination of the PMA-induced inhibition (Fig. 5A, B). A similar effect was seen with chelerythrine (50 μM for 1 hour), though to a lesser degree (Fig. 5B). Pre-incubation with genistein, a potent inhibitor of tyrosine kinases did not block the PMA effect (Fig. 4C, F). These results strongly suggest that the PMA inhibition of the Kir4.1-Kir5.1 channel is mediated by PKC, but neither by PKA nor by tyrosine kinase activation.

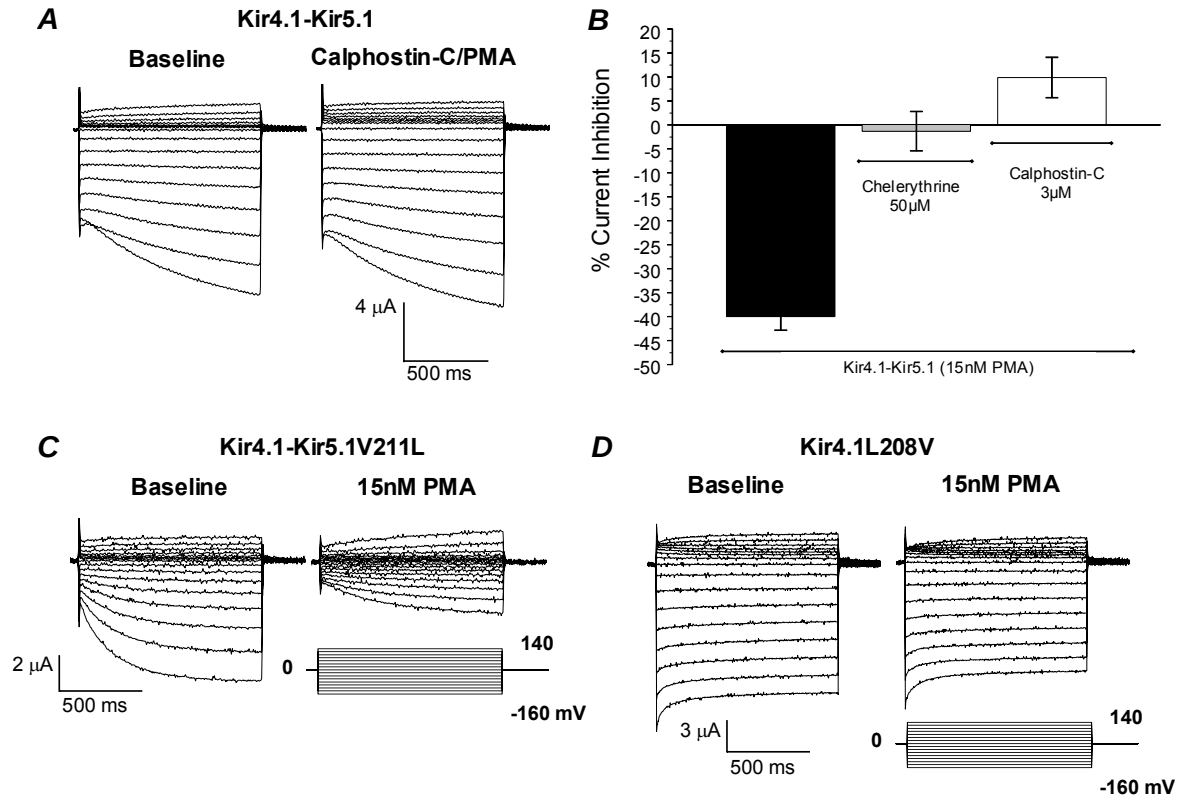

Fig III-5. PKC is necessary for inhibition of Kir4.1-Kir5.1 by PMA. *A*. Using TEVC whole-cell Kir4.1-Kir5.1 currents were recorded from an oocyte 3 days post-injection of the Kir4.1-Kir5.1 dimer cDNA. With 90 mM K^+ in the extracellular solution inward rectifying currents were recorded at baseline. Membrane potential (V_m) was held at 0 mV. A series of command pulse potentials from –160 mV to 140 mV with a 20-mV increment was applied to the cell. Before exposure to 15 nM PMA the oocyte was pre-incubated with 3 μM Calphostin-C (a potent and specific inhibitor of PKC) for 2 hours. Inhibition of PKC drastically attenuated the effect of PMA. PMA exposure after incubation with calphostin-C slightly activated the Kir4.1-Kir5.1 currents by 9.8%. *B*. Pre-incubation of oocytes with specific PKC inhibitors (50 μM chelerythrine or 3 μM calphostin-C) strongly attenuated the effect of 15 nM PMA (n≥4). *C*. Whole-cell currents were recorded from an oocyte 3 days post injection of the Kir4.1-Kir5.1V211L mutant channel recorded under the same condition as in A. This mutant is suggested to have increased PIP_2 affinity. Exposure of the oocytes to 15 nM PMA inhibited the Kir4.1-Kir5.1V211L currents by 57.6%. *D*. The converse mutant was created on the Kir4.1 channel (Kir4.1L208V) and tested in an oocyte under the same experimental conditions as for Figure 4C. Similarly as for the wild-type channel this mutant failed to be inhibited by 15 nM PMA.

IIIb-3. ***Inhibition of the Kir4.1-Kir5.1 Channel by PKC activation in HEK293 cells***

The Kir4.1-Kir5.1 channel was transiently expressed in HEK293 cells. Whole-cell voltage clamp was performed on GFP-positive cells. Both the bath and pipette solutions contained 145 mM K^+. The Kir4.1-Kir5.1 positive transfected cells showed typical Kir4.1-Kir5.1 currents that were relatively big at the basal level upon the formation of the whole-cell configuration. Without any treatment the currents remained at this level for more than 5 min. The cells were held at a membrane potential of 0 mV. Command pulses of -80 mV were applied to the cell every 3 seconds and the Kir4.1-Kir5.1 currents were recorded. Application of 15 nM PMA strongly inhibited the Kir4.1-Kir5.1 channel by 39.3±2.1% (n=10) (Fig. 6A, D). The inhibition by 15 nM PMA was greatly diminished [1.40±2.6% (n=6)] in the presence of the PKC inhibitor peptide (10 μM PKCi) that was added to the pipette solution (Fig. 6B, D). 100 nM thymeleatoxin similar to 15 nM PMA also inhibited the Kir4.1-Kir5.1 channel [44.7±2.6% (n=10)] expressed in HEK293 cells. However, an inactive analogue of PMA (4α-PDD) only inhibited the Kir4.1-Kir5.1 currents in HEK293 cell by 10.7±2.7% (n=9) (Fig. 6D). Taken together, these results suggest that the Kir4.1-Kir5.1 channel is inhibited by PKC activation in HEK293 cells in a similar manner as in *Xenopus* oocytes.

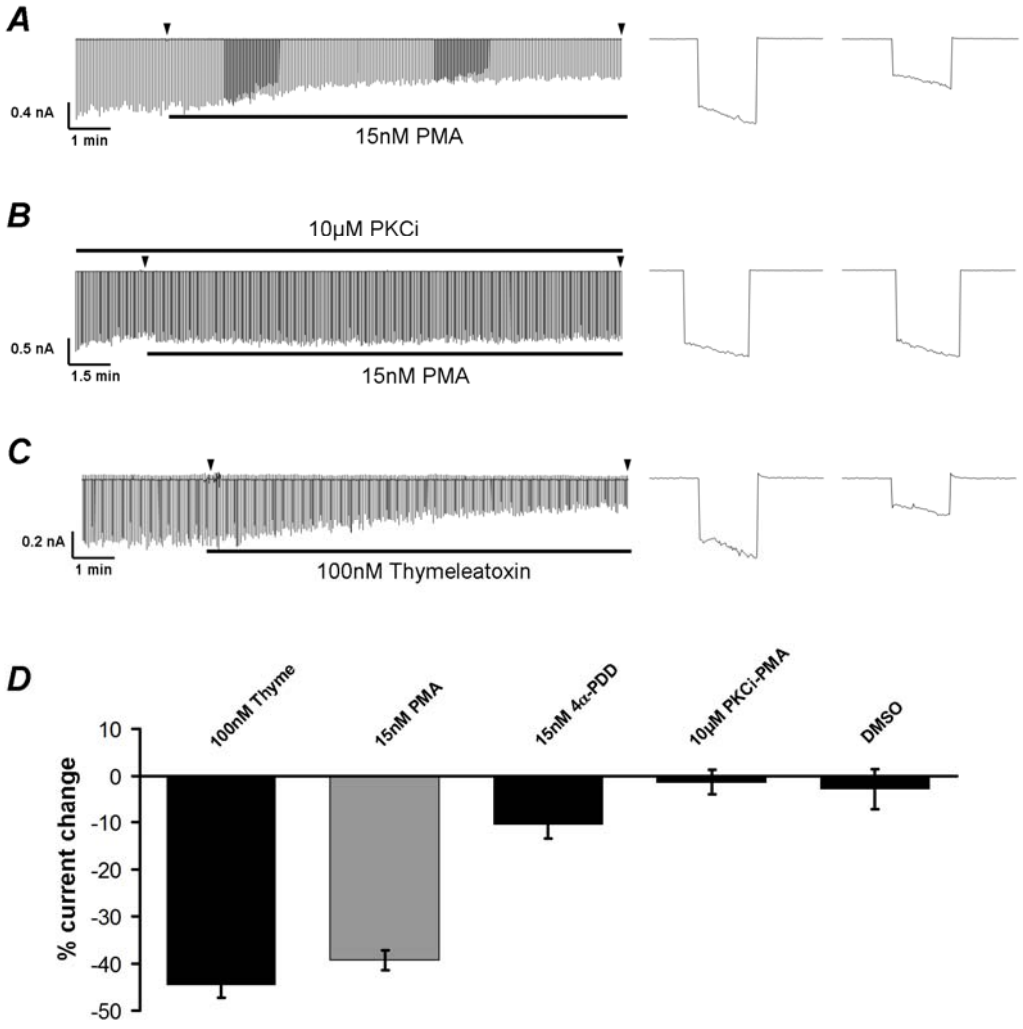

Fig III-6. PKC activation inhibits the Kir4.1-Kir5.1channel in HEK293 cells. *A*. Whole-cell currents were recorded from an HEK293 cell transfected with the Kir4.1-Kir5.1 dimer cDNA with a holding potential at 0mV and command pulses of –80mV in every 3 seconds. After the whole-cell configuration was formed, the cell was perfused with the extracellular solution for a 2-5 min period of baseline recording. The currents were inhibited by exposure to 15nM PMA. The arrow represents the magnification of the current at the time point and shown on the right. *B*. In the presence of the PKC inhibitory peptide (10μM PKCi), 15nM PMA failed to inhibit the Kir4.1-Kir5.1 channel. *C*. Inhibition of the Kir4.1-Kir5.1 channel was also seen with exposure to 100nM thymeleatoxin. *D*. Bargraph showing that PKC activation results in inhibition of the Kir4.1-Kir5.1 channel. In each experiment n≥6.

IIIb-4. *Single-channel Properties Affected*

The effect of PMA on the single-channel biophysical properties was studied in *Xenopus* oocytes using cell-attached patches with 145 mM K^+ applied to the extracellular solution at a membrane potential of -80 mV. Only patches containing ≤4 active channels were considered in the experiment. Inward rectifying currents with single-channel conductance of ~40 pS were recorded from oocytes that were injected with the Kir4.1-Kir5.1 cDNA 2-3 days prior to recordings. These currents were inhibited with an exposure of the cells to 15 nM PMA (Fig. 7A). The current inhibition was mainly produced by a suppression of the channel open-state probability (P_{open}), while the single-channel conductance was barely effected (Fig. 7).

IIIb-5. *Independence of PIP_2*

A number of Kir channels are regulated by membrane lipids including phosphatidylinositol bisphosphate (PIP_2). The presence of this phospholipid has been shown to increase Kir channel activity, and consequently depletion of PIP_2 leads to channel inhibition. To test the possibility that the PMA-induced Kir4.1-Kir5.1 channel inhibition is related to PIP_2 depletion, we mutated the potential PIP_2 binding sites in the channel to increase or decrease the channel affinity for the phospholipid based on a sequence alignment with other Kir channels (Du et al., 2004; Lopes et al., 2002; Mao et al., 2004). One mutant R178Q, that has previously been reported to increase PIP_2 binding affinity (Yang et al., 2000), was created in the Kir5.1 and expressed with wild-type Kir4.1. This mutant channel showed a similar PMA sensitivity as the wild-type (Table 1). Another mutant Kir4.1-Kir5.1V211L, that has also been shown to increase the PIP_2

sensitivity, did not affect the channel inhibition by 15 nM PMA (41.2±5.7%, n=10) (Fig. 5C). A converse mutation, exchanging these residues at a different site on the Kir4.1 (Kir4.1L208V) had no effect (Fig. 5D).

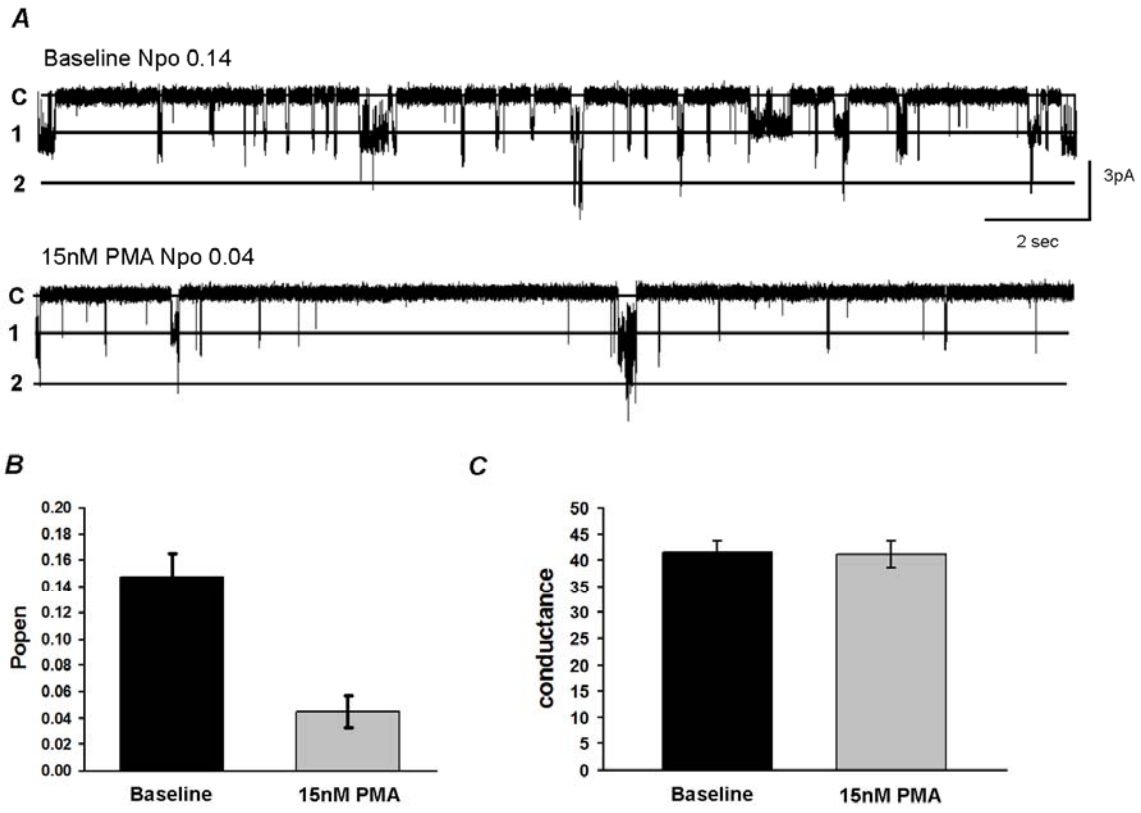

Fig III-7. Effects of PMA on the single channel properties of the Kir4.1-Kir5.1. *A.* Single Kir4.1-Kir5.1 currents were recorded from an oocyte in a cell-attached patch configuration with 145 mM K^+ in the patch pipette. At V_m of -80 mV, two active channels are seen at pH 7.4. Following stabilization, exposure to 15 nM PMA reduced the channel activity by a decrease in the NPo. Labels on the left: c, closure; 1, the first opening; 2, the second opening; etc. *B, C*. Bargraph showing that 15 nM PMA drastically reduced the Po, but did not affect the single-channel conductance (n≥6).

To further assess the effect of PIP_2 depletion in the channel inhibition, wortmannin that inhibits the phosphoinositide kinase-3 (PI3K) and thus the resynthesis of PIP_2 from PIP_3 was used to treat the oocytes prior to PMA exposure. Following incubation of oocytes with 10 μM wortmannin, PMA continued to inhibit the Kir4.1-Kir5.1 channel by 41.4±8.8% (n=5) (Fig. 4F). Taken together these results suggest that PIP_2 depletion does not seem to underlie the PMA-induced Kir4.1-Kir5.1 channel inhibition.

IIIb-6. ***Lack of Evidence for Endocytosis***

Several recent studies indicate that protein kinase activation can lead to endocytosis and thus the suppression of surface Kir channel activity (Lin et al., 2002; Sterling et al., 2002; Wang et al., 2002; Wang et al., 2006; Zeng et al., 2002). To evaluate the role of endocytosis in the inhibition of the Kir4.1-Kir5.1 channel by PKC activation, we carried out experiments with dynamin II and its dominant negative mutant where lysine at position 44 is mutated to alanine (K44A). We reasoned that co-expression of this dominant-negative dynamin II may abolish the effect of PKC if the Kir4.1-Kir5.1 channel inhibition by PKC results in dynamin dependent endocytosis. The Kir4.1-Kir5.1 channel was co-expressed with the wild-type dynamin II as well as the dynamin II K44A mutant. Exposure to 15 nM PMA led to inhibition of the currents by 53.2±4.4% (n=4) in the cells expressing the wild-type dynamin II (Fig. 8A, D) and by 49.5±6.8% (n=5) in cells expressing the dynamin II K44A mutant (Fig. 8B, D).

Another mechanism of endocytosis involves clathrin-coated pits. Proteins that undergo clathrin-dependent endocytosis contain an internalization recognition motif in at

least one of the intracellular domains, usually in the C-terminal (Zeng et al., 2002). This motif [(Y/F)(D/E)NPXY] shares high homology in many proteins. A primary scan of the Kir4.1 amino acid sequence failed to show any similar recognition motif. However, a scan of the Kir5.1 led to the identification of such a motif. The second and third amino acids of the motif have been found to be critical for endocytosis of Kir1.1 (Zeng et al., 2002).

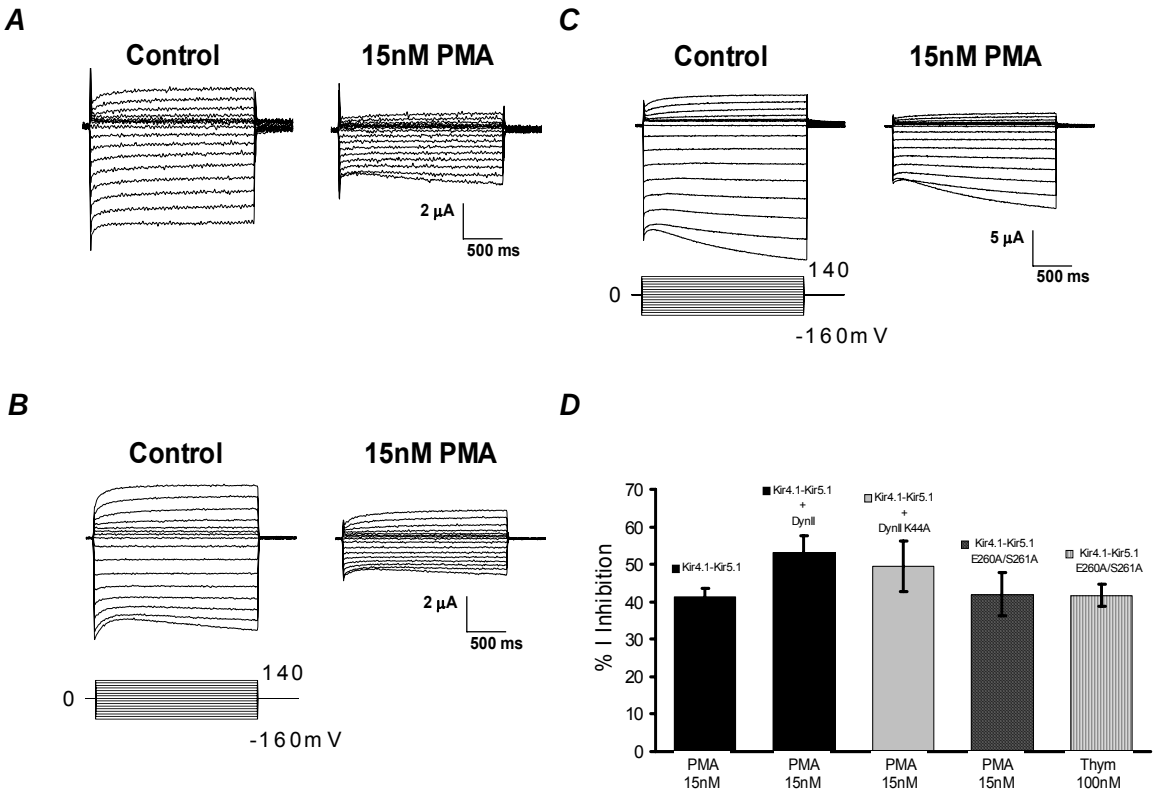

Fig III-8. PKC activation inhibits Kir4.1-Kir5.1 currents independent of endocytosis. *A.* Whole-cell currents were recorded from an oocyte 3 days following injection of the Kir4.1-Kir5.1 + dynamin II cDNAs (co-injection) under the same conditions as described for Figure 1A. PMA exposure inhibited the Kir4.1-Kir5.1+ dynamin II currents by 53%. *B.* Whole-cell Kir4.1-Kir5.1 currents were recorded from an oocyte 3 days following injection of the Kir4.1-Kir5.1 + dynamin II K44A mutant cDNAs (co-injection) using TEVC. Exposure to 15 nM PMA also inhibited the Kir4.1-Kir5.1+ dynamin II K44A (-49%). *C.* Whole-cell currents were recorded from an oocyte 3 days following injection of the Kir4.1-Kir5.1E260A/S261A mutant channel. This mutant has lost the recognition site for CCV endocytosis. Exposure of the oocyte to 15 nM PMA inhibited the Kir4.1-Kir5.1E260A/S261A currents by 42%. *D.* Bargraph summarizing panels A, B, and C. Note that the Dynamin K44A mutant and the Kir4.1-Kir5.1E260A/S261A mutant showed no significant difference to the Kir4.1-Kir5.1 in respect to inhibition by PMA. n≥4 for each experiment.

Therefore, we mutated these residues in Kir5.1. Consistent with the dynamin experiment we found that the Kir4.1-Kir5.1E260A/S261A mutant remained highly sensitive to PMA (Fig. 8C, D).

To further assess the possibility of channel endocytosis, whole cell currents were recorded from HEK293 cells before and during a treatment with thymeleatoxin. The whole cell capacitance (CAP) and series resistance (SR) were measured. If the Kir4.1-Kir5.1 channel inhibition by PKC activation was a result of endocytosis, the whole cell capacitance would decrease following application of thymeleatoxin to the bath solution. The percent change in the whole cell capacitance of HEK293 cells expressing the Kir4.1-Kir5.1 channel exposed to 100 nM thymeleatoxin for 15 min was 5.9±8.2% (n=4). This change in capacitance did not significantly differ from that of cells exposed to DMSO only (3.1±9.9%, n=4) (Fig. 9). The series resistance did not show a significant difference between cells exposed to DMSO versus cells exposed to 100 nM thymeleatoxin (Fig. 9).

We also performed immunocytochemistry to demonstrate membrane expression of the Kir4.1-Kir5.1 channel. Both the Kir4.1 and Kir5.1 antibodies are commercially available. By taking advantage of these antibodies and using immunocytochemistry we decided to look at membrane expression of the Kir4.1-Kir5.1 channel before and after exposure to PMA. HEK293 cells were transfected with the Kir4.1-Kir5.1 dimer. Immunocytochemistry was performed as described in the methods section. Prior to PMA exposure the channel showed membrane surface expression (Fig. 10A1-A3). After exposure to 15 nM PMA for 25 min the membrane expression was retained (Fig. 10B1-

B3). Taken together these results suggest that the Kir4.1-Kir5.1 channel inhibition does not seem to be a result of endocytosis.

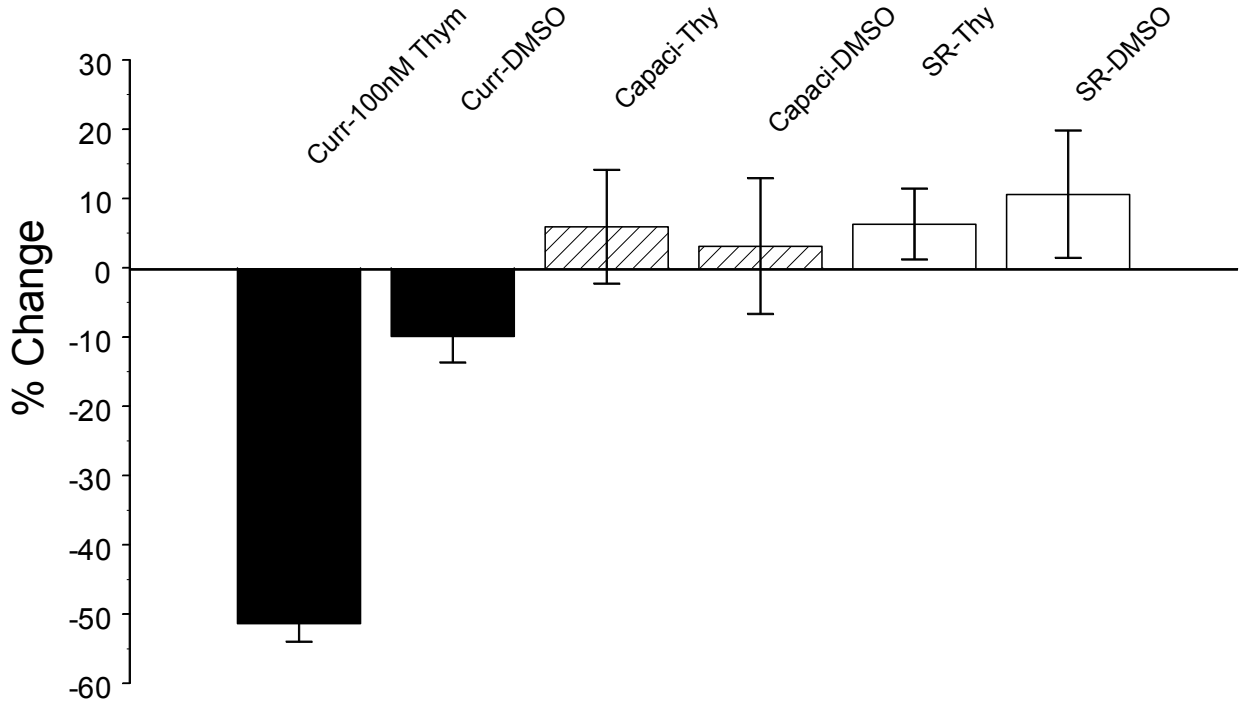

Fig III-9. Endocytosis independent inhibition of Kir4.1-Kir5.1 in HEK293 cells. Whole-cell currents were recorded from HEK293 cells 3 days post-transfection of the Kir4.1-Kir5.1 cDNA. Membrane potential (V_m) was held at 0 mV. A series of command pulse potentials from –120 mV to 80 mV was applied to the cell and the corresponding currents were recorded. Following stabilization 100 nM thymeleatoxin was applied to the bath solution and inhibited the Kir4.1-Kir5.1 currents by 51.4±2.6% (n=4). Application of DMSO alone barely inhibited the Kir4.1-Kir5.1 currents. During the experiments with thymeleatoxin and DMSO, the whole cell capacitance and series resistance were monitored. Neither capacitance nor series resistance changed significantly upon application of 100 nM thymeleatoxin or DMSO to the bath solution.

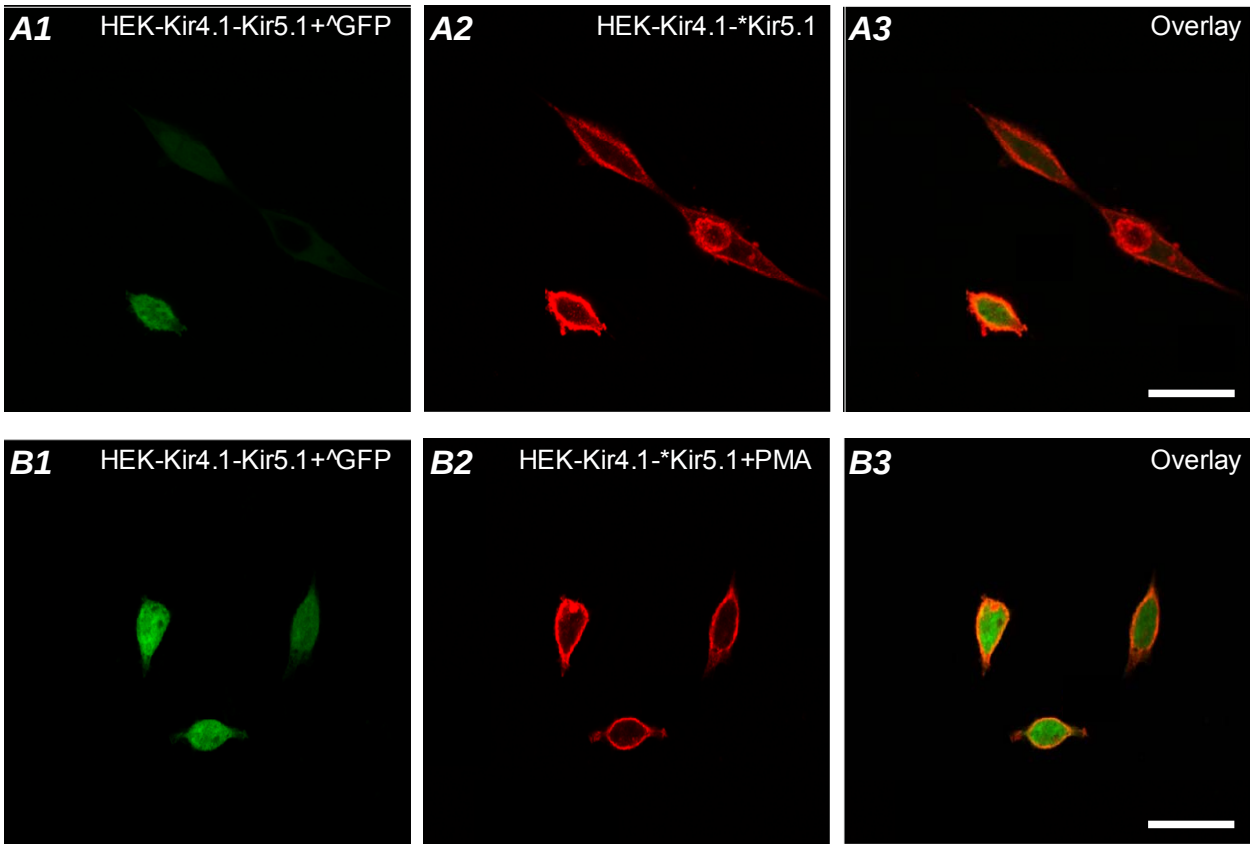

Fig III-10. Surfacce expression of the Kir4.1-Kir5.1. Immunocytochemistry was performed on HEK293 cells 48 hours post-transfection of the Kir4.1-Kir5.1dimer cDNA together with the GFP cDNA. *A*. Prior to PMA exposure the channel was mainly expressed on the surface of the HEK293 cells, suggesting membrane expression. *B*. Following application of 15 nM PMA for 25 minutes the channel maintained expression on the cell surface. ^ Denotes GFP fluorescence imaging. * Denotes Kir5.1 antibody was used as the primary antibody. GFP was used as an indicator of transfection efficiency. Note that all HEK293 cells expressing GFP also expressed the Kir4.1-Kir5.1 channel although the GFP intensity was compromised by the fixation process. Bar=10 μm.

IIIb-7. *Phosphorylation Sites*

To identify the PKC phosphorylation site, a sequence scan of amino acids was made for both the Kir4.1 and Kir5.1 channels. Numerous putative PKC phosphorylation sites were found in Kir4.1 and Kir5.1, according to the consensus sequence, i.e., R(K)-X_{0-2}-T/S-X_{0-2}-R(K). Four different phosphorylation prediction programs were also used to predict potential PKC phosphorylation sites (NetPhos, Scansite, ScanProsite, Phosphobase). We performed systematic screening of these predicted sites according to the prediction programs in both Kir4.1 and Kir5.1 by single mutation of the serines or threonines to an alanine residue. The effect of PMA on these mutants was tested subsequently in *Xenopus* oocytes. The mutant channels were grouped: the first group of mutants consisted of the potential phosphorylation sites that were predicted using all prediction programs and had the highest score for potential phosphorylation by PKC; the second group consisted of those residues that had a lower phosphorylation prediction score; and the third group was residues not predicted by the phosphorylation prediction programs, but was found in a sequence similar to the consensus sequence for PKC. We tested 30 mutant channels with a single mutation representing each group and 9 channels with double mutations. All single mutants tested except for Kir4.1-Kir5.1T174D remained highly sensitive to PMA (Fig. 11A, B, Table 1). Further analysis of the Kir4.1-Kir5.1T174 position suggests that it is involved in another channel function as mutants carrying an alanine or lysine at this position remained sensitive to PMA (Fig. 11G, Table 1). Also the Kir4.1-Kir5.1T174D mutant also failed to respond to 15% CO_2. Single channel analysis showed that the T174D mutant has an increased P_{open} (Fig. 11D).

Taken together we concluded that the T174 position is not a PKC phosphorylation site. The double mutants were created by comparing the PMA effect of the single mutants and selecting those that had a slightly lower PMA sensitivity. When tested, the double mutants also showed a PMA sensitivity similar to the wild-type. Therefore, the PKC phosphorylation sites remain to be demonstrated.

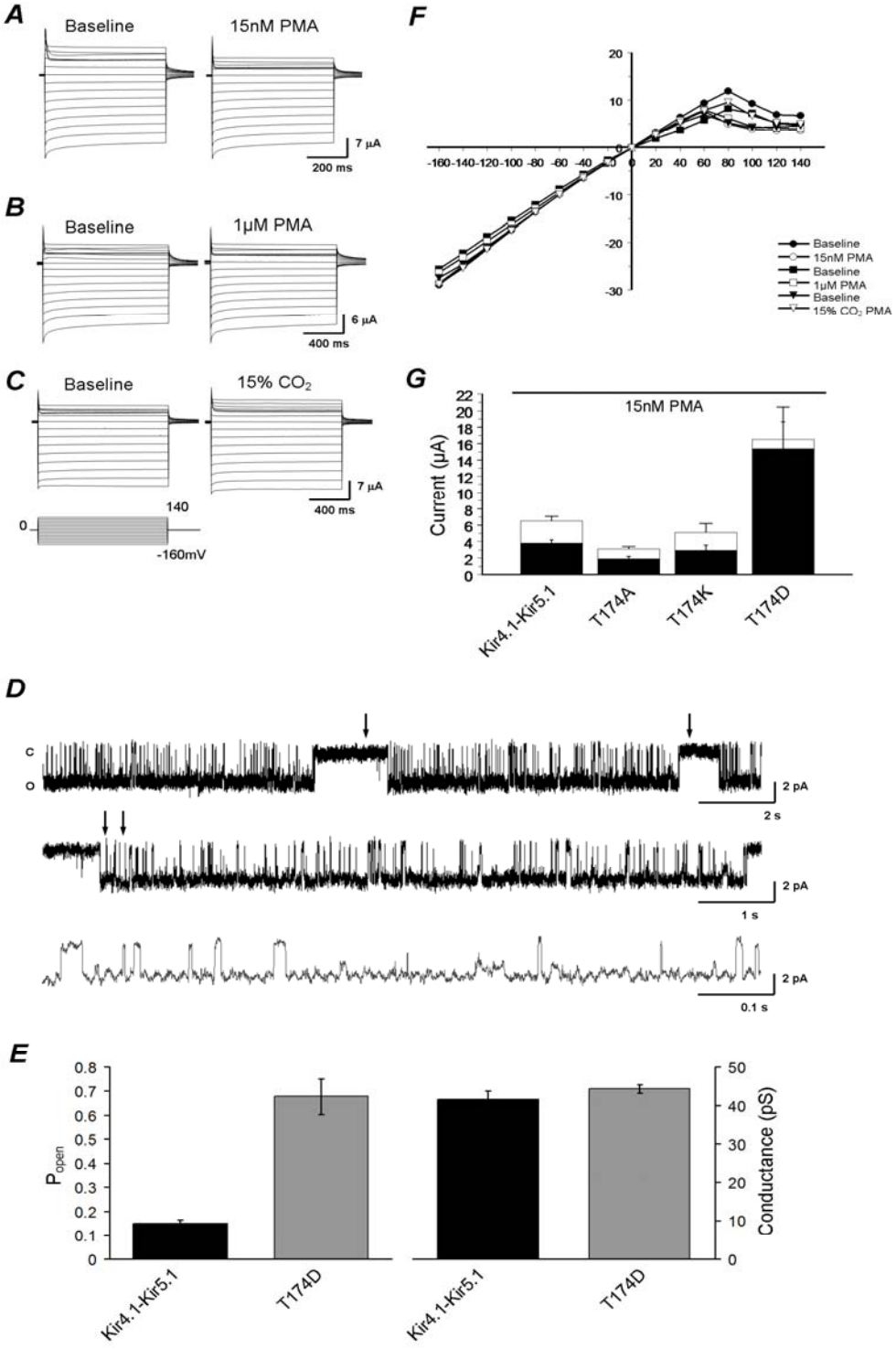
A
Baseline
15nM PMA
7 µA
200 ms
B
Baseline
1µM PMA
6 µA
400 ms
C
Baseline
15% CO2
7 µA
400 ms
140
0
-160mV
F
Baseline
15nM PMA
Baseline
1µM PMA
Baseline
15% CO2 PMA
G
15nM PMA
Current (µA)
Kir4.1-Kir5.1
T174A
T174K
T174D
D
c
o
2 pA
2 s
2 pA
1 s
2 pA
0.1 s
E
Popen
Conductance (pS)
Kir4.1-Kir5.1
T174D
Kir4.1-Kir5.1
T174D

Fig III-11. *A*. T174 as a potential phosphorylation site. Using TEVC whole-cell currents were recorded from an oocyte 3 days post-injection of the Kir4.1-Kir5.1T174D mutant. With 90 mM K^+ in the extracellular solution inward rectifying currents were recorded at baseline. Membrane potential (V_m) was held at 0 mV. A series of command pulse potentials from –160 mV to 140 mV with a 20-mV increment was applied to the cell. Exposure to 15 nM PMA failed to inhibit the T174D currents. *B*. The same experiment was carried out using 1μM PMA. Exposure to 1μM PMA also failed to inhibit the Kir4.1-Kir5.1T174D channel. *C*. Unlike the wild-type Kir4.1-Kir5.1 channel that is strongly inhibited by 15% CO_2, the T174D currents were unaffected by such an exposure. *D, E*. Single channel recordings and analyses shows that the T174D mutant has a higher basal P_{open} than the wild-type Kir4.1-Kir5.1 although the conductances are the very similar (n≥5). *F*. Shows the I-V curve relationships for the experiments carried out in A, B and C. *G*. Bargraph showing the effects of 15nM PMA on the T174 mutants. Note that the T174D mutant had a much larger basal current and failed to be inhibited by PMA in comparison to the wild-type and the other T174 mutants (n≥5).

IIIb-8. *Direct Phosphorylation of Kir4.1 and Kir5.1*

The failure to demonstrate PKC phosphorylation sites raises a question as the whether the channel proteins are indeed phosphorylated by PKC. Thus, we performed in-vitro phosphorylation experiments. Since most of the predicted PKC sites are located in the C-terminus of Kir4.1 and Kir5.1, MBP fusion peptides with the Kir4.1-C-terminus and Kir5.1C-terminus were produced as described in the Materials and Methods. After extraction and purification, the fusion peptides were incubated with ^{32}P-γ-ATP in the presence of the catalytically active subunit of PKC (20 ng). Such a treatment led to positive phosphorylation of these peptides suggesting that both Kir4.1 and Kir5.1 are directly phosphorylated by PKC (Fig. 12; Fig. 13).

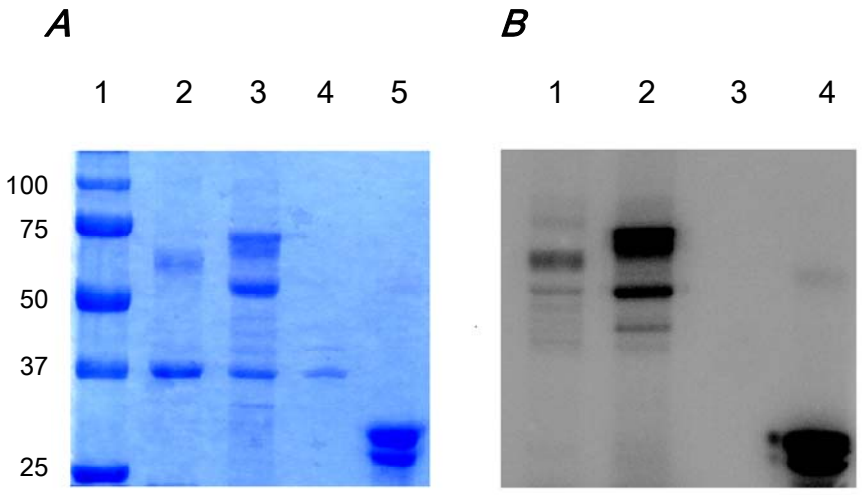

Fig III-12. Phosphorylation of MBP fusion proteins. *A*. 10% SDS-PAGE gel showing the presence of the Kir4.1-C-terminus-MBP (~65 kDa) (lane 2), Kir5.1-C-terminus-MBP (~70 kDa) (Lane 3), MBP alone (~42 kDa) (Lane 4) and Histone III-S (Lane 5). The size is indicated by the ladder (Lane 1) (precision plus protein standards) (Biorad). *B*. Autoradiograph after 12 hours showing phosphorylation of Kir4.1-C-terminus-MBP, Kir5.1-C-terminus-MBP, MBP, and Histone III-S. The proteins were incubated in the presence of ^{32}P-γ-ATP and the catalytically active PKC subunit.

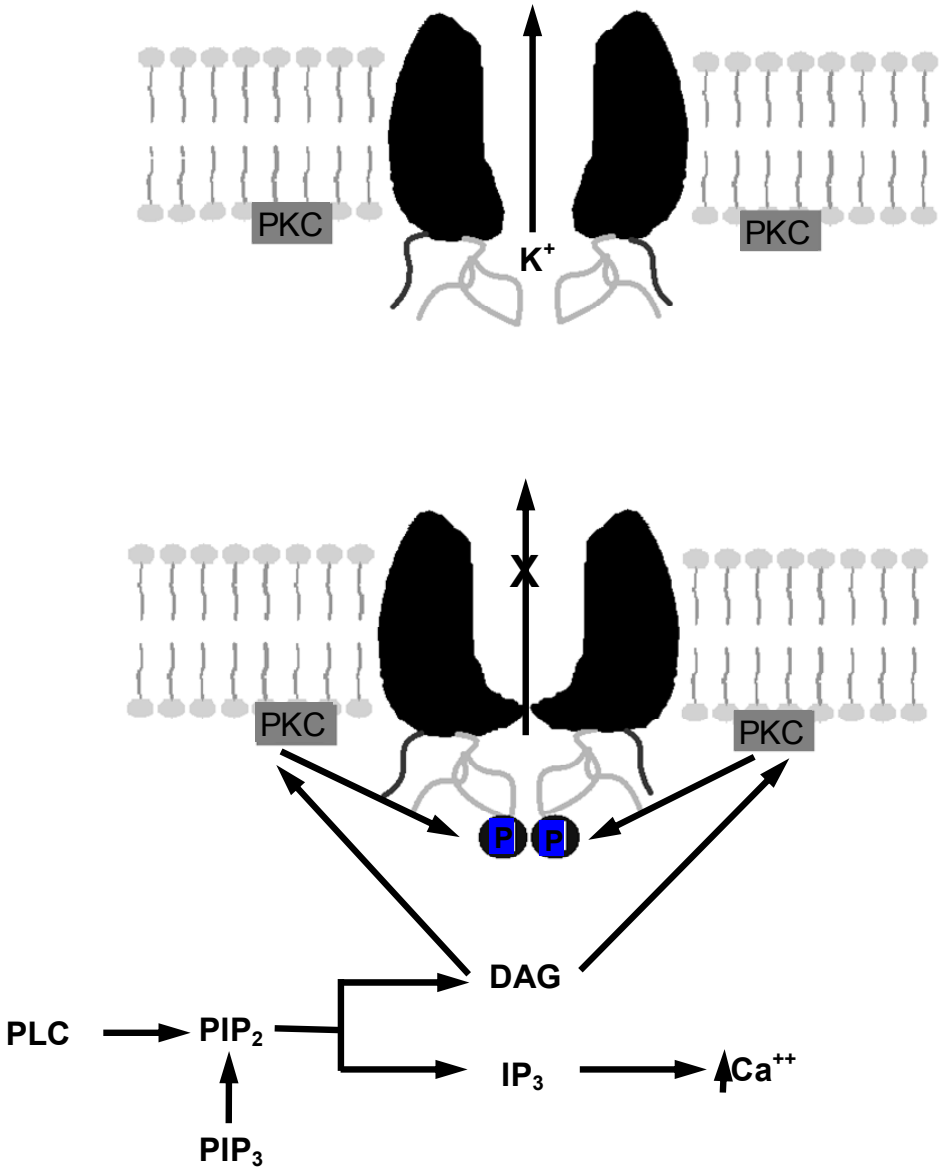

Fig III-13. Schematic for the inhibition of Kir4.1-Kir5.1 channels by PKC. The inhibition of the Kir4.1-Kir5.1 channel is through the activation of PKC by way of DAG activation. The channel appears to be inhibited by PKC directly (phosphorylation) and not by a reduction of PIP_2.

IIIc. DISCUSSION

Protein phosphorylation is an important process in regulating cellular functions. Several inward rectifying K^+ channels have been shown to be regulated by protein kinase phosphorylation (Beguin et al., 1999; Fakler et al., 1994; Henry et al., 1996; Light et al., 2000; Lin et al., 2000; Mao et al., 2004; Stevens et al., 1999; Vorobiov et al., 1998; Wischmeyer et al., 1996; Zhang et al., 2004; Zhu et al., 1999; Zitron et al., 2004). For example, the heteromeric GIRK1/GIRK4 channel has previously been shown to be phosphorylated by protein kinase C at specific serine residues in the channel protein affecting channel gating (Mao et al., 2004). This phosphorylation underscored the effect of substance-P on this channel allowing the channel to partake in the cellular response to this neurotransmitter.

In the present study we have presented evidence for the inhibition of the heteromeric Kir4.1-Kir5.1 channel by PKC. The Kir4.1-Kir5.1 channel is inhibited by nanomolar concentrations of PMA in a dose-dependent manner. Several experiments show that the effect of PMA is specific. Pre-incubation of the oocytes with specific PKC blockers (chelerythrine and calphostin-C) abolishes the PMA effect. Exposure of oocytes to 4α-PDD (an analogue of PMA incapable of activating PKC) fails to inhibit the Kir4.1-Kir5.1 channel. On the other hand, two other PKC activators (OAG & thymeleatoxin) strongly inhibit the channel. The biophysical mechanism for the inhibition of the Kir4.1-Kir5.1 channel by PKC appears to be mediated by reducing the channel open state probability without affecting the single channel conductance. The Kir4.1-Kir5.1 channel

inhibition does not seem to be produced by PKA and tyrosine kinase as forskolin and genistein have rather small effects.

The PKC induced inhibition of the Kir4.1-Kir5.1 channel is independent of PIP_2 and does not seem to be mediated by endocytosis. Since PIP_2 has been shown to regulate many Kir channels it is possible that the PKC induced inhibition of the Kir4.1-Kir5.1 was a result of PIP_2 depletion. The above experiments show that PMA inhibits the Kir4.1-Kir5.1 channel independent of PIP_2 depletion. Similarly, mutant channels with increased PIP_2 binding remains to be inhibited by PMA exposure to the same degree as the wild-type. Also, pre-incubation of oocytes with worthmannin (a PI3K inhibitor that reduces PIP_2) fails to abolish the PMA induced inhibition of the channel, suggesting that the channel inhibition is not a result of PIP_2 depletion. Immunocytochemistry experiments demonstrating surface expression in addition to experiments using a defective dynamin II mutant show that the effect of PMA is not a result of endocytosis. Although there may be other mechanisms involved, these results suggest that activation of PKC inhibits the Kir4.1-Kir5.1 channel by changing the channel gating mechanism.

Our biochemical experiments suggest a direct phosphorylation of the channel protein as both C-termini of Kir4.1 and Kir5.1 can be phosphorylated by PKC. To find the PKC phosphorylation sites, we screened more than 30 serine / threonine residues (some identified as phosphorylation sites by prediction software programs) by mutation to a non-phosphorylatable amino acid. None of the single mutations led to identification of the phosphorylation site, as all single mutants tested except for Kir5.1T174D remained highly sensitive to PMA. The Kir5.1T174 is not a PKC phosphorylation site either, as the

Kir5.1T174A and Kir5.1T174K mutants are strongly inhibited by PMA. The effect of the T174D mutation suggests that this residue or its surrounding area may play a role in the channel gating mechanism and/or regulation by other intracellular factors. This mutant channel lost the sensitivity to both CO_2 and PKC. Since this area contains several charged residues it is possible that a change in electrostatic charge in this area by the T174D affects the process of channel gating. Several double mutations based on single sites shown by phosphorylation prediction programs were also tested. None of these double mutations affects the PMA sensitivity. Therefore, we believe that the heteromeric combination of the Kir4.1-Kir5.1 channel may introduce multiple phosphorylation sites whose phosphorylation collectively may result in a change in channel activity. Removal of one or two of the phosphorylation sites may not be adequate to abolish the channel inhibition by PKC. This is further supported by the in vitro phosphorylation experiments that shows both Kir4.1 and Kir5.1 C-termini are directly phosphorylated by PKC. The Kir4.1 channel can express as a homomeric channel in several tissues (Ishii et al., 2003; Hibino et al., 1999; Hibino et al., 2004; Higashi et al., 2001; Ito et al., 1996; Kusaka et al., 1999). However, this channel has low pH sensitivity (Xu et al., 2000a; Xu et al., 2000b; Xu et al., 2000c) and is insensitive to phosphorylation by PKC according to our current studies.

IIId. SUMMARY AND CONCLUSION

The Kir4.1-Kir5.1 channel expressed using a tandem dimer construct was inhibited by the PKC activator PMA in a dose-dependent manner. The channel inhibition was produced via reduction of the P_{open}. The effect of PMA was abolished by specific PKC inhibitors. In contrast, exposure of oocytes to forskolin (a PKA activator) had no significant effect on Kir4.1-Kir5.1 currents. The channel inhibition appeared to be independent of PIP_2 depletion and PKC-dependent internalization. Several consensus sequences of potential PKC phosphorylation sites were identified in the Kir4.1 and Kir5.1 subunits by sequence scan. Although the C terminal peptides of both Kir4.1 and Kir5.1 were phosphorylated in vitro, site-directed mutagenesis of individual residues failed to reveal the PKC phosphorylation sites suggesting that the channel may have multiple phosphorylation sites. Taken together, these results suggest that the Kir4.1-Kir5.1 but not the homomeric Kir4.1 channel is strongly inhibited by PKC activation.

Table III-1. Effect of 15 nM PMA on wild-type Kir4.1, Kir4.1-Kir5.1 and mutant channels

	Baseline (μA)	PMA (μA)	% effect	N
Kir4.1-Kir5.1 (Dim)	6.5±0.6	3.8±0.43	-41.4±1.9	13
Kir4.1+Kir5.1 (Co-inj)	8.9±2.1	5.2±1.2	-40.7±1.9	6
Kir4.1(homomer)	15.3±2.3	15.23±2.2	-0.04±2.2	6
Kir4.1K67M-Kir5.1	20.53±3.0	12.3±2	-41.35±3.23	6
Kir4.1T178A-Kir5.1	3.4±0.7	2.22±0.43	-33.1±2.9	6
Kir4.1S206A-Kir5.1	6.0±1.3	3.8±0.84	-36.7±3.7	13
Kir4.1T214A-Kir5.1	3.3±0.2	2.1±0.2	-37.2±4.6	11
Kir4.1T262A-Kir5.1	16.96±1.5	11.1±1.3	-34.9±3.5	5
Kir4.1T262S-Kir5.1	14.1±0.7	9.7±0.6	-31.4±2.9	5
Kir4.1S263A-Kir5.1	9.7±1.0	6.2±1.0	-36.2±3.9	4
Kir4.1S299A-Kir5.1	8.8±1.6	5.4±1.0	-38.6±2.9	7
Kir4.1S320A-Kir5.1	4.7±0.6	3.0±0.6	-39.0±5.0	7
Kir4.1T346A-Kir5.1	4.8±0.4	2.75±0.48	-44.1±7.1	6
Kir4.1S360A-Kir5.1	4.0±0.4	2.3±0.23	-40.3±5.8	4
Kir4.1S373A-Kir5.1	4.1±0.4	2.46±0.23	-38.1±7.3	7
Kir4.1-Kir5.1T68A	11.9±0.8	8.2±0.5	-30.5±1.5	7
Kir4.1-Kir5.1T174A	3.1±0.3	1.9±0.27	-38.1±4.1	5
Kir4.1-Kir5.1T174D	16.5±3.9	15.38±3.3	-0.9±7.2	8
Kir4.1-Kir5.1T174K	5.1±1.1	2.94±0.61	-40.1±9.6	7
Kir4.1-Kir5.1R178Q	6.2±0.5	3.88±0.54	-37.8±4.0	7
Kir4.1-Kir5.1T181A	3.8±0.3	2.08±0.31	-45.8±4.7	5
Kir4.1-Kir5.1S185A	10.1±0.6	6.28±0.64	-37.8±5.1	4
Kir4.1-Kir5.1T215A	3.6±0.2	2.08±0.17	-40.8±7.2	5
Kir4.1-Kir5.1T232A	4.0±0.5	2.3±0.27	-41.4±5.6	4
Kir4.1-Kir5.1S298A	10.2±0.4	6.12±0.82	-39.4±8.5	4
Kir4.1-Kir5.1T370A	3.6±0.4	2.26±0.25	-36.6±5.2	7
Kir4.1T32A-S299A-Kir5.1	22.5±3.3	14.8±3.17	-36.4±5.8	6
Kir4.1K67M-Kir5.1T68A	8.5±3.3	5.95±2.6	-35.8±5.2	4
Kir4.1T262A-Kir5.1T68A	11.04±0.6	7.1±0.27	-35.3±3.4	5
Kir4.1-Kir5.1V211L	4.5±0.6	2.6±0.4	-41.2±5.7	10
Kir4.1L208V	10.4±2.0	9.45±1.9	-10.1±4.7	7
Kir4.1L208I	n.f.	n.f.		
Kir4.1L208V-Kir5.1	7.8±1.46	4.77±0.8	-37.8±2.9	6
Kir4.1L208I-Kir5.1	n.f.	n.f.		

Abbreviations: n, number of observation; n.f., nonfunctional

IV. GATING OF THE ATP-SENSITIVE K^+ CHANNEL BY A PORE-LINING PHENYLALANINE RESIDUE*

These results have been published:

Asheebo Rojas, Jianping Wu, Runping Wang, and Chun Jiang. Gating of the ATP-sensitive K^+ Channel by a Pore-lining Phenylalanine Residue. *BBA-Biomembranes.* (2007) 1768 (1):39-51.

*In this part, Dr. Jianping Wu did 80 % of the single channel patch clamp recordings for me. Ms. Runping Wang created 20 % of the mutations on the Kir6.2. Their help is greatly appreciated.

IVa. INTRODUCTION

The K_{ATP} channels are heteromeric consisting of four subunits of Kir6 and four subunits of sulphonylurea receptor (SUR). The Kir6, that forms the ion-conduction pathway with two transmembrane domains, possesses the essential machineries for channel opening and closure controls (Tucker et al., 1997). A central question in understanding the K_{ATP} channel function is how the channel opening and closure is produced following ligand binding, a process that is known as channel gating. Experimental evidence suggests that transmembrane domains, especially the pore-lining membrane helices, play an important role in the channel gating (Bichet, et al., 2003; Doyle, 2004; Yellen, 2002). The Ca^{++}-dependent gating of the bacterial MthK channel occurs through lateral movements of the inner transmembrane helices (TM2) while the outer transmembrane domain (TM1) remains relatively rigid and stable (Jiang et al., 2002). Such TM2 helical movements during channel gating have also been implied in the KirBac1.1 and mammalian GIRK channels based on crystal structures (Jin et al., 2002; Kuo et al., 2003). In the latter two Kir channels, a phenylalanine located at the narrowest region of the inner vestibule appears to play a critical role in the channel gating (Jin et al., 2002; Kuo et al., 2003). In Kir1.1 a leucine homologous to this phenylalanine was found to be essential for pH gating (Sackin et al., 2005). Such a phenylalanine residue (Phe168) is also found at the cytosolic end of the TM2 of the Kir6.2 subunit, which faces the ion-conduction pathway when its amino acid (AA) sequence is aligned with the KirBac1.1. Phenylalanine is hydrophobic with an aromatic side group. Recent studies on crystal structures of the bacterial mechanosensitive MscL channel, nicotinic acetylcholine

receptor and the KirBac1.1 channel have indicated that nonpolar residues may form a gate through their hydrophobic interaction (Kuo et al., 2003; Sukharev et al., 2001; Unwin, 1995; Unwin, 2003). It is necessary to demonstrate that such a gate is not only a structural existence but also a functional entity. The functional role of Phe168 in Kir6.2 gating was investigated by replacing this residue with amino acids having side chains of different size and hydrophobicity. Our results suggest that the aromatic group of phenylalanine may occlude the ion conduction pathway in the closed state (Jin et al., 2002; Kuo et al., 2003). However, other residues with bulky or hydrophobic side chains at this location can also gate Kir6.2 in a similar manner. In addition to blockade of the ion pathway during the closed state, the Phe168 appears to lower the energy barrier necessary for the gating transition. Thus this phenylalanine may act as a hinderer and a facilitator in the Kir6.2 channel gating.

IVb. RESULTS

IVb-1. *Phenylalanine 168 at the narrowest region of the ion conduction pathway*

AA sequence of several mammalian Kir channels were aligned with sequences of the bacterial KirBac1.1 and KcsA channels in a region from the selectivity filter to the proximal C-terminus. Based on the crystallographic structures of KcsA and KirBac1.1, a phenylalanine is found at the narrowest region of the inner vestibule of the ion-conduction pathway in the Kir6 and Kir3 subfamilies (Fig. 1A, also see Sackin et al., 2005). These Kir channels have rather low basal channel activity. A hydrophobic residue with an intermediate size side group (Leucine, methionine) is also seen in other Kir

channels, most of which show high baseline P_o. Based on the crystal structure of the KirBac1.1 and KcsA channels (Doyle et al., 1998; Kuo et al., 2003), the phenylalanine residue faces the pore with its side chain projecting into the ion pathway (Fig. 1B).

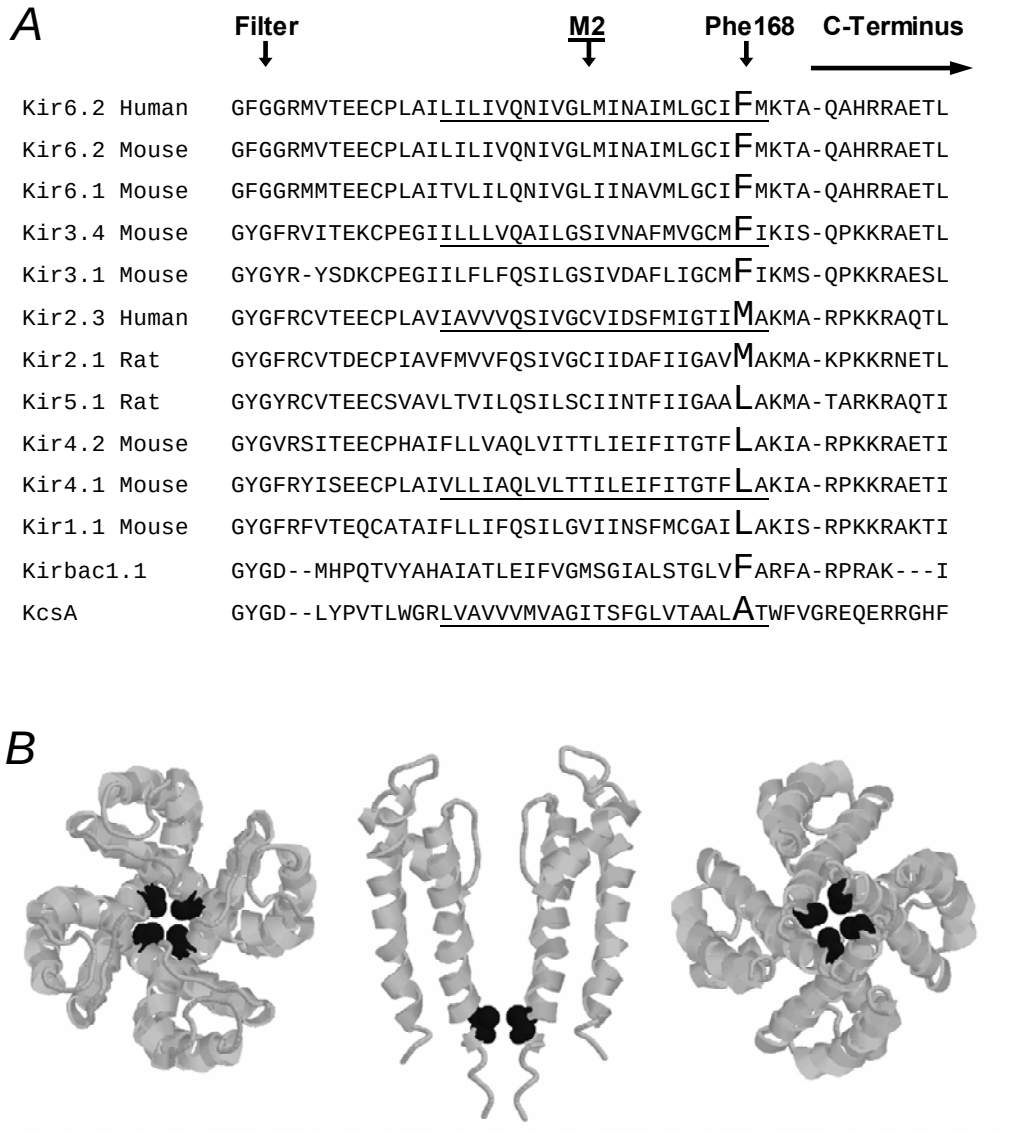

Fig. IV-1. *A*. Phe168 is located in the narrowest sector of the ion conductive pore. Alignment of the Kir6.2 with other K^+ channels in a region from the selectivity filter to the proximal C-terminus. *B*. Phe168 is located in the narrowest sector of the inner pore when aligned with the KcsA sequence and viewed using RasMol modeling (Capener et al., 2000).

IVb-2. ***ATP- and H^+-dependent channel gating with different residue mass and hydrophobicity at position 168***

Site-specific mutations of the Phe168 to small amino acids (alanine, glycine or serine) allowed expression of functional inward rectifying currents. However, these mutations severely disrupted the channel gating by intracellular ATP. The mutant channels barely responded to 3mM ATP, whereas the wild-type Kir6.2ΔC36 channel was strongly inhibited by micromolar concentrations of ATP (Figs. 2C-E, F). In contrast to these mutations, the ATP-dependent channel gating was well maintained when the Phe168 was mutated to a bulky tryptophan (Fig. 2A). The F168W mutant showed a similar ATP sensitivity as the wild-type channel (Figs. 2F, 3F), suggesting that a bulky amino acid is necessary for the ATP-dependent channel gating. Slightly smaller than phenylalanine, histidine is a hydrophilic amino acid with a bulky side chain. The F168H mutation produced a channel that was poorly gated by intracellular ATP (Fig. 2F), suggesting that the residue mass is not the only player in the Kir6.2 channel gating, and hydrophobicity is also important. Further supporting this idea was that mutant channels carrying a hydrophilic amino acid (i.e., glutamine, asparagine, glutamate) at residue 168 were also poorly gated by ATP (Fig. 2F, Table 1). Mutations to other massive and hydrophilic residues (tyrosine, arginine) did not yield functional channels. A similar phenomenon was observed in the presence of the sulphonylurea receptor 1 subunit (SUR1). In the presence of SUR1 the 168 position showed a size dependent effect similar to the Kir6.2ΔC36. The presence of the SUR1 increased the channel sensitivity to ATP without affecting the gating mechanism (Fig. 3, Table 1).

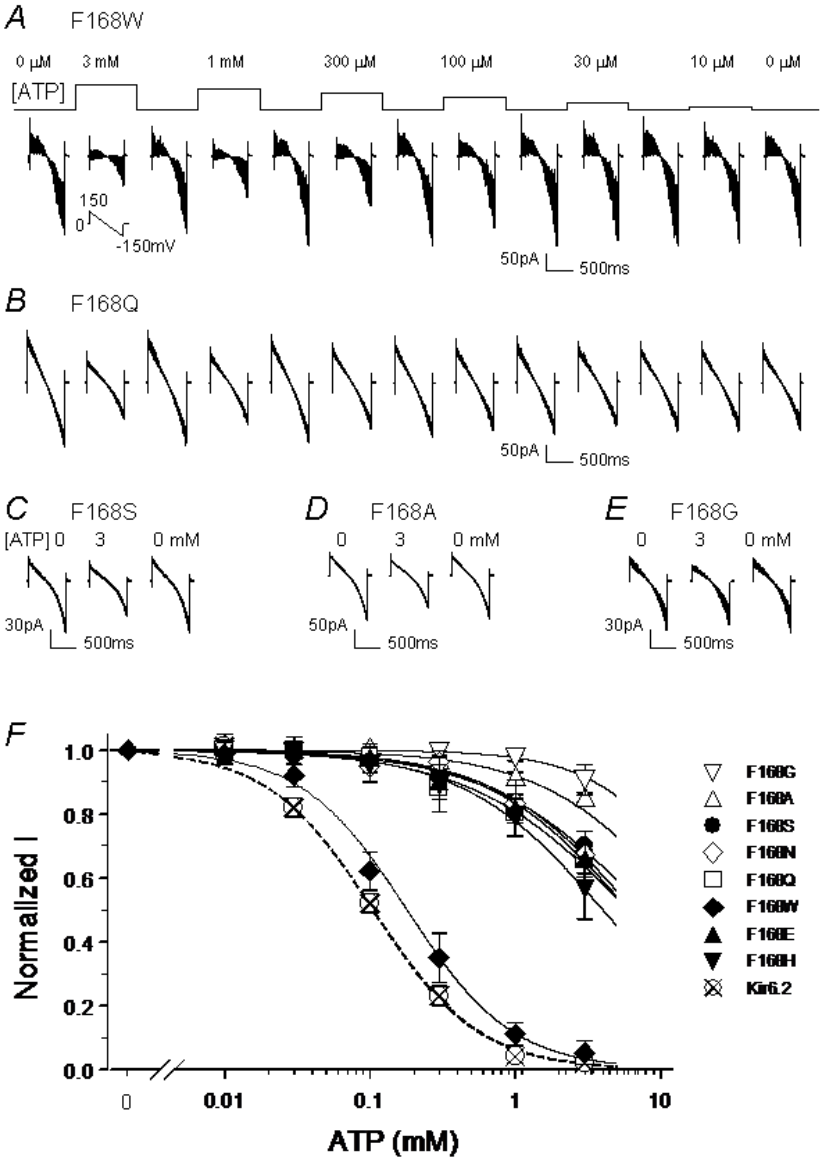

Fig. IV-2. ATP sensitivity of the Kir6.2 channel and its mutants. *A.* Currents were recorded from an inside-out patch obtained from a cell expressing the Kir6.2ΔC36 F168W. With ramp potentials from –150 to 150mV applied to the patch membrane inward rectifying currents were recorded. Exposures to ATP produced a dose-dependent inhibition of these currents with the ATP concentration for 50% current inhibition (IC_{50}) ~300μM. *B.* The Kir6.2ΔC36 F168Q mutant was only modestly inhibited by 1mM ATP. Note that eight superimposed traces are shown in each panel. *C-E.* The F168S, F168A, and F168G mutants of Kir6.2ΔC36 barely responded to 3mM

ATP. *F*. The dose-response curves were produced using the Hill equation (see Methods). All mutants were obtained from Kir6.2ΔC36. Data are presented as means ± s.e with IC_{50} shown in Table 1.

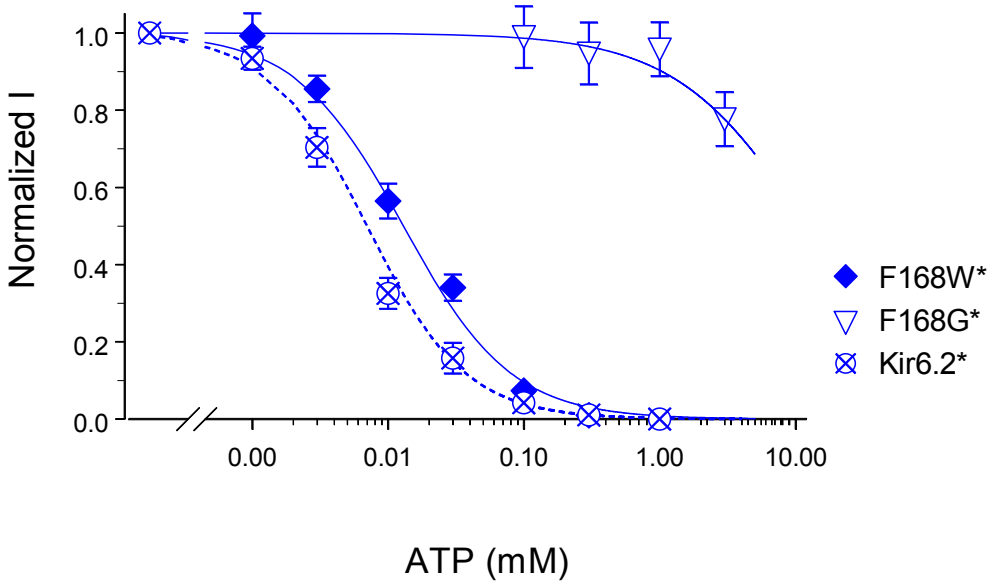

Fig. IV-3. ATP sensitivity of Kir6.2 channel and its mutants expressed with SUR1. Currents were recorded from an inside-out patch obtained from a cell expressing the Kir6.2-F168W+SUR1. With ramp potentials from –150 to 150mV applied to the patch membrane inward rectifying currents were recorded. Exposures to ATP produced a dose-dependent inhibition of the currents with the ATP concentration for 50% current inhibition (IC_{50}) ~10μM. The Kir6.2-F168G+SUR1 mutant barely responded to 3mM ATP. The dose-response curves were produced using the Hill equation (see methods).

The same gating pattern was observed for the proton-dependent gating of the Kir6.2. The F168A and F168G mutations greatly diminished or completely eliminated the channel gating by pH (Fig. 4D-F). The pH sensitivity was well maintained when the Phe168 was mutated to a bulky tryptophan (Fig. 4B). Mutation to an AA with a medium side-chain (glutamine, asparagine) had an intermediate effect (Figs. 4C, F), while mutation to glutamate or histidine reversed the pH response (Table 1).

When the ATP and pH sensitivities were plotted against the residue mass, we found that the effect of ATP and pH on channel activity was a function of the residue mass (Fig. 4F). With a residue of 165 Daltons or larger, the channels were fully functional. They were strongly activated by protons and inhibited by ATP, whereas mutations to a residue smaller than glutamine (146 Daltons) disrupted the channel gating by both ATP and pH. The transition occurs between 146 and 165 Daltons (Fig. 4F), suggesting that residue mass at this location is critical for the Kir6.2 channel gating.

To understand whether the hydrophobic nature of phenylalanine is adequate for the channel gating, we also studied mutant channels with several other nonpolar amino acids such as valine, leucine, isoleucine and methionine at residue 168. None of these mutants produced detectable K^+ currents (Table 1).

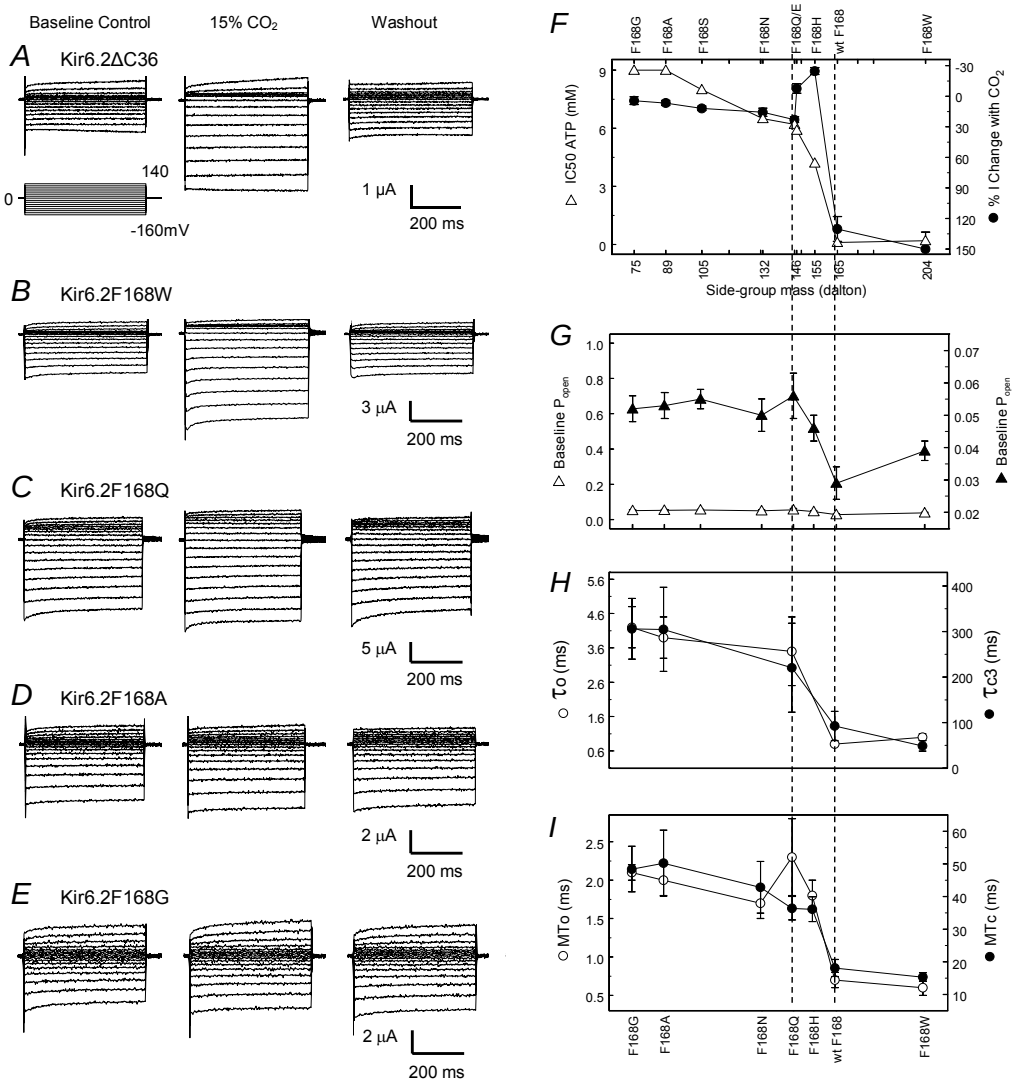

Fig. IV-4. *A.* Activation of Kir6.2ΔC36 by hypercapnic acidosis. Whole-cell currents were studied in an oocyte injected with the Kir6.2ΔC36 3 days earlier. With 90mM K^+ in the extracellular solution inward rectifying currents were recorded at baseline. The currents were reversibly activated with a 5min exposure to 15% CO_2 that acidifies the cytosol to pH 6.6. *B.* Mutation of Phe168 to tryptophan resulted in current activation similar to the Kir6.2ΔC36. *C.* The channel was moderately activated when the Phe168 was mutated to glutamine. *D,E.* Mutation to alanine or glycine yielded channels that were insensitivity to CO_2. *F.* The effects of ATP and CO_2 on single-channel and whole-cell currents were plotted against the residue mass (Kyte and Doolittle, 1982) at the Phe168 location. A marked reduction in the pH and ATP sensitivities occurred with residues smaller than glutamine (146 Daltons). In contrast, the channels showed fair ATP and pH sensitivities with residue mass greater than 165 Daltons. When both plots

combined, the critical mass of this residue is shown to be >155 Daltons for the full ATP and pH sensitivities. Note that the channel response to acidic pH is inversely plotted. IC_{50}= concentration for 50% inhibition. I= current. The open triangle represents the IC_{50} and the closed circles represent the % current change with CO_2. *G.* The relationship of baseline P_o with residue mass. The P_o remained low no matter what AA the Phe168 was substituted with (open triangle). In higher magnification (solid triangle), the baseline P_o was significantly higher with small residues than with large ones with the transition between 145-165 Daltons. *H.* The open-time constant (τo) and the long period of closed-time constant ($\tau c3$) obtained by fitting the dwell-time histogram as illustrated in Fig. 4 show a clear residue-mass dependence. Note that for comparison purpose, the open time was fitted with a single exponential for all channels. *I.* Similar mass-dependence was observed with the mean open time (MT_o) and mean closed time (MT_c).

IVb-3. ***Effects of residue mass and hydrophobicity on the single channel properties***

Consistent with previous reports (Tucker et al., 1997; Wu et al., 2002), single-channel Kir6.2ΔC36 currents showed short periods of openings with low baseline P_o (Fig. 5, Table 2). The F168W-mutant channel showed similar single-channel activity with moderate bursting activity (Fig. 7). It is worth noting that the F168W channel did not show rapid rundown. With a small residue at this position, the F168G channel had much longer openings and closures than the Kir6.2ΔC36 (Figs. 5, 8), leading to a marked decrease in the closure-opening frequency. These mutant channels ran down rather fast in contrast to the F168W, especially when the patches were exposed to acidic pH that causes rundown in wild-type Kir6.2 as well, though to a lesser degree (Xu et al., 2001; Wu et al., 2002).

Although the baseline P_o of all mutant channels remained low (Table 1), significant differences in the baseline P_o was observed between large and small residues. The baseline P_o of the F168G was almost twice as high as the Kir6.2ΔC36 ($P<0.01$), despite the fact that its rapid rundown may have led to an under-estimation of the P_o value. When the residue mass was plotted against P_o, a clear transition of P_o levels was also seen at the residue mass of 146-165 Daltons (Fig. 4G). We also examined the channel open- and closed-time properties and when plotted, the residue-mass dependence was observed in these open and closed time properties with a transition at 146-165 Daltons (Fig. 4H, I).

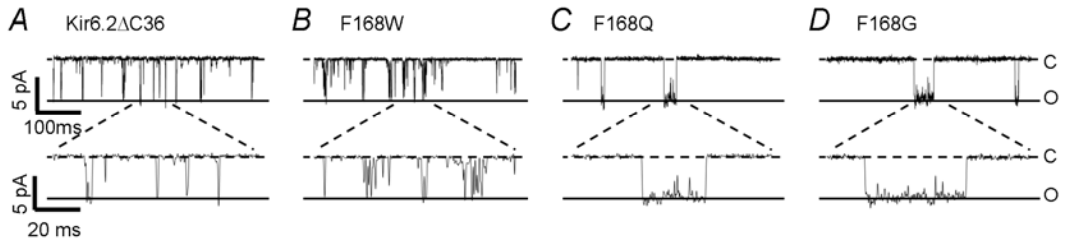

Fig. IV-5. Single-channel analysis of the open and closed times of the Kir6.2ΔC36 and its representative mutants. *A-D.* The Kir6.2ΔC36 and F168W show brief openings and closures, while the openings and closures are much longer in F168G and F168Q. Labels on the right indicate the opening (o) and closure levels (c).

IVb-4. ***Mutations at position 168 in Kir6.2 also affect single-channel kinetics***

Channel open-time and closed-time properties were studied on the F168W, F168Q and F168G mutants that represent residues of different size and hydrophobicity (Figs. 7, 8, 9). The open time constant (τ_o) and the mean open time (MT_o) of the F168W were comparable to those of Kir6.2ΔC36 (Table 2, Table 4), although its bursting activity caused a reduction in long periods of closures leading to a modest decrease in the closed-time constants (τ_c) and the mean closed time (TM_c) (Table 2). The F168G and F168Q channels all showed much longer openings and closures (Table 2). They also had longer τ_o and τ_c as well as longer MT_o and MT_c (Table 2, Table 4). Thus the mutant channels without a bulky and hydrophobic residue at the 168 position tend to stay in long periods of openings and closures (Fig. 5C, D), strongly suggesting that the Phe168 is not only involved in blocking the ion pathway by its bulky side-group, but also facilitates the transition between channel openings and closures.

Like Kir6.2ΔC36 (Fig. 6), the F168W channel was fairly sensitive to ATP. The inhibition by ATP was produced by selective augmentation of the long closures with little or no effect on the openings (Fig. 7D, E). This led to an increase in the MT_c with little effect on the MT_o (Table 2). The F168G mutant was unaffected by ATP up to 3mM ATP. As a result, there were no evident changes in its single-channel kinetics with 1mM ATP (Fig. 8, Table 4). The F168Q was modestly inhibited by ATP. Such a small effect was also mediated by changes in the closed time constants (Fig. 9). Taken together, these

results suggest that the mechanism for ATP inhibition remains similar in the F168W and F168Q mutants although the magnitude of the inhibition is different.

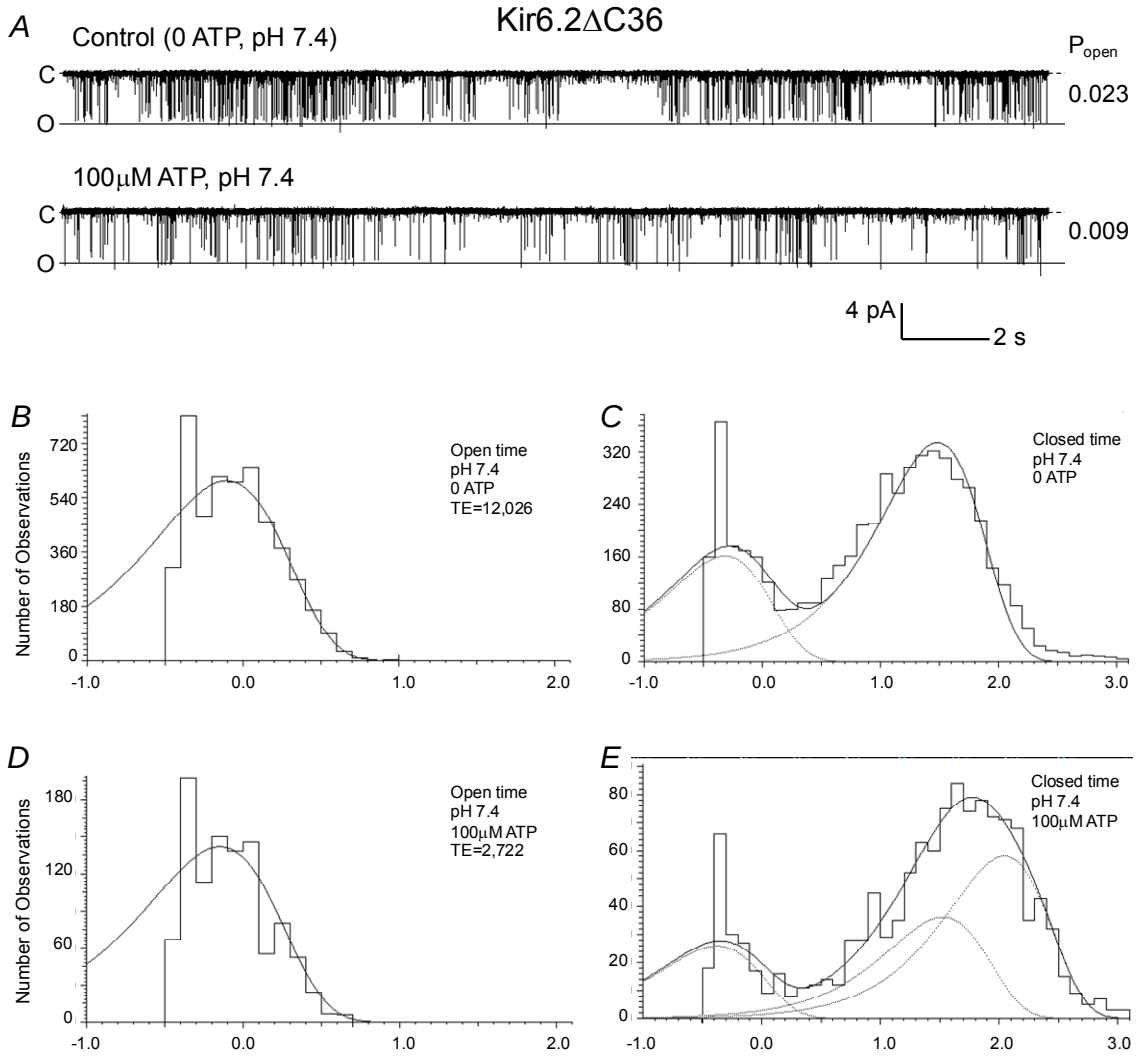

Fig. IV-6. Single-channel kinetics analysis of Kir6.2ΔC36 channel. Data were obtained from an inside-out patch with each histogram constructed using >1min recording. *A.* Single-channel current recorded from the patch was studied with different levels of ATP. Channel activity (P_o, shown on the right) decreased in the presence of 100μM ATP (lower trace). Labels on the left indicate the opening (o) and closure levels (c). The total number of events (TE) used to compute the histogram is also in the caption. *B,C.* Baseline open-time and closed-time histograms at pH 7.4 in the absence of ATP. *B.* The open-time histogram was fitted with one exponential with τo = 0.7 ms. *C.* The closed time was fitted with two exponentials with τc1 = 0.3 ms and τc2 = 28.8 ms. *D, E*. In the presence of 100μM ATP (pH 7.4), a third closure event appeared and was very long.

The time constant for the second closure was slightly changed, but the third closure was prolonged ($\tau c2$ = 33.7 ms, $\tau c3$ = 110.9 ms), while the other time constants were barely affected.

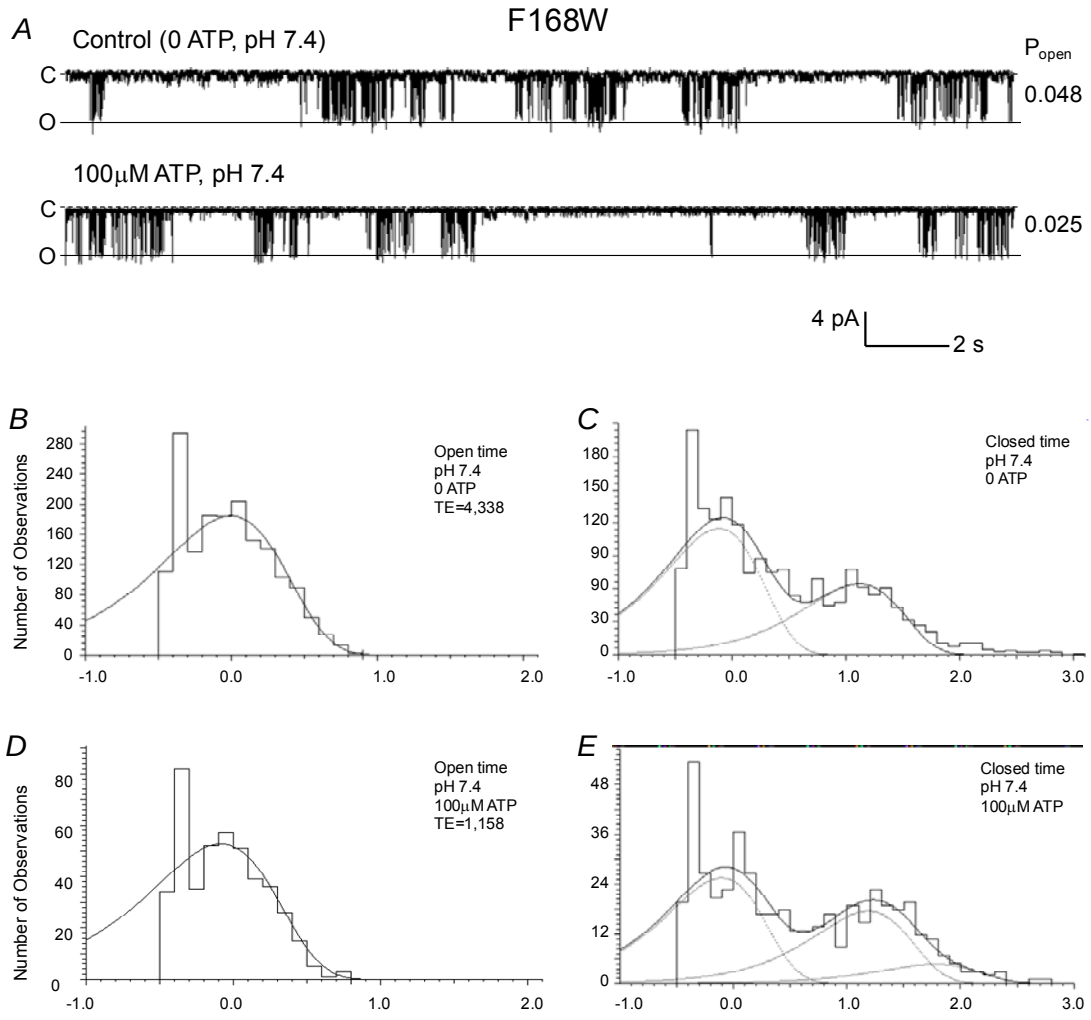

Fig. IV-7. Single-channel kinetics analysis of F168W. Data were obtained from an inside-out patch with each histogram constructed using two stretches of 20 s recording in *B, C, F* and *G* and one stretch in *D* and *E. A.* Single-channel current recorded from the patch was studied with different levels of ATP. Channel activity (P_o, shown on the right) decreased in the presence of 100μM ATP (lower trace). Labels on the left indicate the opening (o) and closure levels (c). The total number of events (TE) used to compute the histogram is also in the caption. *B, C.* Baseline open and closed time histograms at pH 7.4 in the absence of ATP. *B.* The open time histogram was fitted with one exponential with τo = 1.0 ms. *C.* The closed time was fitted with two exponentials with τc1 = 0.8 ms and τc2 = 13.1 ms. *D, E*. In the presence of 100μM ATP (pH 7.4), time constants for the second closure changed a little and a third closures became apparent

and was prolonged ($\tau c2$ = 15.4 ms, $\tau c3$ = 60.3 ms), while the other time constants were barely affected.

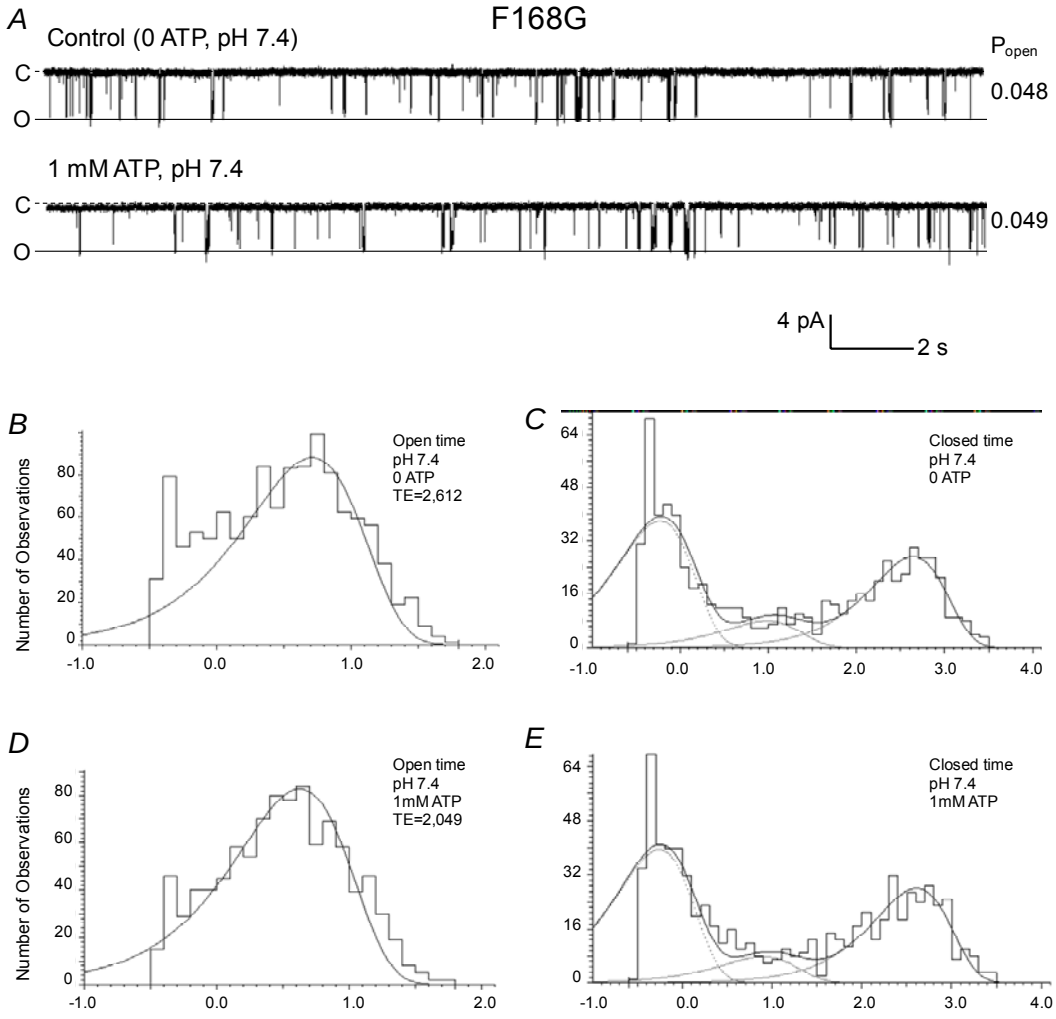

Fig. IV-8. Single-channel kinetics analysis of F168G. Data were obtained from an inside-out patch with each histogram constructed using ≥1min recordings. *A.* Single-channel current recorded from the patch was studied with different levels of ATP. Channel activity (P_o, shown on the right) decreased in the presence of 1mM ATP (lower trace). Labels on the left indicate the opening (o) and closure levels (c). The total number of events (TE) used to compute the histogram is also in the caption. *B,C.* Baseline open and closed time histograms at pH 7.4 in the absence of ATP. *B.* The open time histogram was fitted with one exponential with $\tau o1 = 5.14$ ms. *C.* The closed time was fitted with three exponentials with $\tau c1 = 0.6$ ms, $\tau c2 = 9.6$ ms, $\tau c3 =$

437.9 ms. *D, E*. ATP (1mM, pH 7.4) had no effect on the time constants ($\tau c1$ = 0.5 ms, $\tau c2$ = 7.9 ms, $\tau c3$ = 407.9 ms).

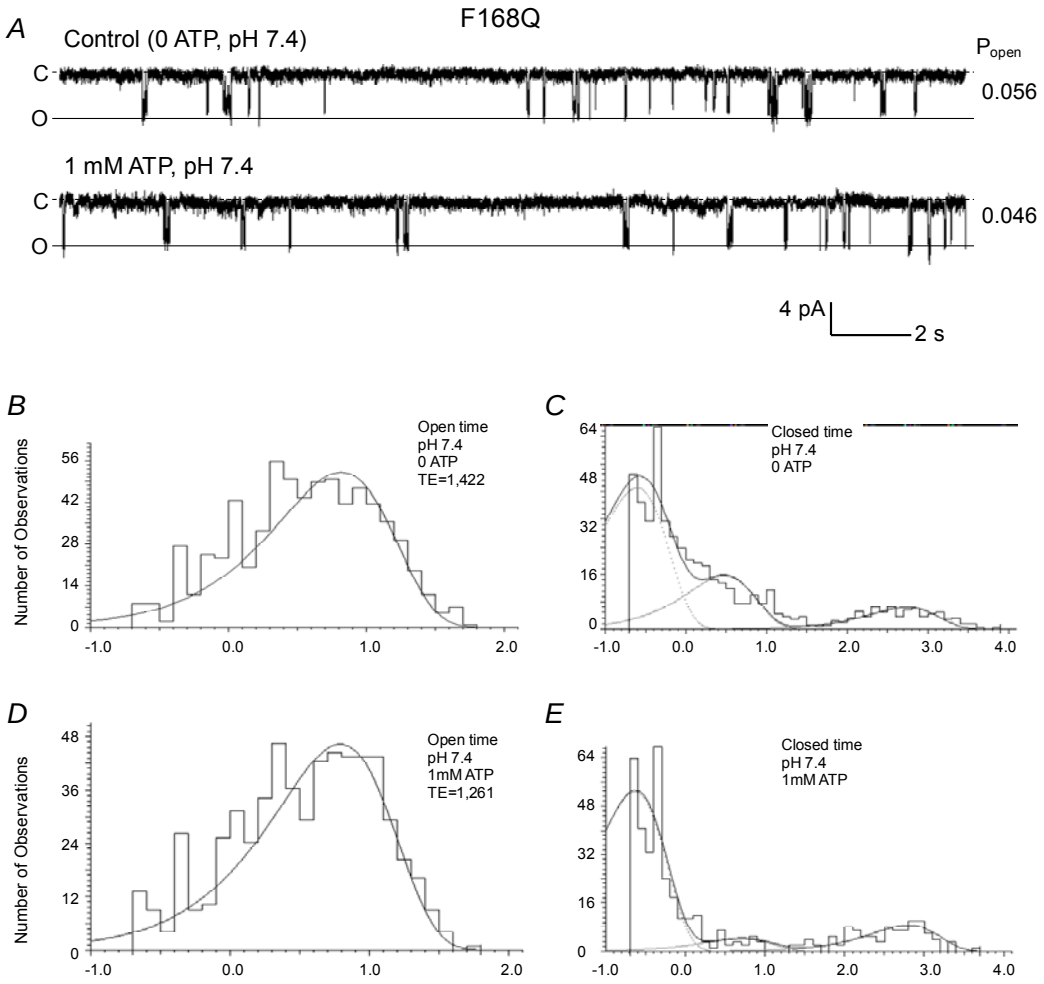

Fig. IV-9. Single-channel kinetics analysis of F168Q. Data were obtained from an inside-out patch with each histogram constructed using ≥1min recordings. *A.* Single-channel current recorded from the patch was studied with different levels of ATP. Channel activity (P_o, shown on the right) decreased in the presence of 1mM ATP (lower trace). Labels on the left indicate the opening (o) and closure levels (c). The total number of events (TE) used to compute the histogram is also in the caption. *B,C.* Baseline open and closed time histograms at pH 7.4 in the absence of ATP. *B.* The open time histogram was fitted with one exponential with $\tau o1 = 6.6$ ms. *C.* The closed time was fitted with three exponentials with $\tau c1 = 0.2$ ms, $\tau c2 = 3.0$ ms, $\tau c3 = 563.6$ ms. *D, E.* In the presence of 1mM ATP (pH 7.4), time constants for the second and third

closures were slightly prolonged ($\tau c1$ = 0.2 ms, $\tau c2$ = 5.0 ms, $\tau c3$ = 640.0 ms), while the other time constants were barely affected.

IVb-5. ***Kinetics modeling***

The rate constant kinetics was determined for the Kir6.2ΔC36 in the basal condition as well as in the presence of ATP (Colquhoun & Hawkes, 1995; Trapp et al., 1998). We adopted a simple kinetic scheme used previously for the K_{ATP} channel (Trapp et al., 1998). In an ATP-free condition, the Kir6.2ΔC36 channel has a single O with C1, and C2. The C1 is the short-lived closed state that can be seen in bursts of openings, and C2 is the long-lived closed state that determines the duration between bursts. During baseline levels the Kir6.2ΔC36 channel exhibits bursting that is reflective in the rate time kinetics (Table 1). This channel tends to have alternating fast and slow kinetics between open and closed states. The scheme is supported by the rate constant kinetics calculated based on the equations described in the methods section. The kinetic model suggests that the Kir6.2ΔC36 channel spends very little time in either the closed or open states. The transitions between the states are very rapid. During channel opening there is a fast transition to the short-lived closed state. In the absence of ATP the kinetics favor a very fast transition from the short-lived closure to the open state and also a very fast transition from the open state to the long-lived closed state. This explains why in the basal condition this channel exhibits bursting or flickering activity. When ATP is present, a second long-lived closed state (C3) appears in the Kir6.2ΔC36 (Scheme 1). The kinetics favors a very fast transition towards C3 in the presence of ATP as indicated by the bold arrow. As a result the C2 is shortened by ATP. Therefore, ATP inhibits the channel by extending the long-lived closed state.

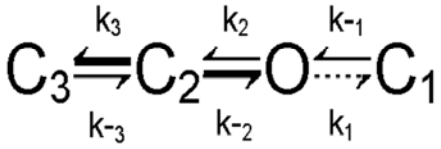

Kir6.2ΔC36-F168G

Scheme 2

To determine whether the Phe168 is critical for this gating transition, we calculated the rate constant kinetics for the F168G mutant that causes severe disruption of channel gating, and compared them with the rate constant kinetics of the Kir6.2ΔC36. The data for the F168G was fitted with the kinetic scheme 2. When the kinetics was entered into the scheme it supported the idea that the F168G mutation has an increased barrier of energy necessary for the gating transitions. The rate constant kinetics for this mutant favors the transition towards openings from both C1 and C2 allowing the channel to stay in the open state (Table 3). The transition from open to C1 is lessened as noted by the dashed arrow (Table 3). Furthermore, the kinetics also favors the transition from C2 to C3 stabilizing at the long-lived close state (Table 3). Therefore, the F168G mutant unlike the Kir6.2ΔC36 has long periods of closures followed by long periods of openings. This results in the slow transition between channel opening and closure, a completely opposite effect to the bursting activity seen in the Kir6.2ΔC36.

IVc. DISCUSSION

Our results have shown that a bulky and hydrophobic AA is required at residue 168 for the Kir6.2 channel gating. With a small residue at this site, the mutant channels remain conducting inward rectifying K^+ currents, but fail to be gated by ATP and protons. The requirement of a bulky residue on the ion-conduction pathway for channel gating therefore suggests a steric hindrance effect. In addition to the residue-mass dependence, hydrophobicity of residue 168 is important for the Kir6.2 channel gating. The size of the residue at position 168 cannot completely account for full channel gating. Various side chain characteristics may contribute to the gating properties. This is apparent in channels carrying charges at the 168 position such as F168E and F168H. These two channels show disrupted pH gating which may attribute to the charge carried by these amino acids. The Kir6.2 channel is well gated with a hydrophobic but not a hydrophilic residue. These results are consistent to what has been reported for the pH gating of Kir1.1 (Sackin et al., 2005).

Based on crystal structures of the bacterial mechanosensitive MscL channel, nicotinic acetylcholine receptor and the KirBac1.1 channel, a hydrophobic residue is often found at the narrowest region of the ion-conduction pathways (Kuo et al., 2003; Sukharev et al., 2001; Unwin, 1995; Unwin, 2003), leading to the "hydrophobic gate" hypothesis: Gating of these channels involves movements of the pore-lining helices with the pore widened during channel opening, while constriction of these pore-lining helices during channel closure brings the nonpolar residues in each subunit of a multimeric channel in contact with each other, thereby sealing the ion-conduction pathway (Doyle,

2004). Our studies have evaluated this hypothesis by looking at functional consequences of different amino acid properties at residue 168. Our results have shown that a hydrophobic residue is necessary for the Kir6.2 channel gating. The channel gating is severely compromised when the Phe168 is mutated to a hydrophilic amino acid including histidine that has almost the same residue mass as phenylalanine. Thus, these results provide functional evidence supporting the hydrophobic gate hypothesis.

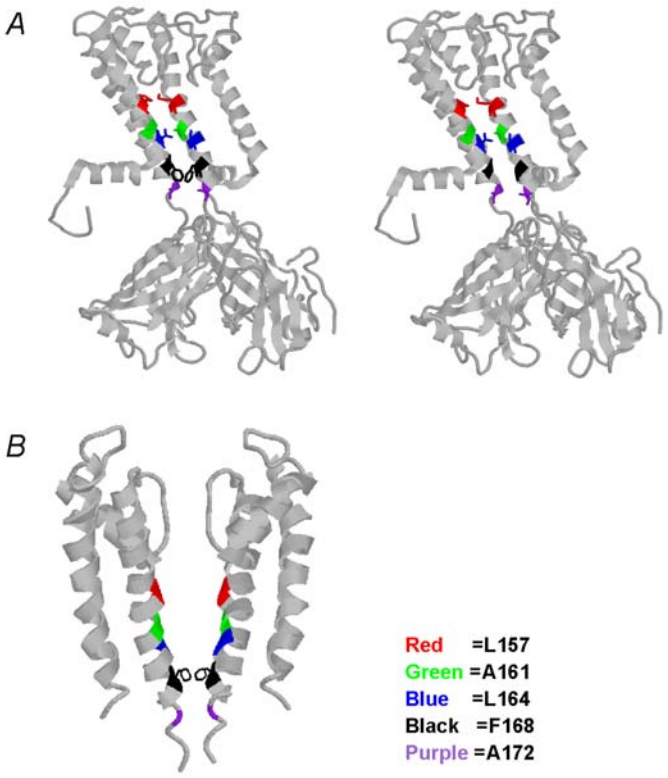

Fig. IV-10. *A.* A structural representation of the residues in the lower TM2 domain. The Kir6.2 was aligned with the KirBac1.1 and displayed based on the KirBac1.1 X-ray crystallographic structure [Kuo et al., 2003]. Shown are two of the channel subunits in a *cis* configuration. The Phe168 is labeled in black. Also labeled by color are other hydrophobic residues located in the

TM2 domain that may possibly interact with each other in the absence of the Phe168. *B.* When the Phe168 is aligned with the KscA model [Doyle et al., 1998], the Phe168 is located at the narrowest part of the ion-conduction pathway of the inner vestibule, and points its side chain toward the pore.

Phenylalanine has an aromatic side group. According to the KirBac1.1 model (Kuo et al., 2003), the Phe168 faces the pore and may block the ion-conduction pathway by the bulky side group (Fig. 10). The involvement of such a phenylalanine residue in channel gating has been suggested in KirBac1.1 and GIRK channels. In the GIRK4 channel, Phe187 is located at the narrowest part of the ion-conduction pathway. The channel gating requires flexibility of the TM2 helix above the Phe187, while introduction of flexibility at the helical turn below the Phe187 renders the TM2 helix unable to transduce the force exerted at its end by the channel-G-protein interaction and fails to produce functional channels (Jin et al., 2002). In the KirBac1.1 channel, a phenylalanine (Phe146) is identified at the corresponding site to the Phe187 in GIRK4 and Phe168 in Kir6.2. Side chains of the Phe146 have been shown to form structural obstacles in the ion-conduction pathway in the closed state (Kuo et al., 2003). Similarly, leucine residues at a homologous position on Kir1.1 occlude the permeation path of Kir1.1 in the closed state (Sackin et al., 2005). According to the White-Wimley hydropathy scale (Wimley & White, 1996; White & Wimley, 1999), leucine is more hydrophobic than its counterpart isoleucine and valine, suggesting that this leucine residue in the Kir1.1 channel may act similarly as Phe168 in the Kir6.2 channel.

In Kir6.2, the baseline channel openings are maintained by the intrinsic conformation of the channel protein, phosphorylation and other K_{ATP} channel regulators such as phospholipids, ADP and protons (Baukrowitz et al., 1998; Light et al., 2000; Lin et al., 2000; Shyng & Nichols,1998; Wu et al., 2002; Xu et al., 2001). ATP binding to intracellular protein domains (Tanabe et al., 1999; Tsubo et al., 2004) may produce a

conformational change of the inner helices. When the phenylalanine from each subunit are close enough, they can interact with each other through hydrophobic forces and close the ion pathway (Fig. 10), as indicated in the KirBac1.1 crystallographic structure (Kuo et al., 2003). Substitution of this Phe168 residue with a smaller amino acid eliminates the gating ring, and disrupts the channel gating. The pore blockade may be removed during channel opening, as it is known that the inner helix bundle-crossing moves and the inner pore is widened with channel opening (Armstrong, 1966; Davies, 1990; Flynn & Zagotta, 2001; Jiang et al., 2002; Johnson & Zagotta, 2001; Perozo et al., 1999; Phillips et al., 2003; Shin et al., 2001), suggesting that the Phe168 also acts on the channel gating by the steric hindrance effect.

A kinetic model is helpful to understand how this phenylalanine can have this steric hindrance effect. We thus used the simplest kinetic scheme to explain our data for the Kir6.2ΔC36 and the F168G mutant channels. In the basal condition, the Kir6.2ΔC36 channel contains two close states (C1, C2) and one open state (O). A third long-lived closed state appears when ATP is present in the solution. In contrast to the Kir6.2ΔC36, the F168G mutant contains one open state and three closed states (C1, C2, C3) in the absence of ATP. The C1 and C2 are similar to those in the Kir6.2ΔC36, while the C3 is a long-lived closed state independent of ATP. Kinetic analysis shows that the F168G mutant tends to be stabilized in the open and long-lived closed states. Under such a condition, higher free energy is needed to fulfill the gating transitions. This is consistent with the observation that this mutant channel is no longer sensitive to ATP concentrations that strongly inhibit the Kir6.2ΔC36. The mere presence of a phenylalanine at position

168 in the Kir6.2ΔC36 appears sufficient to lower the barrier of energy necessary for the gating transitions. In this respect, phenyalanine is likely to act as a facilitator of the channel gating. Thus, a bulky and hydrophobic residue like phenylalanine and tryptophan may block the ion-conduction pathway in the closed state and facilitate the closure-opening transition in channel gating. Apparently this is a consequence of evolutionary optimization of protein function. This phenylalanine is not seen in several other Kir channels including Kir1.1, Kir2.1 and Kir4.1. Instead, a leucine or methionine is found in those channels. It is known that some of these hydrophobic residues with an intermediate side chain also serve as a gate as in the Kir1.1 channel (Sackin, 2005). Under such a condition, a reduced hydrophobicity of the pore-lining residues may be necessary for preventing pore collapse or channel rundown.

IVd. SUMMARY AND CONCLUSION

ATP-sensitive K^+ (K_{ATP}) channels are gated by intracellular ATP, proton and phospholipids. The pore-forming Kir6.2 subunit has all essential machineries for channel gating by these ligands. It is known that channel gating involves the inner helix bundle of crossing in which a phenylalanine residue (Phe168) is found in the TM2 at the narrowest region of the ion-conduction pathway in the Kir6.2. Here we present evidence that Phe168-Kir6.2 functions as an ATP- and proton-activated gate via steric hindrance and hydrophobic interactions. Site-specific mutations of Phe168 to a small amino acid resulted in losses of the ATP- and proton-dependent gating, whereas the channel gating was well maintained after mutation to a bulky tryptophan, supporting the steric hindrance

effect. The steric hindrance effect, though necessary, was insufficient for the gating, as mutating Phe168 to a bulky hydrophilic residue severely compromised the channel gating. Single-channel kinetics of the F168W mutant resembled the wild-type channel. Small residues increased P_{open}, and displayed long-lasting closures and long-lasting openings. Kinetic modeling showed that these resulted from stabilization of the channel to open and long-lived closed states, suggesting that a bulky and hydrophobic residue may lower the energy barrier for the switch between channel openings and closures. Thus, it is likely that the Phe168 acts as not only a steric hindrance gate but also potentially a facilitator of gating transitions in the Kir6.2 channel.

Table IV-1. WT and mutant channels tested and their pH and ATP sensitivities

	IC_{50} ATP	% CO_2 Effect	Baseline P_o	MW	Hydropathy[1]	Hydropathy[2]
F168G	>9,000 (4)	4.5 ± 3.8 (8)	0.052 ± 0.004 (6)	75	−0.4	0.01
F168A	>9,000 (4)	6.7 ± 2.6 (9)	0.053 ± 0.004 (6)	89	1.8	0.17
F168S	8,061 ± 1,254 (6)	11.9 ± 2.2 (7)	0.055 ± 0.003 (4)	105	−0.8	0.13
F168V	NF	NF	NF	117	4.2	0.07
F168C	NF	NF	NF	121	2.5	-0.24
F168I	NF	NF	NF	131	4.5	-0.31
F168L	NF	NF	NF	131	3.8	-0.56
F168N	6,562 ± 797 (5)	15.8 ± 4.0 (5)	0.050 ± 0.005 (6)	132	-3.5	0.42
F168Q	6,274 ± 656 (4)	23.1 ± 2.9 (10)	0.056 ± 0.006 (13)	146	−3.5	0.58
F168K	NF	NF	NF	146	−3.9	0.99
F168E	5,989 ± 1,441 (6)	−7.5 ± 4.6 (6)	0.036 ± 0.005 (4)	147	−3.5	2.02
F168M	NF	NF	NF	149	1.9	-0.23
F168H	4,198 ± 375 (4)	−24.6 ± 3.4 (6)	0.046 ± 0.005 (4)	155	−3.2	0.96
Kir6.2ΔC36	109 ± 17 (14)	130.3 ± 12.2 (9)	0.029 ± 0.005 (7)	165	2.8	-1.13
F168R	NF	± NF	NF	174	−4.5	0.81
F168Y	NF	NF	NF	181	−1.3	-0.94
F168W	195 ± 24 (6)	150 ± 16.6 (10)	0.039 ± 0.003 (13)	204	-0.9	-1.85
***Kir6.2F168G**	>9,000 (6)		0.070 ± 0.004 (5)			
***Kir6.2^{+}Sur1**	7 ± 0.6 (11)		0.169 ± 0.014 (4)			
***Kir6.2F168W**	13 ± 2.6 (5)		0.243 ± 0.016 (11)			

The ATP sensitivity was studied in excised patches and is expressed by fitting the data using the Hill equation. Hill coefficients are 1.0−1.2 (not shown). All mutants were created on Kir6.2ΔC36. Abbreviations: MW, molecular weight; NF, nonfunctional. Data are presented as means ± s.e with n (in the parentheses) = number of patches. Hydropathy was used to indicate whole-residue hydrophobicity according to the interface scale (Kyte & Doolittle, 1982; Wimley & White, 1996; White & Wimley, 1999). Hydropathy[1] refers to the Kyte-Doolittle hydropathy scale and hydropathy[2] refers to the White-Wimley scale. Asterisk indicates the channel expressed with SUR1.

Table IV-2. Single channel data of wild-type and representative mutant channels

	F168G	F168Q	Kir6.2ΔC36 F168	F168W
pH7.4, no ATP				
P_o	0.049 ± 0.003 (17)	0.056 ± 0.007 (14)	0.029 ± 0.004 (7)	0.039 ± 0.004 (9)
MT_o	2.1 ± 0.1 ms (11)	2.3 ± 0.5 ms (14)	0.7 ± 0.1 ms (6)	0.6 ± 0.1 ms (9)
MT_c	48.4 ± 7.0 ms (11)	36.4 ± 3.6 ms (14)	18.1 ± 2.6 ms (6)	15.3 ± 1.3 ms (9)
pH7.4, 100μM ATP				
P_o	–	–	0.008 ± 0.002 (4)	0.021 ± 0.002 (4)
MT_o	–	–	0.8 ± 0.0 ms (4)	0.6 ± 0.0 ms (4)
MT_c	–	–	67.1 ± 4.3 ms (4)	22.4 ± 2.7 ms (5)
pH7.4, 1mM ATP				
P_o	0.047 ± 0.008 (7)	0.040 ± 0.007 (6)	–	–
MT_o	2.6 ± 0.3 ms (7)	2.7 ± 0.5 ms (6)	–	–
MT_c	60.2 ± 7.6 ms (7)	64.0 ± 7.5 ms (6)	–	–

The open-state probability (P_o), mean open time (MT_o), and mean closed time (MT_c) were studied in patches with a single active channel. Excised inside-out patches were exposed to 100μM ATP or 1mM ATP as dependent upon the IC_{50} of the mutant and compared to controls with no ATP. All mutants were based on the Kir6.2ΔC36. Data are presented as means ± s.e. with n shown in parentheses and represents the number of patches.

Table IV-3. Rate constants used for kinetic modeling

	Kir6.2ΔC36	Kir6.2ΔC36-F168G
τo1	0.6	4.2
τc1	0.2	0.3
τc2	38.0	2.5
τc3	–	255.6
τc2'	27.4	–
τc3'	197.3	–
k_1	720.2	162.1
k_{-1}	4,545.4	4,000.0
k_2	1,065.5	76.0
k_{-2}	26.3	257.5
k_3	–	138.5
k_{-3}	–	3.9
k'_3	102,230.0	–
k'_{-3}	5.1	–

The average rate constants were calculated at -80mV. The τc2', τc3', k'_3 and k'_{-3} were obtained in the presence of 100μM ATP.

Table IV-4. Open and closed time constants for wild-type and mutant channels

	Kir6.2ΔC36	Kir6.2ΔC36-F168W	Kir6.2ΔC36-F168Q	Kir6.2ΔC36-F168G
τo1	0.56±0.04 (5)	0.5±0.06 (5)	3.5±1.0 (5)	4.2±0.55 (4)
τc1	0.22±0.02 (5)	0.3±0.0 (5)	0.3±0.1 (5)	0.3±0.03 (4)
τc2	38.02±11.18 (5)	17.86±2.72 (5)	10±2.4 (5)	2.5±0.74 (4)
τc3	-	-	162.2±74.2 (5)	255.55±79.65 (4)
∗τo1	0.68±0.066 (5)	0.95±0.1 (4)	4.0±0.7 (5)	4.2±0.6 (4)
∗τc1	0.3±0.05 (5)	0.65±0.06 (4)	0.4±0.0 (5)	0.3±0 (4)
∗τc2	27.38±12.83 (5)	14.13±2.76 (4)	13.8±2.1 (5)	2.9±0.8 (4)
∗τc3	197.26±84.55 (5)	94.53±25.16 (4)	240.5±64.4 (5)	254.9±78.7 (4)

The open time constant (**τo1**) and the closed time constants (**τc1, τc2, τc3**) were studied in patches with a single active channel. Excised inside-out patches were exposed to 100μM ATP or 1mM ATP as dependent upon the IC_{50} of the mutant and compared to controls with no ATP. All mutants were based on the Kir6.2ΔC36. Data are presented as means ± s.e. with n shown in parentheses and represents the number of patches. Asterisk represent data obtained in the presence of ATP.

K. GENERAL DISCUSSION

K-1. *Central CO_2 chemoreception*

The process by which the body senses CO_2 is finely tuned, covering a wide range of CO_2 changes. The basal level of CO_2 in the body is ~5% CO_2. This is a partial pressure of CO_2 (pCO_2) ~ 38 mmHg. In humans the range of pCO_2 detected is from 38 mmHg to ~80 mmHg. pCO_2 levels above 80 mmHg is considered a patho-physiological condition that rapidly results in the stoppage of breathing. Even with such a broad range of pCO_2 levels being detected the central CO_2 chemoreception system remains highly sensitive to changes in CO_2. A change in pCO_2 as low as 1 mmHg results in a significant change in ventilation (Nattie, 1999; Putnam et al., 2004). This minute change in the partial pressure of CO_2 results in only a minuscule change in blood pH (~0.001%). This creates a paradox that is: how can the CO_2 sensing mechanism in the brainstem maintain such a high sensitivity to CO_2 and at the same time cover a wide range of changes in the pCO_2? Researchers have been trying to address this question for many years.

K-2. *Neuromodulation and central chemoreception*

In some cases instead of changing the frequency of action potentials, neurotransmitters may change the pattern of the firing. For example, neurons that are normally tonic bursters may become phasic burster following the neurotransmitter binding and vice versa. The response of the neuron to these neurotransmitters depends on several factors such as the receptor subtype, the intracellular cascades activated, receptor number, target molecule number and distribution, as well as the amount of neurotransmitter released. Some neurotransmitters such as serotonin have many receptor

subtypes. These different receptors although share a commonality in binding serotonin may all lead to the activation of different intracellular cascades and molecules leading to different neuromodulations. In this way it becomes extremely important in identifying which receptor subtype is present in these chemosensitive neurons and what intracellular cascades are activated following ligand binding. With such specificity the neuromodulation may be confined to a specific cell type. In this way neuromodulation may affect the cellular response to CO_2 that may also explain how the CO_2 signal may be amplified leading to a highly sensitive detection system. In this thesis I have performed experiments to test the hypothesis that blockade of synaptic transmission results in a lower sensitivity to CO_2 in cultured brainstem neurons. Brainstem neurons were dissociated and cultured on MEA dishes. The response to CO_2 was determined for individual units. Following the blockade of synaptic transmission by the application of specific neurotransmitter blockers to the bath solution the CO_2 sensitivity of identified units were determined to be lower than that prior to the application of the neurotransmitter blocker. I was able to demonstrate that blockade of synaptic transmission involving substance P, serotonin, and glutamate resulted in a lower response to acidification, suggesting that cultured brainstem neurons have adopted synaptic transmission as a means of amplifying the response to changes in CO_2.

The high pH sensitivity of the Kir4.1-Kir5.1 channel in the physiological range suggests that this channel may be a good candidate CO_2 chemoreceptor molecule. To strengthen the candidacy of this channel as a chemoreceptor molecule we found it necessary to demonstrate how the neurotransmitters and CO_2 affect the channel activity.

We hypothesized that the neurotransmitters and CO_2 inhibits the channel activity via different mechanisms. Therefore, we performed experiments to test this hypothesis. We found that although both CO_2 and the neurotransmitters (SP, 5-HT, and TRH) can inhibit the channel, the inhibition appeared to be though different and independent mechanisms. This is an important finding as this suggests that both modulators combined may have a greater effect on the channel than either modulator alone. This potentially implies that the presence of the neurotransmitters may increase the channel's sensitivity to CO_2. This is significant as we know that the have to be amplification of the signal during central CO_2 chemoreception (discussed earlier). This potentially may be one mechanism for amplifying the signal the signal in central CO_2 chemoreception.

K-3. ***Inward rectifier potassium channels as chemoreceptor molecules***

A previous study performed by Wu et al., in 2004 demonstrated the presence of mRNA for both Kir4.1 and Kir5.1 in the same brainstem chemosensitive neurons. This study used in situ hybridization to identify mRNA of Kir4.1 and Kir5.1 in CO_2 chemosensitive sites. Although mRNA for the Kir4.1 and Kir5.1 positively identified in the same chemosensitive brainstem neurons suggested that the heteromeric Kir4.1-Kir5.1 is expressed, the weakness of this study is that mRNA is only suggestive. The presence of mRNA is not indicative of the protein expression. The presence of mRNA does not necessarily confer that the Kir4.1 and Kir5.1 proteins are present. Therefore, in this dissertation I wanted to solidify the expression of the heteromeric Kir4.1-Kir.1 channel in chemosensitive brainstem neurons. It was very imperative that we demonstrate expression of the Kir4.1 and Kir5.1 proteins in neurons as both Kir4.1 and Kir5.1

subunits are suggested to express only in glial cells where they function in potassium recycling. Although we agree that the Kir4.1 and Kir5.1 subunits are expressed in glial cells we also believe that they are expressed in neurons as well where they may form the heteromeric Kir4.1-Kir5.1 channel that would have a different function than potassium recycling. Using DAB immunocytochemistry and immunofluorescence I have presented evidence in this thesis for the expression of the Kir4.1-Kir5.1 channel in chemosensitive neurons. This neuronal expression suggests that this channel may have a different function than potassium recycling in neurons compared to the homomeric counterparts expressed in glial cells. In addition to demonstrating neuronal expression I also have demonstrated expression of the Kir4.1-Kir5.1 channel in chemosensitive neurons. I showed that the channel is expressed in primary sensory neurons such as LC neurons as well as in chemosensitive motor neurons such as the hypoglossal motor neurons. The demonstration of the presence of this Kir4.1-Kir5.1 channel in these chemosensitive brainstem nuclei strengthens the candidacy of this channel as a central CO_2 chemoreceptor molecule.

In this thesis I have also demonstrated another important regulation of the Kir4.1-Kir5.1 channel critical for central chemoreception that is the modulation by neurotransmitters critical for respiratory control. Recall that one of the requirements of a central CO_2 chemoreceptor molecule is that it should be subject to modulation by neurotransmitters critical for respiratory control. The neurotransmitters 5-HT, SP, and TRH are all critical for respiratory control. Therefore, I hypothesized that the Kir4.1-Kir5.1 channel is regulated by these neurotransmitters as the immunocytochemistry

experiments show co-expression of the Kir4.1-Kir5.1 channel with the NK1R. Xenopus laevis oocytes co-expressing the natural receptors for these neurotransmitters and the Kir4.1-Kir5.1 channel were exposed to the neurotransmitters. Bath application of all three neurotransmitters inhibited Kir4.1-Kir5.1 currents and reduced the channel activity. The effects of the neurotransmitters were dose dependent and specific. More importantly, the effects of the neurotransmitters required co-expression of the Kir5.1 as the homomeric Kir4.1 channel expressed with the neurotransmitters failed to be regulated by the neurotransmitters. This important finding may prove to be a useful tool for future experiments with the heteromeric channel in vivo. The activation of PKC has been demonstrated to underscore the inhibition of G-protein gated inward rectifier potassium channels (GIRK) by SP (Mao et al., 2004). Therefore we wanted to know whether protein kinase C was involved in the inhibition of the Kir4.1-Kir5.1 by the neurotransmitters 5-HT, SP, and TRH. Indeed, similar to GIRK channels we showed that PKC activation was involved in the inhibition of the channel by the neurotransmitters.

Since the channel modulation by neurotransmitters depended upon protein kinase C activation, we hypothesized that the Kir4.1-Kir5.1 channel may be phosphorylated by PKC. Indeed, several other Kir channels have been shown to be phosphorylated by PKC and PKC phosphorylation sites have been identified (Fakler et al., 1994; Henry et al., 1996; Light et al., 2000; Lin et al., 2000; Mao et al., 2004; Stevens et al., 1999; Vorobiov et al., 1998; Zhang et al., 2004; Zhu et al., 1999; Zitron et al., 2004). Both the Kir4.1 and Kir5.1 channels were screened to identify potential PKC phosphorylation sites. Both subunits contained numerous putative PKC phosphorylation sites in the C-termini,

suggesting that PKC may phosphorylate the Kir4.1-Kir5.1 channel at residues in the C-termini. In this thesis I showed that Kir4.1-Kir5.1 is inhibited by PKC activation and that PKC could directly phosphorylate the C-termini of both Kir4.1 and Kir5.1. Unfortunately, I was unable to identify the PKC phosphorylation site(s) as I think that the channel contains multiple phosphorylation sites. In this way, single mutation of potential phosphorylation sites may not lead to an identification of the phosphorylation site. Indeed, the biochemistry experiments demonstrated that both Kir4.1 and Kir5.1 C-termini can be directly phosphorylated by PKC which supports the idea that the heteromeric interaction introduces additional potential phosphorylation sites. Although the Kir4.1 C-terminus was shown to contain phosphorylation sites that could be phosphorylated directly by PKC the Kir4.1 channel expressed in xenopus oocytes failed to be regulated by PKC activation suggesting that the presence of Kir5.1 allows for the regulation by PKC. This is another regulatory function displayed by the Kir4.1-Kir5.1 channel that is absent in the Kir4.1 homomeric channel. This may be proven to be a useful tool for characterizing the heteromeric channel function in the future.

K-4. *Kir channel gating*

Ligand modulated ion channels have four properties that are: ion selectivity; ion permeation, ligand binding, and gating. Of all these properties channel gating is the least understood. Gating refers to the opening and closure of ion channels. Ion channels can adopt at least two conformations; an open conformation and a closed conformation. This suggests that ion channels can switch between these two conformations at any giving time (gating). In ligand modulated channels, ligand binding results in a change in

the channel gating mechanism. With the discovery that CO_2 and the neurotransmitters affect the Kir4.1-Kir5.1 channel via different mechanisms, I then tried to identify the exact mechanism for the channel inhibition by these modulators. I hypothesized that Kir channels have common gate that can be modulated by CO_2. Since the protonation site in the Kir4.1-Kir5.1 channel has not been clearly identified I decided to examine the gating mechanism by CO_2 using the Kir6.2+SUR1 channel. The Kir6.2+SUR1 channels have several advantages over the Kir4.1-Kir5.1 channel for studying gating. The Kir6.2+SUR1 channel's CO_2 sensitivity have been well documented. This channel in addition to being pH sensitive is also ATP sensitive. And the channel has clearly demonstrated ligand binding sites as well as gating sites.

I noticed that in the Kir6.2+SUR1 there was only one bulky hydrophobic residue in the TMD2 domain (Phenylalanine 168). Therefore, I hypothesized that the bulky hydrophobic phenylalanine 168 in the Kir6.2 was involved in channel gating by exposing its bulky side chain to block the channel pore. I tested this hypothesis using site directed mutagenesis and found that Phe168 acts as a gate in the Kir6.2+SUR1 channel. I found that Phe168 not only hinders ion flow, but also facilitates it. How can one residue hinder and facilitate ion flow? During basal conditions the bulky side chain of Phe168 clogs the channel pore and hinders the flow of ions though the ion conducting pathway. Upon ligand binding the TMD2 undergoes elaborate conformational changes that results in the moving away of the bulky phenylalanine side chain from the pore. I showed that when the 168 position is mutated to small amino acids the mutant channels tend to lose their sensitivity to ATP and pH. Single channel analysis demonstrated that this is a result of

the channels staying in long periods of openings and closures with more closures than openings. However, the presence of a bulky hydrophobic residue at the 168 position allows the channels to gate more readily. I demonstrated that the presence of phenylalanine 168 lowers the energy barrier necessary for the transition from open to close; thus being a facilitator of channel gating. I found that both ATP and proton binding regulated the channel gating at this position, suggesting that the gate is shared by multiple ligands. This is the first demonstration of a functional gate in the Kir6.2+SUR1 channel. As mentioned before, all Kir channels have a bulky hydrophobic residue located around the narrowest region of the ion conductive pathway. It now becomes necessary to demonstrate the importance of this gate during ligand modulation in other Kir channels. For the Kir6.2+SUR1 and the Kir4.1-Kir5.1 channel, the demonstration of a functional pH modulation gate is critical for understand the role these channels may play in central CO_2 chemoreception.

The Kir6.2+SUR1 channel is a strong chemoreceptor molecule. We now know that this channel is expressed in brainstem inspiratory neurons, the channel is sensitive to pH within a physiological range, it can change the membrane excitability of neurons, and it is gated by protons. The presence of the Kir6.2+SUR1 channel in inspiratory neurons suggests that the channel functions in these cells (Haller et al., 2001). Since the Kir6.2+SUR1 channel is stimulated by intracellular acidification, then channel may be involved in the inhibition of these expiratory neurons during acidosis that is necessary. The activation of this potassium channel would lead to release of potassium to the extracellular space resulting in hyper polarization of these expiratory neurons. This

hyper polarization would inhibit these neurons leading to a decrease in their firing frequency and thus a decrease in their information relay to the respiratory muscles. This is important physiologically as we know that the brain contains inspiratory and expiratory neurons. During inspiration the respiratory neurons are inhibited where as during expiration the inspiratory neurons are inhibited. Therefore, during inspiration activation the Kir6.2+SUR1 channel is a mechanism that can potentially lead to the inhibition of expiratory neurons. Recordings from brainstem expiratory neurons containing the Kir6.2+SUR1 channels demonstrating the importance of this channel in these neurons now becomes necessary for solidifying the role of this channel in central CO_2 chemoreception.

The Kir4.1-Kir5.1 is also a strong central CO_2 chemoreceptor candidate molecule. We now know that this channel is expressed in the brainstem, it has high pH sensitivity within the physiological range, it can detect both alkaline and acidic pH levels, it can change the cellular excitability, it is subject to neuromodulation by neurotransmitters critical for respiratory control, it is gated by protons. Similar to the Kir6.2+SUR1 the presence of the Kir4.1-Kir5.1 channel in chemosensitive brainstem neurons suggest that the channel may play an important role in these cells. The Kir4.1-Kir5.1 channel unlike the Kir6.2+SUR1 is inhibited by intracellular acidosis. The heteromeric Kir4.1-Kir5.1 channel unlike the Kir6.2+SUR1 channel is inhibited by intracellular acidification. As discussed earlier the inhibition appears to occur via protonation of lysine residues. Since the Kir4.1-Kir5.1 channel is inhibited by intracellular acidosis its role in primary sensory chemosensitive neurons may be to augment the firing activity of these neurons. The

inhibition of the Kir4.1-Kir5.1 channel by CO_2 would result in the cease of flow of potassium out of the neurons resulting in the depolarization of the neurons. Depolarization would lead to an increase in the firing frequency of these brainstem neurons that would be relayed to the respiratory muscle leading to an increase in ventilation. In addition to being inhibited by CO_2 the Kir4.1-Kir5.1 channel may also be inhibited by neurotransmitters critical for respiratory control thereby increasing the CO_2 stimulus and the response during the relay to the respiratory muscles. The demonstration of the modulation of the Kir4.1-Kir5.1 channel by neurotransmitters critical for respiratory control is important physiologically as this suggests that the channel may play in role in the control of respiration. This also suggests that the Kir4.1-Kir5.1 channel has an additional function that the homomeric channels do not have.

The two channels studied and discussed in this dissertation are just two of the potential chemoreceptor candidates. There are other candidates that were not studied as they are weak candidates failing to satisfy the requirements for a central CO_2 chemoreceptor molecule. For many years researchers have searched for the central CO_2 chemoreceptor molecule. What we are proposing in this dissertation is that there may be multiple CO_2 chemoreceptor molecules. This idea can explain how central CO_2 chemoreception can maintain a high sensitivity while spanning a broad range of changes in pCO_2. The potential CO_2 receptor molecules may all be able to detect CO_2/pH in different levels such that collectively they would allow for the detection of a broad range of changes in pCO_2. Indeed, this is what is found for temperature sensing in the body. Transient receptor potential channels are non selective cation channels. This channel

super family contains many members that detect temperatures at different levels in such a way that together they span a broad range of temperatures from cold to hot. We propose that CO_2 sensing has adopted a similar mechanism for detecting such a broad range of pCO_2. In this way both the heteromeric Kir4.1-Kir5.1 and the Kir6.2+SUR1 proposed in the beginning of this dissertation may be central CO_2 chemoreceptor molecules.

L. GENERAL CONCLUSION

The experiments performed in this dissertation using heterologous expression systems demonstrate the modulation of Kir channels. The results shown here strengthen the candidacy of these channels as central CO_2 chemoreceptors. In addition to the findings of other researchers my studies demonstrate the ligand regulation of Kir channels. I have presented additional evidence for the expression of the Kir4.1-Kir5.1 channel in the brainstem, modulation of the channel by neurotransmitters critical for respiratory control and CO_2, identification of the molecular mechanism underlying this modulation, as well as identifying a functional pH regulated gate in the Kir6.2+SUR1 channel that appears to be shared by other Kir channels. These properties are critical to the function of these channels as central CO_2 chemoreceptor molecules that can couple CO_2 sensing to cellular excitability and thus an appropriate response by the respiratory system. Therefore, the information obtained and presented in this dissertation about the molecular mechanisms underlying the regulation of Kir channels by neurotransmitters and CO_2 constitutes a significant step towards the understanding of the role that may be played by these channel as CO_2 sensing molecules, and may have an impact on the understanding of respiratory control diseases and on the formation of therapeutic modalities by the manipulation of these channels.

M. REFERENCE LIST

Anton F, Herdegen T, Peppel P, Leah JD (1991). c-FOS-like immunoreactivity in rat brainstem neurons following noxious chemical stimulation of the nasal mucosa. *Neuroscience* **41**:629-641.

Armstrong CM (1966). Time course of TEA^+-induced anomalous rectification in squid giant axons., *J.Gen.Physiol*. **273**, pp. F516-F529.

Ashcroft FM and Gribble FM (1999). ATP-sensitive K^+ channels and insulin secretion: their role in health and disease, *Diabetologia* **42**, pp. 903-919.

Bajic D, Koike M, Albsoul-Younes AM, Nakajima S, and Nakajima Y (2002). Two different inward rectifier K^+ channels are effectors for transmitter-induced slow excitation in brain neurons. *Proc Natl Acad Sci USA* **99**: 14494-14499.

Ballantyne D, Scheid P (2001). Central chemosensitivity of respiration: a brief overview. *Respir Physiol* **129**:5-12.

Baukrowitz T, Fakler B (2000). KATP channels gated by intracellular nucleotides and phospholipids. *Eur J Biochem* **267**:5842-5848.

Baukrowitz T, Schulte U, Oliver D, Herlitze S, Krauter T, Tucker SJ, Ruppersberg JP, and Fakler B (1998). PIP2 and PIP as determinants for ATP inhibition of K_{ATP} channels, *Science* **282**, pp. 1141-1144.

Baukrowitz T, Tucker SJ, Schulte U, Benndorf K, Ruppersberg JP, Fakler B (1999). Inward rectification in KATP channels: a pH switch in the pore. *EMBO J* **18**:847-853.

Beguin P, Nagashima K, Nishimura M, Gonoi T, and Seino S (1999). PKA-mediated phosphorylation of the human $K(_{ATP})$ channel: separate roles of Kir6.2 and SUR1 subunit phosphorylation, *EMBO J.* **18**, pp. 4722-4732.

Bichet D, Haass FA, and Jan LY (2003). Merging functional studies with structures of inward-rectifier K^+ channels, *Nat.Rev.Neurosci*. **4**, pp. 957-967.

Bonham AC (1995). Neurotransmitters in the CNS control of breathing. *Respir Physiol* **101**:219-230.

Budzinska K, von Euler C, Kao FF, Pantaleo T, Yamamoto Y (1985). Effects of graded focal cold block in rostral areas of the medulla. *Acta Physiol Scand* **124**:329-340.

Capener CE., Shrivastava IH, Ranatunga KM, Forrest LR, Smith GR, and Sansom MS (2000). Homology modeling and molecular dynamics simulation studies of an inward rectifier potassium channel, *Biophys.J*. **78**, pp. 2929-2942.

Casamassima M, D'Adamo MC, Pessia M, and Tucker SJ (2003). Identification of a heteromeric interaction that influences the rectification, gating, and pH sensitivity of Kir4.1/Kir5.1 potassium channels, *J Biol.Chem.* **278**, pp. 43533-43540.

Caterina MJ, Rosen TA, Tominaga M, Brake AJ, Julius D (1999). A capsaicin-receptor homologue with a high threshold for noxious heat. *Nature* **398**:436-441.

Chen Z, Hedner J, Hedner T (1990). Substance P in the ventrolateral medulla oblongata regulates ventilatory responses. *J Appl Physiol* **68**:2631-2639.

Coates EL, Li A, Nattie EE (1993). Widespread sites of brain stem ventilatory chemoreceptors. *J Appl Physiol* **75**:5-14.

Colquhoun D and Hawkes AG (1995). *The principles of the stochastic interpretation of ion-channel mechanisms,* In: B. Sakmann and E. Neher, Editors, *Single-Channel Recording*, Plenum Press, New York, pp. 397-482.

Colquhoun D, Hawkes AG (1990). Stochastic properties of ion channel openings and bursts in a membrane patch that contains two channels: evidence concerning the number of channels present when a record containing only single openings is observed. *Proc R Soc Lond B Biol Sci* **240**:453-477.

Cream CL, Li A, and Nattie EE (1997). RTN TRH causes prolonged respiratory stimulation. *J Appl Physiol* **83**: 792-799.

Cuevas J, Bassett AL, Cameron JS, Furukawa T, Myerburg RJ, Kimura S (1991). Effect of H^+ on ATP-regulated K^+ channels in feline ventricular myocytes. *Am J Physiol* **261**:H755-H761.

Cui N, Giwa LR, Xu H, Rojas A, Abdulkadir L, and Jiang C (2001). Modulation of the heteromeric Kir4.1-Kir5.1 channels by $P(CO_2)$ at physiological levels. *J Cell Physiol* **189**: 229-236.

Cukras CA, Jeliazkova I, Nichols CG (2002). The role of NH2-terminal positive charges in the activity of inward rectifier KATP channels. *J Gen Physiol* **120**:437-446.

Davies NW (1990). Modulation of ATP-sensitive K^+ channels in skeletal muscle by intracellular protons, *Nature* **343**, pp. 375-377.

Dean JB, Bayliss DA, Erickson JT, Lawing WL, Millhorn DE (1990). Depolarization and stimulation of neurons in nucleus tractus solitarii by carbon dioxide does not require chemical synaptic input. *Neuroscience* **36**:207-216.

Dean JB, Lawing WL, Millhorn DE (1989). CO_2 decreases membrane conductance and depolarizes neurons in the nucleus tractus solitarii. *Exp Brain Res* **76**:656-661.

Dekin MS, Richerson GB, and Getting PA (1985). Thyrotropin-releasing hormone induces rhythmic bursting in neurons of the nucleus tractus solitarius. *Science* **229**: 67-69.

Doi T, Fakler B, Schultz JH, Schulte U, Brandle U, Weidemann S, Zenner HP, Lang F, Ruppersberg JP (1996). Extracellular K^+ and intracellular pH allosterically regulate renal Kir1.1 channels. *J Biol Chem* **271**:17261-17266.

Donley VR, Hiskett EK, Kidder AC, Schermerhorn T (2005). ATP-sensitive potassium channel (KATP channel) expression in the normal canine pancreas and in canine insulinomas. *BMC Vet Res* **1**:8.

Donnelly DF, Carroll JL (2005). Mitochondrial function and carotid body transduction. *High Alt Med Biol* **6**:121-132.

Doring F, Derst C, Wischmeyer E, Karschin C, Schneggenburger R, Daut J, Karschin A (1998). The epithelial inward rectifier channel Kir7.1 displays unusual K^+ permeation properties. *J Neurosci* **18**:8625-8636.

Doyle DA (2004). Structural changes during ion channel gating, *Trends Neurosci*. **27**, pp. 298-302.

Doyle DA, Morais CJ, Pfuetzner RA, Kuo A, Gulbis JM, Cohen SL, Chait BT, and MacKinnon R (1998). The structure of the potassium channel: molecular basis of K^+ conduction and selectivity, *Science* **280**, pp. 69-77.

Drain P, Li L, Wang J (1998). KATP channel inhibition by ATP requires distinct functional domains of the cytoplasmic C terminus of the pore-forming subunit. *Proc Natl Acad Sci U S A* **95**:13953-13958.

Du X, Zhang H, Lopes C, Mirshahi T, Rohacs T, and Logothetis DE (2004). Characteristic interactions with phosphatidylinositol 4,5-bisphosphate determine regulation of kir channels by diverse modulators, *J Biol.Chem.* **279**, pp. 37271-37281.

Elam M, Yao T, Thoren P, and Svensson TH (1981). Hypercapnia and hypoxia: chemoreceptor-mediated control of locus coeruleus neurons and splanchnic, sympathetic nerves. Brain Res **222**:373-381.

Erlichman JS, Leiter JC (1997). Comparative aspects of central CO_2 chemoreception. *Respir Physiol* **110**:177-185.

Fakler B, Brandle U, Glowatzki E, Zenner HP, and Ruppersberg JP (1994). Kir2.1 inward rectifier K^+ channels are regulated independently by protein kinases and ATP hydrolysis. *Neuron* **13**: 1413-1420.

Feldman JL, Mitchell GS, Nattie EE (2003). Breathing: rhythmicity, plasticity, chemosensitivity. *Annu Rev Neurosci* **26**:239-266.

Flynn GE and Zagotta WN (2001). Conformational changes in S6 coupled to the opening of cyclic nucleotide-gated channels, *Neuron* **30**, pp. 689-698.

Germann WJ and Stanfield CL (2005). The urinary system; fluid and electrolyte balance, in: *Principles of Human Physiology,* Benjamin Cummings, San Francisco, pp 618-631.

Gourine AV (2005). On the peripheral and central chemoreception and control of breathing: an emerging role of ATP. *J Physiol* **568**:715-724.

Gourine AV, Atkinson L, Deuchars J, Spyer KM (2003). Purinergic signalling in the medullary mechanisms of respiratory control in the rat: respiratory neurones express the P2X2 receptor subunit. *J Physiol* **552**:197-211.

Gourine, AV, Llaudet, E, Dale, N, & Spyer, KM (2005). ATP is a mediator of chemosensory transduction in the central nervous system. *Nature* **436**, 108-111.

Gustafsson B and Jankowska E (1976). Direct and indirect activation of nerve cells by electrical pulses applied extracellularly. *J Physiol* **258**: 33-61.

Guyenet PG, Mulkey, DK, Stornetta, RL, & Bayliss, DA (2005). Regulation of ventral surface chemoreceptors by the central respiratory pattern generator. *J Neurosci* **25** , 8938-8947.

Guyenet PG, Stornetta RL, Bayliss DA, Mulkey DK (2005). Retrotrapezoid nucleus: a litmus test for the identification of central chemoreceptors. *Exp Physiol* **90**:247-253.

Haller M, Mironov SL, Karschin A, Richter DW (2001). Dynamic activation of $K(_{ATP})$ channels in rhythmically active neurons. *J Physiol* **537**:69-81.

Haxhiu MA, Yung K, Erokwu B, and Cherniack NS (1996). CO_2-induced c-fos expression in the CNS catecholaminergic neurons. Respir Physiol 105:35-45.

Henry P, Pearson WL, and Nichols CG (1996). Protein kinase C inhibition of cloned inward rectifier (HRK1/KIR2.3) K^+ channels expressed in Xenopus oocytes, *J Physiol.* **495 (Pt 3)**, pp. 681-688.

Hibino H, Fujita A, Iwai K, Yamada M, and Kurachi Y (2004). Differential assembly of inwardly rectifying K^+ channel subunits, Kir4.1 and Kir5.1, in brain astrocytes, *J Biol.Chem.* **279**, pp. 44065-44073.

Hibino H, Horio Y, Fujita A, Inanobe A, Doi K, Gotow T, Uchiyama Y, Kubo T, and Kurachi Y (1999). Expression of an inwardly rectifying K^+ channel, Kir4.1, in satellite cells of rat cochlear ganglia. *Am J Physiol* **277**: C638-C644.

Higashi K, Fujita A, Inanobe A, Tanemoto M, Doi K, Kubo T, and Kurachi Y (2001). An inwardly rectifying $K(^+)$ channel, Kir4.1, expressed in astrocytes surrounds synapses and blood vessels in brain, *Am J Physiol Cell Physiol.* **281**, pp. C922-C931.

Hodges MR, Martino P, Davis S, Opansky C, Pan LG, Forster HV (2004). Effects on breathing of focal acidosis at multiple medullary raphe sites in awake goats. *J Appl Physiol* **97**:2303-2309.

Hodges MR, Opansky C, Qian B, Davis S, Bonis J, Bastasic J, Leekley T, Pan LG, Forster HV (2004). Transient attenuation of CO2 sensitivity after neurotoxic lesions in the medullary raphe area of awake goats. *J Appl Physiol* **97**:2236-2247.

Horio Y (2001). Potassium channels of glial cells: distribution and function. Jpn J Pharmacol **87**:1-6.

Horn CC, Friedman MI (2003). Detection of single unit activity from the rat vagus using cluster analysis of principal components. *J Neurosci Methods* **122**:141-147.

Ishii M, Fujita A, Iwai K, Kusaka S, Higashi K, Inanobe A, Hibino H, and Kurachi Y (2003). Differential expression and distribution of Kir5.1 and Kir4.1 inwardly rectifying K^+ channels in retina, *Am J Physiol Cell Physiol.* **285**, pp. C260-C267.

Isomoto S, Kondo C, Kurachi Y (1997). Inwardly rectifying potassium channels: their molecular heterogeneity and function. *Jpn J Physiol* **47**:11-39.

Ito M, Inanobe A, Horio Y, Hibino H, Isomoto S, Ito H, Mori K, Tonosaki A, Tomoike H, and Kurachi Y (1996). Immunolocalization of an inwardly rectifying K^+ channel, K(AB)-2 (Kir4.1), in the basolateral membrane of renal distal tubular epithelia, *FEBS Lett.* **388**, pp. 11-15.

Jan LY and Jan YN (1997). Voltage-gated and inwardly rectifying potassium channels. *J Physiol* **505 (Pt 2)**: 267-282.

Jiang C and Lipski J (1990). Extensive monosynaptic inhibition of ventral respiratory group neurons by augmenting neurons in the Botzinger complex in the cat. *Exp Brain Res* **81**: 639-648.

Jiang C, Rojas A, Wang R, and Wang X (2005). CO_2 central chemosensitivity: why are there so many sensing molecules?. Respir Physiol Neurobiol 145:115-126.

Jiang C, Xu H, Cui N, Wu J (2001). An alternative approach to the identification of respiratory central chemoreceptors in the brainstem. *Respir Physiol* **129**:141-157.

Jiang Y, Lee A, Chen J, Cadene M, Chait BT, and MacKinnon R (2002). Crystal structure and mechanism of a calcium-gated potassium channel, *Nature* **417**, pp. 515-522.

Jin T, Peng L, Mirshahi T, Rohacs T, Chan KW, Sanchez R, and Logothetis DE (2002). The beta-gamma subunits of G proteins gate a K^+ channel by pivoted bending of a transmembrane segment, *Mol.Cell* **10**, pp. 469-481.

Johnson JP and Zagotta WN (2001). Rotational movement during cyclic nucleotide-gated channel opening, *Nature* **412**, pp. 917-921.

Karschin A, Brockhaus J, Ballanyi K (1998). KATP channel formation by the sulphonylurea receptors SUR1 with Kir6.2 subunits in rat dorsal vagal neurons in situ. *J Physiol* **50**9 (Pt 2):339-346.

Karschin C, Ecke C, Ashcroft FM, Karschin A (1997). Overlapping distribution of $K(_{ATP})$ channel-forming Kir6.2 subunit and the sulfonylurea receptor SUR1 in rodent brain. *FEBS Lett* **401**:59-64.

Karschin C, Karschin A (1997). Ontogeny of gene expression of Kir channel subunits in the rat. *Mol Cell Neurosci* **10**:131-148.

Kawai, A, Onimaru, H, & Homma, I (2006). Mechanisms of CO2/H+ chemoreception by respiratory rhythm generator neurons in the medulla from newborn rats in vitro. *J Physiol* **572**, 525-537.

Kawai, A., Ballantyne, D, Muckenhoff, K, & Scheid, P (1996). Chemosensitive medullary neurones in the brainstem-spinal cord preparation of the neonatal rat. *J Physiol* **492**, 277-292.

Koike-Tani M, Collins JM, Kawano T, Zhao P, Zhao Q, Kozasa T, Nakajima S, and Nakajima Y (2005). Signal transduction pathway for the substance P-induced inhibition of rat Kir3 (GIRK) channel. *J Physiol* **564**: 489-500.

Komai M and Bryant BP (1993). Acetazolamide specifically inhibits lingual trigeminal nerve responses to carbon dioxide. Brain Res 612:122-129.

Konstas AA, Korbmacher C, and Tucker SJ (2003). Identification of domains that control the heteromeric assembly of Kir5.1/Kir4.0 potassium channels. *Am J Physiol Cell Physiol* **284**: C910-C917.

Kuo A, Gulbis JM, Antcliff JF, Rahman T, Lowe ED, Zimmer J, Cuthbertson J, Ashcroft FM, Ezaki T, and Doyle DA (2003). Crystal structure of the potassium channel KirBac1.1 in the closed state, *Science* **300**, pp. 1922-1926.

Kusaka S, Horio Y, Fujita A, Matsushita K, Inanobe A, Gotow T, Uchiyama Y, Tano Y, and Kurachi Y (1999). Expression and polarized distribution of an inwardly rectifying K^+ channel, Kir4.1, in rat retinal pigment epithelium. *J Physiol* **520 Pt 2**: 373-381.

Kyte J and Doolittle RF (1982). A simple method for displaying the hydropathic character of a protein, *J.Mol.Biol*. **157**, pp. 105-132.

Lagrutta AA, Bond CT, Xia XM, Pessia M, Tucker S, Adelman JP (1996). Inward rectifier potassium channels. Cloning, expression and structure-function studies. *Jpn Heart J* **37**:651-660.

Lahiri S, Forster RE (2003). CO2/H($^+$) sensing: peripheral and central chemoreception. *Int J Biochem Cell Biol* **35**:1413-1435.

Lahiri S, Roy A, Baby SM, Hoshi T, Semenza GL, Prabhakar NR (2006). Oxygen sensing in the body. *Prog Biophys Mol Bio*l **91**:249-286.

Lamanna JC, Neal M, Xu K, Haxhiu MA (2003). Differential expression of intracellular acidosis in rat brainstem regions in response to hypercapnic ventilation. *Adv Exp Med Biol* **536**:407-413.

Lei Q, Talley EM, and Bayliss DA (2001). Receptor-mediated inhibition of G protein-coupled inwardly rectifying potassium channels involves $G_{\alpha q}$ family subunits, phospholipase C, and a readily diffusible messenger. *J Biol Chem* **276**: 16720-16730.

Li A, Nattie E (2006). Catecholamine neurones in rats modulate sleep, breathing, central chemoreception and breathing variability. *J Physiol* **570**:385-396.

Li A, Nattie EE (1997). Focal central chemoreceptor sensitivity in the RTN studied with a CO_2 diffusion pipette in vivo. *J Appl Physiol* **83**:420-428.

Li A, Zhou S, Nattie E (2006). Simultaneous inhibition of caudal medullary raphe and retrotrapezoid nucleus decreases breathing and the CO2 response in conscious rats. *J Physiol* **577***:307-318.*

Li L, Rojas A, Wu J, Jiang C (2004). Disruption of glucose sensing and insulin secretion by ribozyme Kir6.2-gene targeting in insulin-secreting cells. *Endocrinology* **145**:4408-4414.

Light PE, Bladen C, Winkfein RJ, Walsh MP, and French RJ (2000), Molecular basis of protein kinase C-induced activation of ATP-sensitive potassium channels, *Proc.Natl.Acad.Sci.U.S A.* **97**, pp. 9058-9063.

Lin D, Sterling H, Lerea KM, Giebisch G, and Wang WH (2002). Protein kinase C (PKC)-induced phosphorylation of ROMK1 is essential for the surface expression of ROMK1 channels, *J Biol.Chem.* **277**, pp. 44278-44284.

Lin YF, Jan YN, and Jan LY (2000). Regulation of ATP-sensitive potassium channel function by protein kinase A-mediated phosphorylation in transfected HEK293 cells, *EMBO J.* **19**, pp. 942-955.

Lopes CM, Zhang H, Rohacs T, Jin T, Yang J, and Logothetis DE (2002). Alterations in conserved Kir channel-PIP2 interactions underlie channelopathies, *Neuron* **34**, pp. 933-944.

Lorier, AR, Peebles, K, Brosenitsch, T, Robinson, DM, Housley, GD, & Funk, GD (2004). P2 receptors modulate respiratory rhythm but do not contribute to central CO_2 sensitivity in vitro. *Respir Physiol Neurobiol* **142**, 27-42.

Luscher C, Jan LY, Stoffel M, Malenka RC, and Nicoll RA (1997). G protein-coupled inwardly rectifying K^+ channels (GIRKs) mediate postsynaptic but not presynaptic transmitter actions in hippocampal neurons. *Neuron* **19**: 687-695.

Ma W, Zhang L, Xing G, Hu Z, Iwasa KH, and Clay JR (1998). Prenatal expression of inwardly rectifying potassium channel mRNA (Kir4.1) in rat brain. Neuroreport 9:223-227.

Mao J, Wang X, Chen F, Wang R, Rojas A, Shi Y, Piao H, and Jiang C (2004). Molecular basis for the inhibition of G protein-coupled inward rectifier K($^+$) channels by protein kinase C, *Proc.Natl.Acad.Sci.U.S A.* **101**, pp. 1087-1092.

Matsuo M, Kimura Y, Ueda K (2005). KATP channel interaction with adenine nucleotides. *J Mol Cell Cardiol* **38**:907-916.

Messier ML, Li A, Nattie EE (2002). Muscimol inhibition of medullary raphe neurons decreases the CO_2 response and alters sleep in newborn piglets. *Respir Physiol Neurobiol* **133**:197-214.

Mikhailov MV, Mikhailova EA, Ashcroft SJ (2000). Investigation of the molecular assembly of beta-cell K($_{ATP}$) channels. *FEBS Lett* **482**:59-64.

Miura M, Okada J, Kanazawa M (1998). Topology and immunohistochemistry of proton-sensitive neurons in the ventral medullary surface of rats. *Brain Res* **780**:34-45.

Mizusawa A, Ogawa H, Kikuchi Y, Hida W, Shirato K (1995). Role of the parabrachial nucleus in ventilatory responses of awake rats. *J Physiol* **489** (Pt 3):877-884.

Moreau C, Prost AL, Derand R, Vivaudou M (2005). SUR, ABC proteins targeted by KATP channel openers. *J Mol Cell Cardiol* **38**:951-963.

Moss IR, Denavit-Saubie M, Eldridge FL, Gillis RA, Herkenham M, and Lahiri S (1986). Neuromodulators and transmitters in respiratory control. *Fed Proc* **45**: 2133-2147.

Mulkey DK, Stornetta RL, Weston MC, Simmons JR, Parker A, Bayliss DA, Guyenet PG (2004). Respiratory control by ventral surface chemoreceptor neurons in rats. *Nat Neurosci* **7**:1360-1369.
Mulkey, DK, Mistry, AM, Guyenet, PG, & Bayliss, DA (2006). Purinergic P2 receptors modulate excitability but do not mediate pH sensitivity of RTN respiratory chemoreceptors. *J Neurosci* **26**, 7230-7233.

Mutolo D, Bongianni F, Carfi M, and Pantaleo T (1999). Respiratory responses to thyrotropin-releasing hormone microinjected into the rabbit medulla oblongata. *Am J Physiol* **277**: R1331-R1338.

Nattie E (1999). CO_2, brainstem chemoreceptors and breathing. *Prog Neurobiol* **59**: 299-331.

Nattie E (2000). Multiple sites for central chemoreception: their roles in response sensitivity and in sleep and wakefulness. *Respir Physiol* **122**:223-235.

Nattie E, Li A, Meyerand E, Dunn JF (2002). Ventral medulla pHi measured in vivo by 31P NMR is not regulated during hypercapnia in anesthetized rat. *Respir Physiol Neurobiol* **130**:139-149.

Nattie EE and Li A (2002). Substance P-saporin lesion of neurons with NK1 receptors in one chemoreceptor site in rats decreases ventilation and chemosensitivity. *J Physiol* **544**: 603-616.

Nattie EE, Li A (1994). Retrotrapezoid nucleus lesions decrease phrenic activity and CO_2 sensitivity in rats. *Respir Physiol* **97**:63-77.

Nattie EE, Li A (2002). CO_2 dialysis in nucleus tractus solitarius region of rat increases ventilation in sleep and wakefulness. *J Appl Physiol* **92**:2119-2130.

Nattie EE, Li A, Richerson G, and Lappi DA (2004). Medullary serotonergic neurones and adjacent neurones that express neurokinin-1 receptors are both involved in chemoreception in vivo. *J Physiol* **556**: 235-253.

Nattie EE, Li AH, St John WM (1991). Lesions in retrotrapezoid nucleus decrease ventilatory output in anesthetized or decerebrate cats. *J Appl Physiol* **71**:1364-1375.

Necakov A, Peever JH, Shen L, and Duffin J (2002). Acetazolamide and respiratory chemosensitivity to CO_2 in the neonatal rat transverse medullary slice. Respir Physiol Neurobiol 132:279-287.

Nichols CG, Lopatin AN (1997). Inward rectifier potassium channels. *Annu Rev Physiol* **59**:171-191.

Nink M, Krause U, Lehnert H, Heuberger W, Huber I, Schulz R, Hommel G, and Beyer J (1991). Thyrotropin-releasing hormone has stimulatory effects on ventilation in humans. *Acta Physiol Scand* **141**: 309-318.

Nink M, Krause U, Lehnert H, Schulz V, Schulz R, Beyer J (1991). [Studies on the influence of releasing hormones TRH and CRH on respiratory regulation]. *Pneumologie 45 Suppl* **1**:246-248.

Oliver D, Baukrowitz T, Fakler B (2000). Polyamines as gating molecules of inward-rectifier K^+ channels. *Eur J Biochem* **267**:5824-5829.

O'Regan RG, Majcherczyk S (1982). Role of peripheral chemoreceptors and central chemosensitivity in the regulation of respiration and circulation. *J Exp Biol* **100**:23-40.

Oyamada Y, Andrzejewski M, Muckenhoff K, Scheid P, and Ballantyne D (1999). Locus coeruleus neurones in vitro: pH-sensitive oscillations of membrane potential in an electrically coupled network. Respir Physiol 118:131-147.

Oyamada Y, Ballantyne D, Muckenhoff K, and Scheid P (1998). Respiration-modulated membrane potential and chemosensitivity of locus coeruleus neurones in the in vitro brainstem-spinal cord of the neonatal rat. J Physiol 513 (Pt 2):381-398.

Paterson DS, Thompson EG, Kinney HC (2006). Serotonergic and glutamatergic neurons at the ventral medullary surface of the human infant: Observations relevant to central chemosensitivity in early human life. *Auton Neurosci* **124**:112-124.

Perozo E, Cortes DM, and Cuello LG (1999). Structural rearrangements underlying K^+-channel activation gating, *Science* **285**, pp. 73-78.

Pessia M, Imbrici P, D'Adamo MC, Salvatore L, and Tucker SJ (2001). Differential pH sensitivity of Kir4.1 and Kir4.2 potassium channels and their modulation by heteropolymerisation with Kir5.1, *J Physiol.* **532**, pp. 359-367.

Pessia M, Tucker SJ, Lee K, Bond CT, and Adelman JP (1996). Subunit positional effects revealed by novel heteromeric inwardly rectifying K^+ channels. *EMBO J* **15**: 2980-2987.

Pete G, Mack SO, Haxhiu MA, Walbaum S, and Gauda EB (2002). CO_2-induced c-Fos expression in brainstem preprotachykinin mRNA containing neurons. *Respir Physiol Neurobiol* **130**: 265-274.

Phillips LR, Enkvetchakul D, and Nichols CG (2003). Gating dependence of inner pore access in inward rectifier K^+ channels, *Neuron* **37**, pp. 953-962.

Pineda J, Aghajanian GK (1997). Carbon dioxide regulates the tonic activity of locus coeruleus neurons by modulating a proton- and polyamine-sensitive inward rectifier potassium current. *Neuroscience* **77**:723-743.

Poopalasundaram S, Knott C, Shamotienko OG, Foran PG, Dolly JO, Ghiani CA, Gallo V, and Wilkin GP (2000). Glial heterogeneity in expression of the inwardly rectifying $K(^+)$ channel, Kir4.1, in adult rat CNS. Glia 30:362-372.

Putnam RW, Filosa JA, Ritucci NA (2004). Cellular mechanisms involved in $CO(_2)$ and acid signaling in chemosensitive neurons. *Am J Physiol Cell Physiol* **287**:C1493-C1526.

Quayle JM, Nelson MT, Standen NB (1997). ATP-sensitive and inwardly rectifying potassium channels in smooth muscle. *Physiol Rev* **77**:1165-1232.

Reimann F, Ashcroft FM (1999). Inwardly rectifying potassium channels. *Curr Opin Cell Biol* **11**:503-508.

Ribas-Salgueiro JL, Matarredona ER, Ribas J, Pasaro R (2006). Enhanced c-Fos expression in the rostral ventral respiratory complex and rostral parapyramidal region by inhibition of the Na^+/H^+ exchanger type 3. *Auton Neurosci* **126**-127:347-354.

Richerson GB (2004). Serotonergic neurons as carbon dioxide sensors that maintain pH homeostasis, *Nat.Rev.Neurosci.* **5**, pp. 449-461.

Richerson GB, Wang W, Hodges MR, Dohle CI, and Diez-Sampedro A (2005). Homing in on the specific phenotype(s) of central respiratory chemoreceptors. *Exp Physiol* **90**: 259-266.

Richerson GB, Wang W, Tiwari J, Bradley SR (2001). Chemosensitivity of serotonergic neurons in the rostral ventral medulla. Respir Physiol **129**:175-189.

Richerson, GB (1995). Response to CO_2 of Neurons in the Rostral Ventral Medulla In-Vitro.
J Neurophysiol **73**, 933-944.

Sackin H, Nanazashvili M, Palmer LG, Krambis M, and Walters DE (2005). Structural locus of the pH gate in the Kir1.1 inward rectifier channel, *Biophys.J*. **88**, pp. 2597-2606.

Salvatore L, D'Adamo MC, Polishchuk R, Salmona M, Pessia M (1999). Localization and age-dependent expression of the inward rectifier K^+ channel subunit Kir 5.1 in a mammalian reproductive system. *FEBS Lett* **449**:146-152.

Sato M, Severinghaus JW, Basbaum AI (1992). Medullary CO_2 chemoreceptor neuron identification by c-fos immunocytochemistry. *J Appl Physiol* **73**:96-100.

Schultz JH, Czachurski J, Volk T, Ehmke H, Seller H (2003). Central sympathetic chemosensitivity and Kir1 potassium channels in the cat. *Brain Res* **963**:113-120.

Schulz R, Nink M, Werner GS, Andreas S, Kreuzer H, Beyer J, and Lehnert H (1996). Human corticotropin-releasing hormone and thyrotropin-releasing hormone modulate the hypercapnic ventilatory response in humans. *Eur J Clin Invest* **26**: 989-995.

Severson CA, Wang W, Pieribone VA, Dohle CI, Richerson GB (2003). Midbrain serotonergic neurons are central pH chemoreceptors. *Nat Neurosci* **6**:1139-1140.

Shin KS, Rothberg BS, and Yellen G (2001). Blocker state dependence and trapping in hyperpolarization-activated cation channels: evidence for an intracellular activation gate, *J.Gen.Physiol* **117**, pp. 91-101.

Shyng, SL and Nichols CG (1998). Membrane phospholipid control of nucleotide sensitivity of K_{ATP} channels, *Science* **282**, pp. 1138-1141.

Solomon IC (2003). Focal CO_2/H^+ alters phrenic motor output response to chemical stimulation of cat pre-Botzinger complex in vivo. *J Appl Physiol* **94**:2151-2157.

Solomon IC (2003). Influence of respiratory network drive on phrenic motor output evoked by activation of cat pre-Botzinger complex. *Am J Physiol Regul Integr Comp Physiol* **284**:R455-R466.

Sterling H, Lin DH, Gu RM, Dong K, Hebert SC, and Wang WH (2002). Inhibition of protein-tyrosine phosphatase stimulates the dynamin-dependent endocytosis of ROMK1, *J Biol.Chem.* **277**, pp. 4317-4323.

Stevens EB, Shah BS, Pinnock RD, and Lee K (1999). Bombesin receptors inhibit G protein-coupled inwardly rectifying K^+ channels expressed in Xenopus oocytes through a protein kinase C-dependent pathway, *Mol Pharmacol.* **55**, pp. 1020-1027.

Story GM, Peier AM, Reeve AJ, Eid SR, Mosbacher J, Hricik TR, Earley TJ, Hergarden AC, Andersson DA, Hwang SW, McIntyre P, Jegla T, Bevan S, Patapoutian A (2003).

ANKTM1, a TRP-like channel expressed in nociceptive neurons, is activated by cold temperatures. *Cell* **112**:819-829.

Stunden, CE, Filosa, JA, Garcia, AJ, Dean, JB, & Putnam, RW (2001). Development of in vivo ventilatory and single chemosensitive neuron responses to hypercapnia in rats. *Respir Physiol* **127**, 135-155.

Su J, Jiang C (2006). Multicellular recordings of cultured brainstem neurons in microelectrode arrays. *Cell Tissue Res* **326**: 25-33.

Su J, Yang L, Zhang X, Rojas A, Shi Y, Jiang C (2007). High CO_2 chemosensitivity versus wide sensing spectrum: a paradoxical problem and its solutions in cultured brainstem neurons. *J Physiol* **578**:831-841.

Sugama S, Shimokawa N, Okada J, Miura M (1997). In vitro study of H^+-sensitive neurons in the ventral medullary surface of neonate rats. *Brain Res* **777**:95-102.

Sukharev S, Betanzos M, Chiang CS, and Gu HR (2001). The gating mechanism of the large mechanosensitive channel MscL, *Nature* **409**, pp. 720-724.

Takakura A, Moreira CT, Colombari TS, West, GH, Stornetta, RL, & Guyenet, PG (2006). Peripheral chemoreceptor inputs to retrotrapezoid nucleus (RTN) CO_2-sensitive neurons in rats. *J Physiol* **572**, 503-523.

Takano M, Kuratomi S (2003). Regulation of cardiac inwardly rectifying potassium channels by membrane lipid metabolism. *Prog Biophys Mol Biol* **81**:67-79.

Tanabe K, Tucker SJ, Matsuo M, Proks P, Ashcroft FM, Seino S, Amachi T, and Ueda K (1999). Direct photoaffinity labeling of the Kir6.2 subunit of the ATP-sensitive K^+ channel by 8-azido-ATP, *J.Biol.Chem*. **274**, pp. 3931-3933.

Tanemoto M, Abe T, Onogawa T, and Ito S (2004). PDZ binding motif-dependent localization of K^+ channel on the basolateral side in distal tubules, *Am J Physiol Renal Physiol.* **287**, pp. F1148-F1153.

Tanemoto M, Kittaka N, Inanobe A, and Kurachi Y (2000). In vivo formation of a proton-sensitive K^+ channel by heteromeric subunit assembly of Kir5.1 with Kir4.1. *J Physiol* **525 Pt 3**: 587-592.

Taylor NC, Li A, Nattie EE (2005). Medullary serotonergic neurones modulate the ventilatory response to hypercapnia, but not hypoxia in conscious rats. *J Physiol* **566**:543-557.

Thomas, T., Ralevic, V., Gadd, C. A., & Spyer, K. M (1999). Central CO_2 chemoreception: a mechanism involving P2 purinoceptors localized in the ventrolateral medulla of the anaesthetized rat. *J Physiol* **517**, 899-905.

Trapp S, Proks P, Tucker SJ, and Ashcroft FM (1998). Molecular analysis of ATP-sensitive K channel gating and implications for channel inhibition by ATP, *J Gen.Physiol* **112**, pp. 333-349.

Tryba, AK, Pena, F, & Ramirez, JM (2006). Gasping activity in vitro: a rhythm dependent on 5-HT2A receptors. *J Neurosci* **26**, 2623-2634.

Tsubo TI, Lippiat JD, Ashcroft FM, and Rutter GA (2004). ATP-dependent interaction of the cytosolic domains of the inwardly rectifying K^+ channel Kir6.2 revealed by fluorescence resonance energy transfer, *Proc.Natl.Acad.Sci.U.S.A* **101**, pp. 76-81.

Tucker SJ, Gribble FM, Zhao C, Trapp S, and Ashcroft FM (1997). Truncation of Kir6.2 produces ATP-sensitive K^+ channels in the absence of the sulphonylurea receptor, *Nature* **387**, pp. 179-183.

Unwin N (1995). Acetylcholine receptor channel imaged in the open state, *Nature* **373**, pp. 37-43.

Unwin N (2003). Structure and action of the nicotinic acetylcholine receptor explored by electron microscopy, *FEBS Lett*. **555**, pp. 91-95.

van den Pol AN, Ghosh PK, Liu RJ, Li Y, Aghajanian GK, and Gao XB (2002). Hypocretin (orexin) enhances neuron activity and cell synchrony in developing mouse GFP-expressing locus coeruleus. J Physiol 541:169-185.

Vivaudou M, Forestier C (1995). Modification by protons of frog skeletal muscle KATP channels: effects on ion conduction and nucleotide inhibition. *J Physiol* **486** (Pt 3):629-645.

Vonhof S, Siren AL, Feuerstein GZ (1991). Central ventilatory effects of thyrotropin-releasing hormone in the conscious rat. *Neuropeptides* **18**:93-98.

Vorobiov D, Levin G, Lotan I, and Dascal N (1998). Agonist-independent inactivation and agonist-induced desensitization of the G protein-activated K^+ channel (GIRK) in Xenopus oocytes, *Pflugers Arch.* **436**, pp. 56-68.

Wang W, Tiwari JK, Bradley SR, Zaykin RV, and Richerson GB (2001). Acidosis-stimulated neurons of the medullary raphe are serotonergic. *J Neurophysiol* **85**: 2224-2235.

Wang WH (2006). Regulation of ROMK (Kir1.1) channels: new mechanisms and aspects, *Am J Physiol Renal Physiol.* **290**, pp. F14-F19.

Wang WH, Lin DH, and Sterling H (2002). Regulation of ROMK channels by protein tyrosine kinase and tyrosine phosphatase, *Trends Cardiovasc.Med.* **12**, pp. 138-142.

Wang, WG., Pizzonia, JH., & Richerson, GB (1998). Chemosensitivity of rat medullary raphe neurones in primary tissue culture. *J Physiol* **511**, 433-450.

Watanabe H, Vriens J, Suh SH, Benham CD, Droogmans G, Nilius B (2002). Heat-evoked activation of TRPV4 channels in a HEK293 cell expression system and in native mouse aorta endothelial cells. *J Biol Chem* **277**:47044-47051.

Wenninger JM, Pan LG, Klum L, Leekley T, Bastastic J, Hodges MR, Feroah TR, Davis S, and Forster HV (2004a). Large lesions in the pre-Botzinger complex area eliminate eupneic respiratory rhythm in awake goats. *J Appl Physiol* **97**: 1629-1636.

Wenninger JM, Pan LG, Klum L, Leekley T, Bastastic J, Hodges MR, Feroah T, Davis S, and Forster HV (2004b). Small reduction of neurokinin-1 receptor-expressing neurons in the pre-Botzinger complex area induces abnormal breathing periods in awake goats. *J Appl Physiol* **97**: 1620-1628.

White SH and Wimley WC (1999). Membrane protein folding and stability: physical principles, *Annu.Rev.Biophys.Biomol.Struct.* **28**, pp. 319-365.

Wimley WC and White SH (1996). Experimentally determined hydrophobicity scale for proteins at membrane interfaces, *Nat.Struct.Biol.* **3**, pp. 842-848.

Wischmeyer E and Karschin A (1996). Receptor stimulation causes slow inhibition of IRK1 inwardly rectifying K^+ channels by direct protein kinase A-mediated phosphorylation, *Proc.Natl.Acad.Sci.U.S A.* **93**, pp. 5819-5823.

Wu J, Cui N, Piao H, Wang Y, Xu H, Mao J, and Jiang C (2002). Allosteric modulation of the mouse Kir6.2 channel by intracellular H^+ and ATP, *J Physiol.* **543**, pp. 495-504.

Wu J, Xu H, Shen W, Jiang C (2004). Expression and coexpression of CO_2-sensitive Kir channels in brainstem neurons of rats. *J Membr Biol* **197**:179-191.

Wu J, Xu H, Yang Z, Wang Y, Mao J, and Jiang C (2002). Protons activate homomeric Kir6.2 channels by selective suppression of the long and intermediate closures, *J.Membr.Biol*. **190**, pp. 105-116.

Wu M, Haxhiu MA, Johnson SM (2005). Hypercapnic and hypoxic responses require intact neural transmission from the pre-Botzinger complex. *Respir Physiol Neurobiol* **146**:33-46.

Xu H, Cui N, Yang Z, Qu Z, and Jiang C (2000). Modulation of kir4.1 and kir5.1 by hypercapnia and intracellular acidosis. *J Physiol* **524 Pt 3**: 725-735.

Xu H, Cui N, Yang Z, Wu J, Giwa LR, Abdulkadir L, Sharma P, Jiang C (2001). Direct activation of cloned $K(_{atp})$ channels by intracellular acidosis. *J Biol Chem* **276**:12898-12902.

Xu H, Ramsey IS, Kotecha SA, Moran MM, Chong JA, Lawson D, Ge P, Lilly J, Silos-Santiago I, Xie Y, DiStefano PS, Curtis R, Clapham DE (2002). TRPV3 is a calcium-permeable temperature-sensitive cation channel. *Nature* **418**:181-186.

Xu H, Wu J, Cui N, Abdulkadir L, Wang R, Mao J, Giwa LR, Chanchevalap S, Jiang C (2001). Distinct histidine residues control the acid-induced activation and inhibition of the cloned $K(_{ATP})$ channel. *J Biol Chem* **276**:38690-38696.

Xu H, Yang Z, Cui N, Chanchevalap S, Valesky WW, and Jiang C (2000). A single residue contributes to the difference between Kir4.1 and Kir1.1 channels in pH sensitivity, rectification and single channel conductance. *J Physiol* **528 Pt 2**: 267-277.

Xu H, Yang Z, Cui N, Chanchevalap S, Valesky WW, and Jiang C (2000). A single residue contributes to the difference between Kir4.1 and Kir1.1 channels in pH sensitivity, rectification and single channel conductance, *J Physiol.* **528 Pt 2**, pp. 267-277.

Xu H, Yang Z, Cui N, Giwa LR, Abdulkadir L, Patel M, Sharma P, Shan G, Shen W, and Jiang C (2000). Molecular determinants for the distinct pH sensitivity of Kir1.1 and Kir4.1 channels. *Am J Physiol Cell Physiol* **279**: C1464-C1471.

Yamada M, Inanobe A, and Kurachi Y (1998). G protein regulation of potassium ion channels. *Pharmacol Rev* **50**: 723-760.

Yang Z, Xu H, Cui N, Qu Z, Chanchevalap S, Shen W, Jiang C (2000). Biophysical and molecular mechanisms underlying the modulation of heteromeric Kir4.1-Kir5.1 channels by CO_2 and pH. *J Gen Physiol* **116**:33-45.

Yellen G (2002). The voltage-gated potassium channels and their relatives, *Nature* **419**, pp. 35-42.

Zeng WZ, Babich V, Ortega B, Quigley R, White SJ, Welling PA, and Huang CL (2002). Evidence for endocytosis of ROMK potassium channel via clathrin-coated vesicles, *Am J Physiol Renal Physiol.* **283**, pp. F630-F639.

Zhang L, Lee JK, John SA, Uozumi N, and Kodama I (2004). Mechanosensitivity of GIRK channels is mediated by protein kinase C-dependent channel-phosphatidylinositol 4,5-bisphosphate interaction, *J Biol.Chem.* **279**, pp. 7037-7047.

Zhu G, Liu C, Qu Z, Chanchevalap S, Xu H, Jiang C (2000). $CO(_2)$ inhibits specific inward rectifier $K(^+)$ channels by decreases in intra- and extracellular pH. *J Cell Physiol* **183**:53-64.

Zhu G, Qu Z, Cui N, and Jiang C (1999). Suppression of Kir2.3 activity by protein kinase C phosphorylation of the channel protein at threonine 53, *J Biol.Chem.* **274**, pp. 11643-11646.

Zhu G, Zhang Y, Xu H, Jiang C (1998). Identification of endogenous outward currents in the human embryonic kidney (HEK 293) cell line. *J Neurosci Methods* **81**:73-83.

Zitron E, Kiesecker C, Luck S, Kathofer S, Thomas D, Kreye VA, Kiehn J, Katus HA, Schoels W, and Karle CA (2004). Human cardiac inwardly rectifying current Kir2.2 is upregulated by activation of protein kinase A, *Cardiovasc.Res.* **63**, pp. 520-527.